Formation Control of Nonlinear Multi-agent Systems Using Neural Networks

Kiarash Aryankia

A Thesis

in

The Department

of

Electrical and Computer Engineering

Presented in Partial Fulfillment of the Requirements

for the Degree of

Doctor of Philosophy (Electrical and Computer Engineering) at

Concordia University

Montréal, Québec, Canada

May 2023

CONCORDIA UNIVERSITY

School of Graduate Studies

This is to certify that the thesis prepared

By: **Kiarash Aryankia**

Entitled: **Formation Control of Nonlinear Multi-agent Systems Using Neural Networks**

and submitted in partial fulfillment of the requirements for the degree of

Doctor of Philosophy (Electrical and Computer Engineering)

complies with the regulations of this University and meets the accepted standards with respect to originality and quality.

Signed by the Final Examining Committee:

______________________________ Chair
Dr. Sivakumar Narayanswamy

______________________________ External Examiner
Dr. James Forbes

______________________________ External to Program
Dr. Walter Lucia

______________________________ Examiner
Dr. Amir G. Aghdam

______________________________ Examiner
Dr. Shahin Hashtrudi Zad

______________________________ Thesis Supervisor
Dr. Rastko R. Selmic

Approved by ______________________________
Dr. Jun Cai, Graduate Program Director

12/05/2023 ______________________________
Dr. Mourad Debbabi, Dean
Gina Cody School of Engineering and Computer Science

Abstract

Formation Control of Nonlinear Multi-agent Systems Using Neural Networks

Kiarash Aryankia, Ph.D.

Concordia University, 2023

This dissertation presents five main contributions to the field of distance-based formation control and target tracking for multi-agent systems.

The first contribution proposes a neural network-based backstepping controller for distance-based formation control in the presence of disturbance. Agents are modeled as second-order nonlinear systems, and a rigid graph theory is used to develop the controller. The radial basis function neural network (RBFNN) is used to compensate for unknown nonlinearities in the system dynamics, and the neural network (NN) weights tuning law is derived using the Lyapunov stability theory. The uniform ultimate boundedness of the formation distance error and NN weights norm estimation error is proven, and simulation results demonstrate the proposed method's performance on nonlinear multi-agent systems.

The second contribution establishes the properties of the normalized rigidity matrix in two- and three-dimensional spaces. The upper bounds of the normalized rigidity matrix singular values are derived for minimally and infinitesimally rigid frameworks, and it is proven that transformations of a framework do not affect the normalized rigidity matrix properties. The maximum smallest singular value for a three-agent rigid framework in two-dimensional space is derived, along with the necessary and sufficient conditions to reach that value. The results are applied to stability analysis and control design of distance-based formation control, and numerical simulations are provided to illustrate the theoretical results.

The third contribution proposes an adaptive neural network-based backstepping controller for distance-based formation control and target tracking in the presence of bounded time delay and disturbance. The RBFNN is used to overcome unknown nonlinearities and disturbances, and the

control signal is designed based on a Lyapunov function and Young's inequality to alleviate the effect of state time delay. The adaptive NN weights tuning law is derived using the Lyapunov function, and the uniform ultimate boundedness of the formation distance error is proven. The performance of the proposed method is validated through simulation results and comparisons with an existing displacement-based method.

The fourth contribution addresses the leader-following formation control problem for heterogeneous, uncertain, input-affine, nonlinear multi-agent systems modeled by a directed graph. A tunable three-layer NN is proposed to approximate unknown nonlinearities, and the NN weights tuning laws are derived using the Lyapunov theory. The leader-following and formation control problems are addressed using a robust integral of the sign of the error feedback and NN-based control. The results are rigorously proven using the Lyapunov stability theory, and the performance of the proposed method is compared with two other results.

The fifth contribution is the study of formation control with constant communication delays for second-order, uncertain, nonlinear multi-agent systems with asymmetric control gain matrix and unknown control direction. A three-layer NN is proposed to approximate unknown nonlinearities, and the NN weights tuning law is derived using the Lyapunov stability theory. The leader-following formation control problem with communication delay is addressed using a delayed integral of error variables, NN-based control, and a robustifying term. The semi-globally uniformly ultimately bounded solution of closed-loop signals is rigorously proven using a barrier Lyapunov function, and simulation results are provided to evaluate the efficiency and performance of the proposed method.

The thesis concludes with a summary of the contributions, limitations of the proposed methods, and suggestions for future work.

Acknowledgments

First and foremost, I express my heartfelt gratitude to my wife for her unconditional love, unwavering support, and constant encouragement throughout my Ph.D. journey. Your faith in me and my abilities has been my driving force, and without you, this achievement would not have been possible.

My family's love, encouragement, and support throughout my academic journey have been my source of strength and motivation. I am deeply thankful to them for their unwavering belief in me.

My sincerest gratitude goes to my supervisor, Dr. Rastko R. Selmic, whose expertise and mentorship have been the foundation of my Ph.D. experience. I am deeply thankful for his guidance, patience, and encouragement throughout my journey.

I would like to extend my sincere gratitude to my thesis committee members, Dr. Amir G. Aghdam, Dr. Shain Hashtrudi Zad, Dr. Walter Lucia, and Dr. James Forbes for their invaluable insights, constructive criticisms, and expert guidance. Their time and effort in reading and reviewing my work and unwavering support are greatly appreciated.

Moreover, I would like to extend my thanks to my colleagues, especially my office mates, for their help, feedback, and moral support. This thesis is a result of a journey filled with challenges, opportunities, and amazing experiences, and I am grateful to everyone who has supported me along the way and helped me reach this point.

Contents

List of Figures

List of Tables

List of Acronyms

ACI	average of the control inputs cost function
AFDE	average absolute formation distance error
AFE	average of the formation errors cost function
BLF	barrier Lyapunov function
LMI	linear matrix inequality
MIR	minimally and infinitesimally rigid
NN	neural networks
RBF	radial basis function
RBFNN	radial basis function neural networks
RISE	robust integral of the sign of the error
SGUUB	semi-global uniformly ultimately bounded
UAV	unmanned aerial vehicles
UGV	unmanned ground vehicles
UUB	uniformly ultimately bounded

List of Publications

[C1]. K. Aryankia and R. R. Selmic, “Formation Control and Target Tracking for a Class of Nonlinear Multi-Agent Systems Using Neural Networks,” *2020 European Control Conference (ECC)*, 2020, pp. 160-165, doi: 10.23919/ECC51009.2020.9143930.

[J1, C2]. K. Aryankia and R. R. Selmic, “Neuro-Adaptive Formation Control and Target Tracking for Nonlinear Multi-Agent Systems With Time-Delay,” in *IEEE Control Systems Letters*, vol. 5, no. 3, pp. 791-796, July 2021, doi: 10.1109/LCSYS.2020.3006187, presented at *59th IEEE Conference on Decision and Control (CDC)*, Jeju Island, Republic of Korea.

[J2]. K. Aryankia and R. R. Selmic, “Neural Network-Based Formation Control With Target Tracking for Second-Order Nonlinear Multiagent Systems,” in *IEEE Transactions on Aerospace and Electronic Systems*, vol. 58, no. 1, pp. 328-341, Feb. 2022, doi: 10.1109/TAES.2021.3111719.

[J3, C3]. K. Aryankia and R. R. Selmic, “Spectral Properties of the Normalized Rigidity Matrix for Triangular Formations,” in *IEEE Control Systems Letters*, vol. 6, pp. 1154-1159, 2022, doi: 10.1109/LCSYS.2021.3089136, presented at *60th IEEE Conference on Decision and Control (CDC)*, Austin, Texas, USA.

[C4]. K. Aryankia and R. R. Selmic, “Formation Control for a Class of Nonlinear Multi-Agent Systems Using Three-Layer Neural Networks,” *Proc. 2023 American Control Conference (ACC)*, San Diego, California, June 2023 (To appear).

[J4]. K. Aryankia and R. R. Selmic, “Robust Adaptive Leader-Following Formation Control of Nonlinear Multi-Agents Using Three-Layer Neural Networks,” *submitted to IEEE Transactions on Cybernetics*, January 2023.

[J5]. K. Aryankia and R. R. Selmic, “Neuro-Adaptive Formation Control of Nonlinear Multi-Agent Systems With Communication Delays,” *submitted to Journal of Intelligent & Robotic Systems*, March 2023.

Chapter 1

Introduction

Multi-agent systems have gained increasing attention recently. The inspiration for formation control stems from group behaviors of animals in nature, e.g., a flock of birds, a school of fish, and colonies of bees. There are various formation control applications, such as guidance and navigation of autonomous unmanned aerial vehicles (UAV) deployed to perform surveillance, exploration, and search and rescue missions. The general categorization of formation control is based on sensing capability and interaction among the agents and includes position-based control, displacement-based control, and distance-based control [1, 2]. Some studies in the literature still do not fit in these classifications, such as containment control and cyclic pursuit [2].

1.1 Motivation

The formation control has been motivated by group behaviors in nature, for instance, the flock of birds. The V-shaped formation helps a flock of birds during their migrations as they save their fuel and energy. Birds flying in a V-shaped formation benefit from the air currents generated by the leading bird, with each bird following behind experiencing less air resistance and saving energy. This reduced air resistance helps to reduce fatigue during extended flights. In addition to this, birds in the V-formation are able to work together and navigate by following the path of the lead bird and adapting their own flight accordingly [3]. By ”riding wakes” - the air currents created by the flapping wings of the birds ahead - they are able to conserve energy and maintain their position in

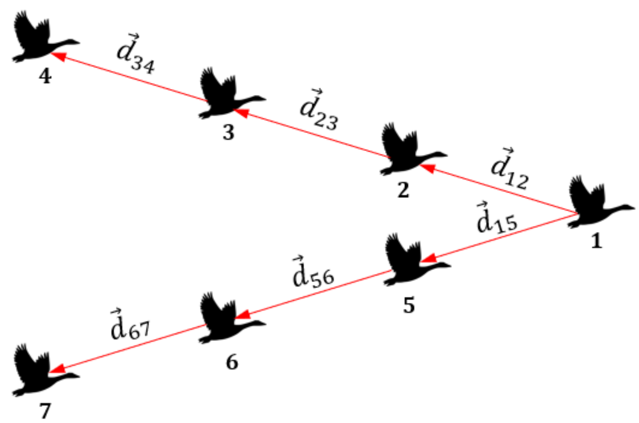

Figure 1.1: Flock of birds flying in a V-shape pattern.

the formation. This allows them to travel greater distances with less effort, making their migration journeys more efficient [4].

Also, the formation makes their seasonal movements easier as they follow the leader [5,6]. The formation control can also be observed in air patrols or groups of autonomous vehicles deployed to perform reconnaissance [7].

The advantages in both cases is clear – reduced energy expenditure or better fuel efficiency and quicker harvesting or data collection. These enable humans and machines to "behave" more efficiently, effectively, and intelligently [8,9]. The applications of formation control in multi-agent systems are not limited to the cases mentioned earlier. Multi-agent systems have also been employed to optimize the number of satellites required in the sky and to make the gathered information of area coverage productive, as well as to allocate resources [9, 10].

1.2 Categorization of Formation Control

In the literature, various varieties for the formation control problem can be categorized into position-based, distance-based, and displacement-based control techniques. Also, there are other terms in the literature, such as shape-producing, consensus, leader-follower, etc.

In a position-based formation control, each agent senses its position in the global coordinate system and moves towards the desired position (formation). In the displacement-based method, the agents control their relative positions with respect to their neighboring agents to achieve the desired

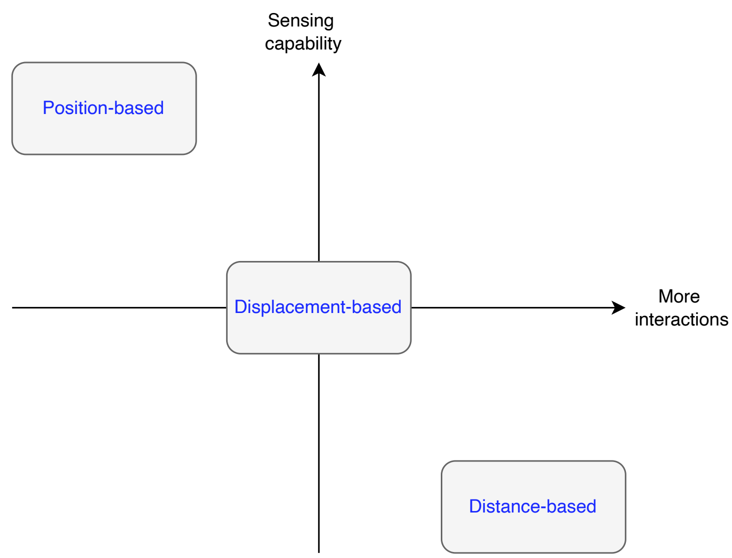

Figure 1.2: Characterization of different formation control methods (source: [2]).

formation. The agents access their neighbors' relative positions with respect to the global coordinate system. In distance-based formation control, agents control inter-agent distances to form the desired formation. The agents sense the relative positions of their neighboring agents and use their local coordinate system to reach desired formation [2, 11]. The relation between the required amount of interactions among agents and the sensing capability for each method is illustrated in Figure 1.2.

1.3 Contributions

In this section, the brief contribution of each chapter is given. More details about each contribution can be found in the chapters that follow.

In this dissertation, we first provide a contribution to the rigid graph theory. We use the normalized rigidity matrix and establish the upper bound of the singular value of minimally and infinitesimally rigid (MIR) graphs in 2D and 2D spaces. Then, we focus on a rigid graph of three vertices and prove that the maximum smallest singular value of a normalized rigidity matrix for a rigid graph with three vertices in 2D space is equal to $\sqrt{\frac{3}{2}}$. Furthermore, the necessary and sufficient conditions for triangular formations to reach this limit value are established.

Moreover, we derive two essential lemmas about three-layer NN and use them to design a control law later in this dissertation.

We develop a controller using backstepping and RBFNN for nonlinear, multi-agent systems in the presence of disturbance to address distance-based formation and target tracking problems. Compared with existing distance-based formation control methods, which considered single- or double-integrator dynamics for agents, the novelty is to consider second-order nonlinear systems with unknown nonlinearity and disturbance. We also provide a rigorous Lyapunov stability analysis for the formation control and target tracking for such a system. We also do not use the Laplacian matrix to model relations among the agents and apply the rigid graph theory.

Second, we extend the results and consider nonlinear multi-agent systems with state time delay. Established results about the normalized rigidity matrix are used to address the formation control problem and target tracking of second-order nonlinear multi-agent systems. This study is the first contribution proposing a formation control using inter-agent distance for nonlinear multi-agent systems with state time delay and disturbance. Compared with the existing methods, we use the rigid graph theory instead of graph Laplacian and design the neuro-adaptive controller using the backstepping technique to address the formation control problem of nonlinear multi-agent systems.

Moreover, using a tunable three-layer NN and robust integral of the sign of the error (RISE) feedback, the leader-following formation control problem of second-order, nonlinear multi-agent systems is addressed. We consider the leader connected to at least one of the other agents. The novelty is that the desired trajectory signals (information from the leader) are not fed into the first layer of the NN. The effects of the leader dynamics and unknown disturbances in the tracking error of each agent are ameliorated by the RISE feedback controller. Unlike commonly-used NN, we determine the number of neurons in each layer and derive the tuning laws for the NN weights matrices. The semi-global, asymptotic, leader-following performance is proved rigorously using a Lyapunov stability theorem.

Finally, we focus on formation control with constant communication delays for second-order, uncertain, nonlinear multi-agent systems with nonsymmetric control gain matrix and unknown control direction. The novelty is that the method does not require the existence or solvability of linear matrix inequalities (LMIs). Moreover, we address the unknown control direction in the presence of the time-invariant communication delay. Compared with existing results, we also consider a three-layer NN to approximate the nonlinearity in closed-loop systems with a predetermined number of neurons in each layer. Only the last layer of the neural network is tuned to improve the online computational burden. Moreover, we use the barrier Lyapunov function to prove the stability of the closed-loop system and prove that the leader-following formation control of second-order, nonlinear multi-agent systems with communication delay is semi-globally uniformly ultimately bounded (SGUUB).

1.4 Thesis Overview

This thesis is organized as follows:

- In Chapter 2, the related notation and preliminaries, as well as the basic graph theory basic, the neural networks, and Nussbaum functions are presented.

- In Chapter 3, the spectral properties of the normalized rigidity matrix for an infinitesimally and minimally rigid graph in two- and three-dimensional spaces are given. For a rigid graph of three vertices, the maximum smallest singular value of the normalized rigidity matrix is given. The results of this Chapter have been published in [J3, C3].

- In Chapter 4, with a backstepping technique and radial basis function neural network, distance-based formation control and target tracking for input-affine, second-order, nonlinear multi-agent systems in the presence of disturbance using rigid graph theory are addressed. The results of this Chapter have been published in [J2, C1].

- In Chapter 5, for nonlinear multi-agent systems with bounded time delay and disturbance, an adaptive neural network-based backstepping controller that uses the normalized rigidity matrix is proposed to address the distance-based formation control problem and target tracking problem. The results of this Chapter have been published in [J1, C2].

- In Chapter 6, using RISE feedback and a three-tunable-layer NN, the leader-following formation control of heterogeneous, second-order, uncertain, input-affine, nonlinear multi-agent systems is addressed when a directed graph models the interactions among the agents. The results of this Chapter appeared in [J4, C4].

- In Chapter 7, using a Nussbaum function, the leader-following formation control problem of second-order, uncertain, nonlinear multi-agent systems with constant communication delays is addressed. The multi-agent systems are considered to have asymmetric control and unknown control direction. The results of this Chapter appeared in [J5].

- In Chapter 8, the conclusion, limitations of each proposed method, and future works are given.

Chapter 2

Background and Related Works

2.1 Introduction

In this chapter, the related notation and preliminaries used in this manuscript are given. The formation control problem is briefly introduced, and the basic graph theory is covered. The definition of the normalized rigidity matrix is provided, and the necessary background and established results on the neural networks are presented.

2.1.1 Notations and Preliminaries

The notations that are used in the report are given here. Let $\mathbb{R}^n$ indicate n-dimensional Euclidean space and $\mathbb{R}^{n\times m}$ denotes the set of $n \times m$ real matrices. Let $\mathbb{I}_n$ denotes $n \times n$ identity matrix and $\mathbf{1}_N = [1, ..., 1]^T$ is $N \times 1$ vector of ones. With $diag(a_1, a_2, ...)$, we denote a block diagonal matrix with diagonal elements of a_i. The notation $vec(.)$ represents a stacked vector of a matrix column-wise. Let $tr(A)$ denote the sum of diagonal terms of matrix A and let $\otimes$ denote the Kronecker product. With A^T, we denote the transpose of a matrix A. Also, by $\|.\|$, we denote the Euclidean norm and $||.||_F$, denotes Frobenius norm where for any matrix A, $||A||_F = \sqrt{tr(A^T A)}$. For any vector $x \in \mathbb{R}^n$, the Manhattan norm is $||x||_1 = \sum_{i=1}^{n} |x_i|$. The notation $\lambda_i(A)$ indicates i-th eigenvalue of matrix A, and with $\bar{\lambda}(A)$, and $\underline{\lambda}(A)$, we denote maximum and minimum eigenvalue of matrix A, respectively. Also, with $\underline{\sigma}(A)$ and $\bar{\sigma}(A)$, we denote the maximum (largest) and minimum (smallest) singular value of matrix A, respectively. The signum function is denoted by $sgn(.)$. The notation $\bigcap\limits_{\mu(H)=0}$ denotes the intersection over all sets H of Lebesgue measure zero, and $\overline{co}$ denotes the convex closure. With $\mathcal{F}(s) = \mathcal{L}[f(t)]$, we denote the Laplace transform of $f(t)$ and its inverse by $f(t) = \mathcal{L}^{-1}[\mathcal{F}(s)]$.

2.2 Formation Control Problem

A formation control problem [2] can be described as follows. Consider a set of N agents described by

$$\begin{aligned} \dot{x_i} &= f_i(x_i, u_i), \\ z_i &= h_i(x_i), \end{aligned} \tag{2.1}$$

where $x_i \in \mathbb{R}^{n_i}$, $u_i \in \mathbb{R}^{m_i}$, and $z_i \in \mathbb{R}^d$, $i = 1, ..., N$ denote the state, input and output of the agent, respectively; n, m, and d are dimensions of state, input, and output, respectively. Also, $f_i : \mathbb{R}^{n_i} \times \mathbb{R}^{m_i} \to \mathbb{R}^{n_i}$, and $h_i : \mathbb{R}^{n_i} \to \mathbb{R}^d$. Defining a variable $\mathbf{z}$ as the output vector $\mathbf{z} = [z_1^T, ..., z_N^T]^T \in \mathbb{R}^{dN}$, where a desired formation [2], is described by a set of M-constraints

$$F(\mathbf{z}) = F(\mathbf{z}^*), \tag{2.2}$$

where $F : \mathbb{R}^{dN} \to \mathbb{R}^M$, for some given $\mathbf{z}^* \in \mathbb{R}^{dN}$. The main goal in a general formation control problem described by a set of N agents as (2.1), is to design a control law $u_i, i = 1, ..., N$ such that the set

$$E_{\mathbf{z}^*} = \Big\{\mathbf{x} |\ F(\mathbf{z}) = F(\mathbf{z}^*)\Big\}, \tag{2.3}$$

becomes asymptotically stable under the control law, where $\mathbf{x} = [x_1^T, ..., x_N^T]^T$ [2].

In formation control problem, position-based, displacement-based, and distance-based approaches can be defined through the given problem formulation (2.3) as follows: [2]:

- In the position-based approach, each agent has access to its information in a global coordinate. The constraint (2.2) is defined as

$$F(\mathbf{z}) := \mathbf{z} = F(\mathbf{z}^*), \tag{2.4}$$

where each agent controls z_i.

- In the displacement-based approach, although the measurements do not contain the absolute states like the position-based method, it is assumed that agents access relative states that are sensed in a global coordinate system. Also, the constraint (2.2) is defined as

$$F(\mathbf{z}) := [...(z_j - z_i)^T...]^T = F(\mathbf{z}^*), \tag{2.5}$$

  where each agent i controls $(z_j - z_i)$ and j denotes its neighboring agent.

- In the distance-based approach, it is assumed that measurements y_i contain only relative variables sensed in the local coordinate system. Unlike position-based and displacement-based methods, agents do not have access to any absolute or relative variables information in the global coordinates system. The constraint (2.2) for this method is defined as

$$F(\mathbf{z}) := [...||z_j - z_i||...]^T = F(\mathbf{z}^*), \tag{2.6}$$

  where each agent actively controls $||z_j - z_i||$.

Note that the consensus problem can be generally considered as a specific form of formation control where $\mathbf{z}^* = 0$ and $F(\mathbf{z}) := [...(z_j - z_i)^T...]^T$ for $i, j = 1, ..., N$.

2.3 Graph Theory

The relation among agents is described by an undirected graph that is denoted by $G = (V, E)$, with $V = \{v_1, ..., v_N\}$ set of vertices and $E \subset V \times V$ set of edges. With $|V| = N$ and $|E|$ we indicate the number of vertices and edges, respectively. We assume the graph is simple, i.e., without repeated edges and no self-loops. Adjacency, or connectivity matrix is $A = [a_{ij}]$ with $a_{ij} > 0$, if $(v_j, v_i) \in E$, and $a_{ij} = 0$, otherwise. Note that we consider $a_{ii} = 0$.

Let us define an in-degree matrix $D = diag(deg_i)$, with $deg_i = \sum_{j \in N_i} a_{ij}$, as the sum of incoming edges weights to the vertex i. The graph Laplacian is $L = D - A$, where the sum of all rows equals zero.

The leader adjacency matrix is defined as $B = diag(b_1, ...b_N)$, with $b_i > 0$, if the leader sends its information to the i-th agent, and $b_i = 0$, otherwise. It is assumed that the leader is connected to at least one agent.

Lemma 2.1 ([12]). *The directed graph G is strongly connected if and only if its Laplacian matrix is irreducible.*

Definition 2.1 ([13, 14]). *A square matrix $P \in \mathbb{R}^{N\times N}$ is said to be a non-singular M-matrix, if it is positive definite, and the off-diagonal elements have non-positive values.*

We present a lemma that extends the results of [15, Lemma 2] and offers greater flexibility by considering a connected graph instead of a strongly connected graph. This lemma is utilized later in this dissertation.

Lemma 2.2 ([16]). *Let the directed graph $G = (V, E)$ be strongly connected. If the leader is connected to at least one of the agents, then $L + B$ is a non-singular M-matrix, and the following inequality holds*

$$\Pi \triangleq P(L + B) + (L + B)^T P > 0, \tag{2.7}$$

where $P = diag(p_i) \triangleq diag(1/q_i)$ is a positive definite matrix and $\mathbf{q} \triangleq (L + B)^{-1}\mathbf{1}_N$, with $\mathbf{q} = [q_1, ..., q_N]^T$.

A pair of $F = (G, p)$ is known as a framework, where $p = (p_1, ..., p_N)$ and $p_i \in \mathbb{R}^d$, $d \in \{2, 3\}$ is the position of vertex i in 2- or 3-dimensional space. Related to any arbitrary ordering of edges in E, let us define the edge function of $\phi : \mathbb{R}^{dN} \to \mathbb{R}^{|E|}$ as follows:

$$\phi_G(p) = (..., ||p_i - p_j||^2, ...), (i, j) \in E, \tag{2.8}$$

where $||.||$ denotes the Euclidean norm. The rigidity matrix $R_p : \mathbb{R}^{dN} \to \mathbb{R}^{|E|\times dN}$ for the framework (G, p) is defined as

$$R_p = \tfrac{1}{2}\tfrac{\partial\phi_G(p)}{\partial p}. \tag{2.9}$$

For instance, consider an undirected graph shown in Figure 2.1. The corresponding rigidity

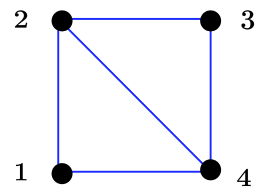

Figure 2.1: Graph model of a system with four agents.

matrix R_p is given by

$$R_p = \begin{bmatrix} p_{12}^T & p_{21}^T & 0 & 0 \\ 0 & p_{23}^T & p_{32}^T & 0 \\ 0 & p_{24}^T & 0 & p_{42}^T \\ p_{14}^T & 0 & 0 & p_{41}^T \\ 0 & 0 & p_{34}^T & p_{43}^T \end{bmatrix}, \tag{2.10}$$

where $p_{ij}^T = p_i^T - p_j^T = [x_i - x_j, y_i - y_j]$, and x_i, y_i denote coordinates of the vertex i. Without the loss of generality, the rigidity matrix can also be defined in 3D [7].

Lemma 2.3 ([17])**.** *Let a framework (G, p) be given in 2D. For any vector $v_r \in R^2$, an N-size vector of ones denoted by $\mathbf{1}_N$, and an $|E|$-size vector of zeros denoted by $\boldsymbol{0}_{|E|}$, the following identity holds*

$$R_p(\mathbf{1}_N \otimes v_r) = \boldsymbol{0}_{|E|}, \tag{2.11}$$

where R_p is the corresponding rigidity matrix.

Two frameworks (G, p) and (G, h) are equivalent, if $\phi_G(p) = \phi_G(h)$, and congruent if $||p_i - p_j|| = ||h_i - h_j||$ for all $i, j \in V$, [18, 19]. Two noncongruent equivalent frameworks are called ambiguous. Figure 2.2 shows that the flip ambiguity of vertex 4 causes the framework to be non-congruent.

Definition 2.2 ([20])**.** *Consider two frameworks $F = (G, p)$ and $F_1 = (G_1, q)$. These two frameworks, with $G = (V, E)$ and $G_1 = (V_1, E_1)$, are said to be isomorphic if they have similar vertex and edge sets where there exists a bijection $f_1 : V \to V_1$ such that $v_i v_j \in E$ if and only if $f_1(v_i) f_1(v_j) \in E_1$.*

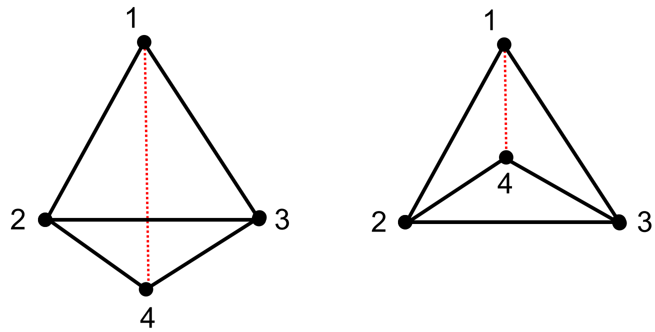

Figure 2.2: Noncongruent framework due to flip ambiguity of vertex 4.

Isomorphic frameworks to a framework F are denoted by Iso(F) [21]. For a framework of F, the notation Amb(F) denotes the set of all ambiguities [21].

The number of edges is important in determining the rigidity of a formation, as well as the distribution of the edges among the graph vertices. Laman's theorem relates rigidity and the number of edges and vertices in 2D.

Theorem 2.1 ([22])**.** *An undirected graph $G(V, E)$ in 2D is rigid, if and only if there exists a subgraph $G_1 = (V, E_1)$ where $E_1 \subset E$ with $|E_1| = 2|V| - 3$ such that for any $V_1 \subset V$, the associated induced subgraph $G_2 = (V_1, E_2)$ of G_1 with $E_2 \subset E_1$, satisfies $|E_2| \leq 2|V_1| - 3$.*

A graph is flexible if it is not rigid [23]. Based on Theorem 2.1, one can conclude that a triangle in 2D is rigid.

Definition 2.3 ([20])**.** *A graph is said to be minimally rigid if it is rigid but does not remain rigid after the removal of an edge.*

A minimally rigid graph in 2D and 3D satisfies $|E| = 2N - 3$ and $|E| = 3N - 6$, respectively [24].

Corollary 2.1 ([23, 25])**.** *A framework with N vertices ($N > 2$) in 2D and 3D is infinitesimally rigid, if and only if $rank(R_p) = 2N - 3$ and $rank(R_p) = 3N - 6$, respectively.*

Lemma 2.4 ([7])**.** *Let the framework (G, p) be MIR in d-dimensional ($d \in \{2, 3\}$), then $R_p R_p^T$ is invertible.*

Definition 2.4. *The neighborhood N_i of the vertex v_i is the set of all edges adjacent to v_i:*

$$N_i = \{v_j \in V |\, v_i v_j \in E\}. \tag{2.12}$$

2.3.1 Normalized Rigidity Matrix

Let us define the normalized rigidity matrix, $\bar{R}_p$, as follows.

Definition 2.5 ([26]). *A normalized rigidity is obtained by row normalization of the rigidity matrix by the length of the corresponding edges.*

For instance, consider an undirected graph shown in Figure 2.1. The corresponding normalized rigidity matrix $\bar{R}_p$ is given by

$$\bar{R}_p = \begin{bmatrix} \frac{p_{12}^T}{\|p_{12}^T\|} & \frac{p_{21}^T}{\|p_{21}^T\|} & 0 & 0 \\ 0 & \frac{p_{23}^T}{\|p_{23}^T\|} & \frac{p_{32}^T}{\|p_{32}^T\|} & 0 \\ 0 & \frac{p_{24}^T}{\|p_{24}^T\|} & 0 & \frac{p_{42}^T}{\|p_{42}^T\|} \\ \frac{p_{14}^T}{\|p_{14}^T\|} & 0 & 0 & \frac{p_{41}^T}{\|p_{41}^T\|} \\ 0 & 0 & \frac{p_{34}^T}{\|p_{34}^T\|} & \frac{p_{43}^T}{\|p_{43}^T\|} \end{bmatrix}, \tag{2.13}$$

As row operations would not affect the rank of a matrixwe can also define the MIR graph based on the normalized rigidity matrix.

2.4 Neural Networks (NN)

2.4.1 Radial Basis Function Neural Networks (RBFNN)

We use an NN to compensate for the unknown nonlinearity in the system. Additional details on NNs can be found in [27, 28]. We assume that the unknown nonlinearity in system dynamics ($f(z) \in \mathbb{R}^m$) is smooth; therefore, it can be approximated on a compact set Ω as:

$$f(z) = W^T \varphi(z) + \epsilon(z), \tag{2.14}$$

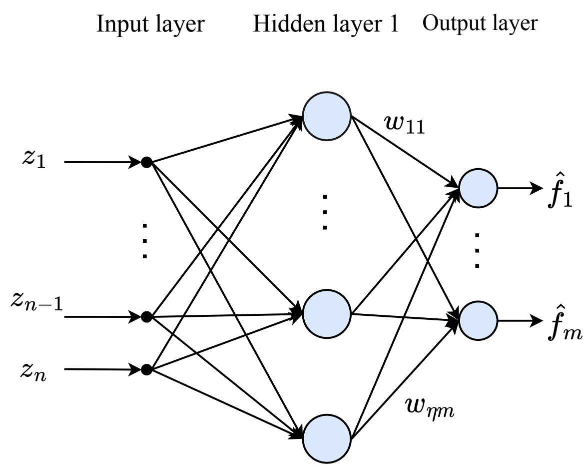

Figure 2.3: Radial basis function neural network architecture.

where $z \in \Omega \subset \mathbb{R}^n$, and $\varphi(z) \in \mathbb{R}^\eta$ is a known smooth function, η is the number of neurons, $W \in \mathbb{R}^{\eta \times m}$ is a set of unknown NN weights, and ϵ is an approximation error [29, 30].

The architecture of the RBFNN is shown in Figure 2.3. The estimation, $\hat{f}$ using RBFNN, is given by

$$\hat{f} = \hat{W}^T \varphi(z), \tag{2.15}$$

where $\hat{W}$ is the tunable NN weights matrix, and $\varphi(z) = [\varphi_1(z), \varphi_2(z), ..., \varphi_\eta(z)]^T$. The activation function $\varphi_i(z)$ is selected as

$$\varphi_i(z) = \exp[\tfrac{-(z-\mu_i)^T(z-\mu_i)}{\Phi_i^2}], \tag{2.16}$$

and $\mu_i = [\mu_{i1}, ..., \mu_{in}]^T \in \mathbb{R}^n$ is the center of the activation function, and Φ_i is the width of the Gaussian function.

Assumption 2.1. *The unknown, ideal NN weights matrix is bounded by $||W||_F \leq W_M$, with a fixed bound W_M.*

Assumption 2.2. *The NN approximation error $\epsilon(z)$ over a compact set Ω is bounded by $||\epsilon_i(z)|| \leq \epsilon_M$.*

Remark 2.1. *Consider the nonlinear function $f(z)$ in be smooth and defined on a compact set of Ω. Since f is a smooth function and Weierstrass high order approximation theorem can be applied, there exists a sufficient number of neurons such that NN approximation error ϵ is bounded by a fixed*

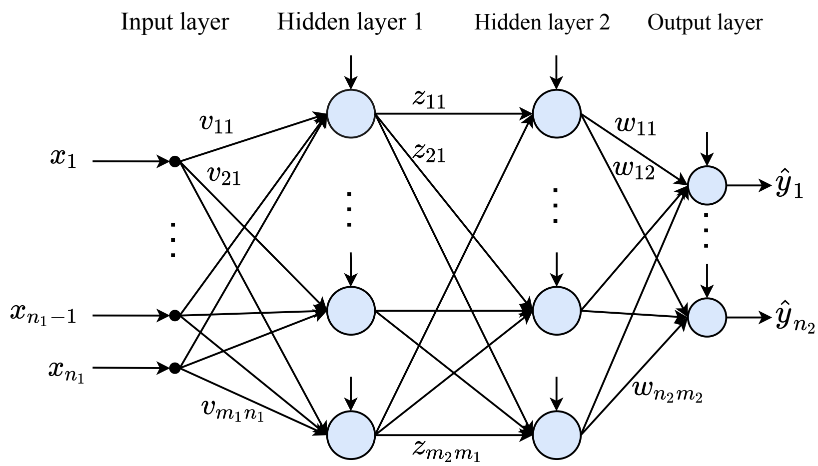

Figure 2.4: Three-layer neural network architecture.

bound $||\epsilon|| \leq \epsilon_M$ *[27, 29].*

2.4.2 Three-Layer Neural Networks

Based on the universal approximation theorem, for a smooth nonlinear function of $y(\mathcal{X})$, over a compact set of $\Omega_{\mathcal{X}}$, there exists a three-layer NN [30], such that

$$y(\mathcal{X}) = W^T \sigma_1(Z^T \sigma_2(V^T \mathcal{X})) + \epsilon, \tag{2.17}$$

where V, Z, and W are ideal NN weights matrices, σ_1 and σ_2 are the activation functions, and ϵ is the NN approximation error. We establish some standard assumptions to estimate the nonlinearity [14, 27, 31].

Assumption 2.3. *The unknown ideal neural network weights matrices V, Z, and W are bounded with fixed bounds such that*

$$\begin{aligned} ||V||_F &\leq V_m, \\ ||Z||_F &\leq Z_m, \\ ||W||_F &\leq W_m. \end{aligned} \tag{2.18}$$

Assumption 2.4. *For the vector $\mathcal{X} \in \mathcal{L}_\infty$, the approximation error ϵ, and its first and second time derivatives are bounded with a fixed bound.*

In this section, we introduce a three-layer NN, as shown in Figure 2.4, to approximate an unknown nonlinear function over a compact set $\Omega_{\mathcal{X}}$. The first hidden layer has m_1 neurons and the second hidden layer has m_2 neurons. Considering $\hat{y} = [\hat{y}_1, ..., \hat{y}_{n_2}]^T \in \mathbb{R}^{n_2}$, the output of NN (Figure 2.4) can be written as

$$\hat{y} = \hat{W}^T \sigma_1(\hat{Z}^T \sigma_2(\hat{V}^T \mathcal{X})), \tag{2.19}$$

where $\mathcal{X} = [1, \bar{\mathcal{X}}^T]^T \in \mathbb{R}^{n_1+1}$ with $\bar{\mathcal{X}} = [x_1, ..., x_{n_1}]^T \in \mathbb{R}^{n_1}$, the NN weights matrices $\hat{V} \in \mathbb{R}^{(n_1+1)\times m_1}$, $\hat{Z} \in \mathbb{R}^{(m_1+1)\times m_2}$, and $\hat{W} \in \mathbb{R}^{(m_2+1)\times n_2}$. We use $\sigma_1(.) \in \mathbb{R}^{m_2+1}$ and $\sigma_2(.) \in \mathbb{R}^{m_1+1}$ to denote the activation functions of hidden layers. We consider the sigmoid function for both hidden layers, i.e., for a scalar s_i, one has $\sigma_k(s_i) = \frac{1}{1+e^{-s_i}}$ for $k \in \{1, 2\}$. The activation function of the output layer is considered to be linear. The ideal NN weights matrices V, Z, and W are defined as follows:

$$V, Z, W = \arg\min_{\hat{V},\hat{Z},\hat{W}} \left\{ \sup_{\mathcal{X}\in\Omega_{\mathcal{X}}} ||y(\mathcal{X}) - \hat{y}(\mathcal{X})|| \right\}. \tag{2.20}$$

Remark 2.2. *For any sufficiently smooth function over a compact set, the Stone-Weierstrass Theorem stipulates that the function can be approximated using enough number of neurons, and the universal approximation property of NN guarantees the boundedness of the approximation error [14, 29, 30, 32].*

2.4.3 Nussbaum Functions

Nussbaum functions were used to estimate the sign of the control gain matrix when the control direction was unknown.

Definition 2.6 ([33, 34])**.** *A function $\mathcal{N}(\zeta)$ is called a Nussbaum function (type A) if the following*

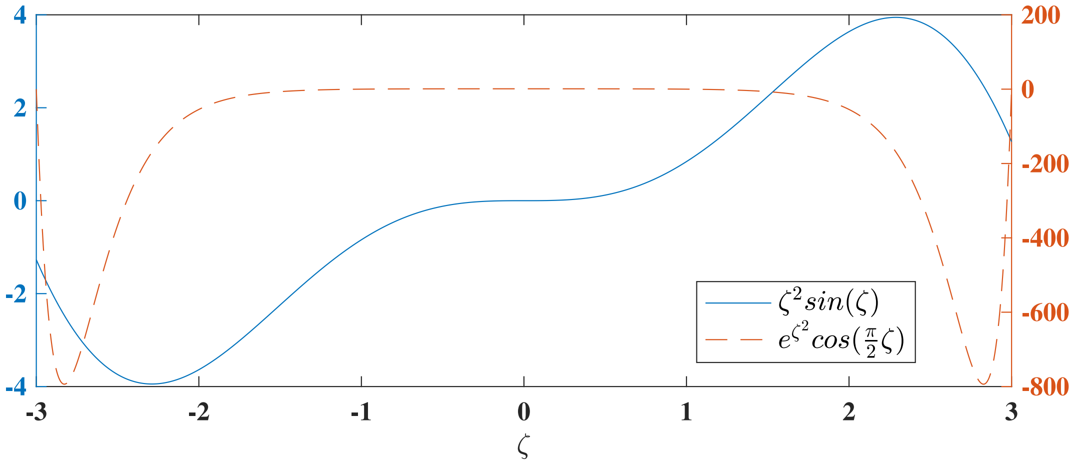

Figure 2.5: Examples of Nussbaum functions $\zeta^2 \sin(\zeta)$ (left y-axis) and $e^{\zeta^2} \cos\left(\frac{\pi}{2}\zeta\right)$ (right y-axis).

properties hold

$$\begin{aligned} \lim_{s\to+\infty} \sup \frac{1}{s}\int_0^s \mathcal{N}(\zeta)d\zeta &= +\infty, \\ \lim_{s\to+\infty} \inf \frac{1}{s}\int_0^s \mathcal{N}(\zeta)d\zeta &= -\infty. \end{aligned} \tag{2.21}$$

Commonly used Nussbaum functions (type A) are $\zeta^2\cos(\zeta), \zeta^2\sin(\zeta)$, and $e^{\zeta^2}\cos\left(\frac{\pi}{2}\zeta\right)$. The Figure 2.5 illustrates $\zeta^2\sin(\zeta)$ and $e^{\zeta^2}\cos\left(\frac{\pi}{2}\zeta\right)$.

Lemma 2.5 ([35]). *Let $V(\cdot)$ and $\zeta(\cdot)$ be smooth functions defined on $[0, t_f)$ with $V(t) \geq 0, \forall t \in [0, t_f)$, and $\mathcal{N}(\zeta)$ be an even smooth Nussbaum function (type A). If the following inequality holds:*

$$V(t) \leq c_0 + \int_0^t (\Gamma(\tau)\mathcal{N}(\zeta) + 1)\dot{\zeta}e^{-c_1(t-\tau)}d\tau, \tag{2.22}$$

where constants $c_0, c_1 > 0$, and $\Gamma(.)$ is a time-varying parameter that takes an unknown value in the closed interval of $\mathcal{I} \triangleq [g^-, g^+]$ with $0 \notin \mathcal{I}$, then $V(t), \zeta(t)$, and $\int_0^t (\Gamma(\tau)\mathcal{N}(\zeta) + 1)\dot{\zeta}d\tau$ must be bounded over $[0, t_f)$.

A reader may refer to [34], where the Nussbaum Functions type B-L were introduced, and a lemma similar to the Lemma 2.5 was proven for them. We use $\mathcal{N}(\zeta) = \zeta^2\cos(\frac{\pi}{2}\zeta)$ for the purpose of this thesis.

Chapter 3

Spectral Properties of the Normalized Rigidity Matrix for Triangular Formations

3.1 Introduction

In this chapter, we provide an explanation of the normalized rigidity matrix and analyze its singular values. Additionally, we present an upper limit for the smallest and largest singular values of the normalized rigidity matrix in both two-dimensional and three-dimensional spaces. We also discuss the maximum smallest singular value of a normalized rigidity matrix for a rigid graph with three vertices in 2D space, along with the necessary and sufficient conditions to achieve this value.

3.1.1 Related Works on Normalized Rigidity Matrix

The rigidity can be used as a fundamental characteristic of a graph that models sensing and communication topologies to achieve distance-based formation [36].

The relation between graph connectivity and its rigidity is studied in [37], where a necessary condition relates connectivity to rigidity. Related to our work, authors in [36] defined a symmetric rigidity matrix and its eigenvalues. The normalized rigidity matrix was first introduced in [26], where it was used to design the controller for single- and double-integrator multi-agent systems. The normalized rigidity matrix is a specific representation of the weighted rigidity matrix [36]. Authors in [36] addressed the formation rigidity of a multi-agent system, while this chapter focuses on the normalized rigidity matrix and establishes the properties of this matrix.

A triangular formation modeled by an undirected graph with three edges is a connected and rigid graph. The Laplacian matrix for any triangular formation always provides position-invariant algebraic connectivity. However, the advantage of the rigid graph theory is that it offers a different normalized rigidity matrix and smallest singular value for different triangular formations in two-dimensional (2D).

We study MIR graphs and provide specific spectral properties for triangular formations. We present a normalized rigidity matrix and its singular values. Moreover, we prove specific properties of the normalized rigidity matrix. Also, for a framework in 2D or 3D spaces, we provide upper bounds for the smallest and largest singular values of the normalized rigidity matrix. We show that the transformation of a framework in 2D and 3D spaces does not affect the rigidity matrix properties.

The proposed results can be exploited to design controllers based on eigenvalues and eigenvectors of the normalized rigidity matrix. Similar to [38], one can develop a practical, fully distributed controller based on the eigenvalue and eigenvector of the symmetric rigidity matrix to achieve the desired formation while maintaining the framework rigidity. Also, the proposed theoretical results can be used for future stability analyses of distance-based formation control and the selection of controller parameters.

We describe the normalized rigidity matrix and its singular values. We study the minimally rigid graphs from a spectral graph theory perspective. We also provide an upper bound of the normalized rigidity matrix's smallest and largest singular values in 2D and 3D spaces.

Although the Laplacian matrix does not provide any information about the formation of a framework, we seek to extract some information from the normalized rigidity matrix. We also show that the transformation of a framework on 2D and 3D spaces not affect this matrix's properties. The main contribution is to show and prove the maximum smallest singular value for a rigid graph with three vertices in 2D space and to provide the necessary and sufficient conditions for it. These results can be used in future stability analyses of distance-based formation control and formation control design in general.

The main contributions here are: (i) The maximum smallest singular value of a normalized rigidity matrix for a rigid graph with three vertices in 2D space is proved to be equal to $\sqrt{3/2}$. (ii) The necessary and sufficient conditions for triangular formations to reach this limit value are established.

3.2 Preliminaries on Normalized Rigidity Matrix

Consider the definition of the normalized rigidity matrix ($\bar{R}_P$) in Section 2.3.1. Then, the following lemmas are valid.

Lemma 3.1. *For a MIR graph in 2D and 3D, the matrix $\bar{R}_P$ is a full-rank matrix.*

Proof. A MIR graph in 2D and 3D has $(2N-3)$ and $(3N-6)$ edges, respectively. From Corollary 2.1, the rigidity matrix has a rank of $(2N-3)$ and $(3N-6)$ in 2D and 3D for an infinitesimally rigid framework, respectively. Moreover, as the row-normalization does not affect a matrix's rank, then the normalized rigidity matrix is full rank. Thus, the result of Lemma 3.1 holds. □

Lemma 3.2. *For a MIR graph in 2D and 3D, the diagonal elements of $\bar{R}_p\bar{R}_p^T$ are equal to two.*

Proof. Proofs for 2D and 3D cases are similar; hence, we only show proof for 3D. Let $\bar{R}_p(m,:)$ be an arbitrary row in the normalized rigidity matrix as

$$\bar{R}_p(m,:) =[[\mathbf{0}], \bar{R}_{m,3n-2},\ \bar{R}_{m,3n-1}, \bar{R}_{m,3n}, [\mathbf{0}], -\bar{R}_{m,3n-2},\ -\bar{R}_{m,3n-1},\ -\bar{R}_{m,3n}, [\mathbf{0}]], \tag{3.1}$$

with $\bar{R}_{m,3n-2} = (x_{mn})/(\sqrt{x_{mn}^2+y_{mn}^2+z_{mn}^2})$ and $\bar{R}_{m,3n-1} = (y_{mn})/(\sqrt{x_{mn}^2+y_{mn}^2+z_{mn}^2})$ and $\bar{R}_{m,3n} = (z_{mn})/(\sqrt{x_{mn}^2+y_{mn}^2+z_{mn}^2})$ being the consecutive elements of m-th row. Then, it is straightforward to verify that $\bar{R}_p(m,:)\bar{R}_p^T(m,:) = 2$. □

In the following theorem, we establish an upper bound for the smallest singular value of a normalized rigidity matrix.

Theorem 3.1. *Let the desired formation of N agents be modeled by an undirected MIR graph in d-dimensional ($d \in \{2, 3\}$) space. The upper bound of the smallest singular value of the normalized rigidity matrix is $\sqrt{2}$.*

Proof. Proofs for 2D and 3D cases are similar; hence, we only show proof for 3D. Consider a normalized rigidity matrix for a MIR graph with N vertices. The normalized rigidity matrix has $3N - 6$ rows (Corollary 2.1), diagonal terms in the matrix $\bar{R} = \bar{R}_p \bar{R}_p^T$ have a value of two (Lemma 3.2), and $\bar{R}$ is full rank (Lemma 3.1). For any symmetric matrix A, one has $\sum \lambda_i(A) = tr(A)$. Therefore, $\sum \lambda_i(\bar{R}) = 2(3N - 6)$. As $\bar{R}$ is a positive definite, one has $(3N - 6)\underline{\lambda}(\bar{R}) \leq 2(3N - 6)$, which yields to $\underline{\sigma}(\bar{R}_p) \leq \sqrt{2}$. ☐

In the following theorem, we establish an upper bound for the singular values of a normalized rigidity matrix.

Theorem 3.2. *Let the desired formation of $N \geq 3$ agents be modeled by an undirected MIR graph in d-dimensional ($d \in \{2, 3\}$) space. The upper bound of singular values of the normalized rigidity matrix in d-dimensional space is $\sqrt{d}\sqrt{N - 1}$.*

Proof. The diagonal elements of matrix $\bar{R} = \bar{R}_p \bar{R}_p^T$ have a value of *two* in d-dimensional space. Consider any row in matrix $\bar{R}$; the number of off-diagonal terms in matrix $\bar{R}$ in 2D (3D) is $2N - 4$ ($3N - 7$). Using Gershgorin Circle Theorem, it is evident that the largest singular value is upper bounded by $\sqrt{d}\sqrt{N - 1}$. ☐

Lemma 3.3. *A graph $G(V, E)$ is infinitesimally rigid if and only if the normalized rigidity matrix singular values are strictly positive.*

Proof. Similar proof for the weighted rigidity matrix can be found in [36], so we skip the proof here. ☐

The following theorem stipulates that the singular values of the normalized rigidity matrix are transformation-invariant.

Theorem 3.3. *Let the desired formation of N agents be modeled by an undirected MIR graph in d-dimensional ($d \in \{2, 3\}$) space. The smallest singular value of the normalized rigidity matrix is* *invariant under uniform scaling (dilation), translation, and rotation transformations of the framework.*

Proof. The proof considers (i) uniform scaling, (ii) translation, and (iii) rotation.

(i) Uniform scaling: consider any arbitrary element, $\bar{R}_p(m,n)$, of the normalized rigidity matrix. This element can be written as $\bar{R}_p(m,n) = \frac{a}{\sqrt{a^2+b^2+c^2}}$, where a, b, c are constants ($\sqrt{a^2+b^2+c^2}$ cannot be zero, otherwise the rigidity condition is violated). One can see that the uniform scaling of each constant does not change elements of normalized rigidity as well as its smallest singular value.

(ii) Translation: one can see that a framework's shift in any direction does not change the normalized rigidity matrix as each tuple is in the form of $(p_i - p_j)^T$. Thus, the smallest singular value of the normalized rigidity matrix is not affected.

(iii) Rotation: let T_d denote the rotation matrix. The rotation matrix in 2D and 3D is an orthogonal matrix. The normalized rigidity of a rotated framework by an angle θ is expressed by $\bar{R}_\theta$. Let $\bar{R}_p(i,:)$ and $\bar{R}_p(k,:)$ be two arbitrary rows in normalized rigidity matrix

$$\begin{aligned} \bar{R}_p(i,:) &= [[\mathbf{0}], p_{ij}^T, [\mathbf{0}], -p_{ij}^T, [\mathbf{0}]], \\ \bar{R}_p(k,:) &= [[\mathbf{0}], p_{km}^T, [\mathbf{0}], -p_{km}^T, [\mathbf{0}]]. \end{aligned} \tag{3.2}$$

Let $\bar{R}_p(i,:)\bar{R}_p^T(k,:) \triangleq p_{ij}^T p_{kj}$. The i-th and k-th rows for a rotated framework can be written as

$$\begin{aligned} \bar{R}_\theta(i,:) &= [[\mathbf{0}], p_{ij}^T T_d^T, [\mathbf{0}], -p_{ij}^T T_d^T, [\mathbf{0}]], \\ \bar{R}_\theta(k,:) &= [[\mathbf{0}], p_{kj}^T T_d^T, [\mathbf{0}], -p_{km}^T T_d^T, [\mathbf{0}]]. \end{aligned} \tag{3.3}$$

Using the orthogonal property of T_d, one can have $\bar{R}_\theta(i,:)\bar{R}_\theta^T(k,:) = p_{ij}^T p_{kj}$. For the two arbitrary rows, we have $\bar{R}_\theta(i,:)\bar{R}_\theta^T(k,:) = \bar{R}_p(i,:)\bar{R}_p^T(k,:)$; thus, it is valid for the other rows. The inner product of any two rows in the matrix $\bar{R}_\theta$ can have a value of two (diagonal terms), or $zero$, or a value within the interval of $(-1, 1)$, which is identical to inner products of the same rows in the matrix $\bar{R}_p$; consequently, $\bar{R}_\theta \bar{R}_\theta^T = \bar{R}_p \bar{R}_p^T$.

Thus, the singular value of a framework's normalized rigidity matrix is invariant under rotation transformation. □

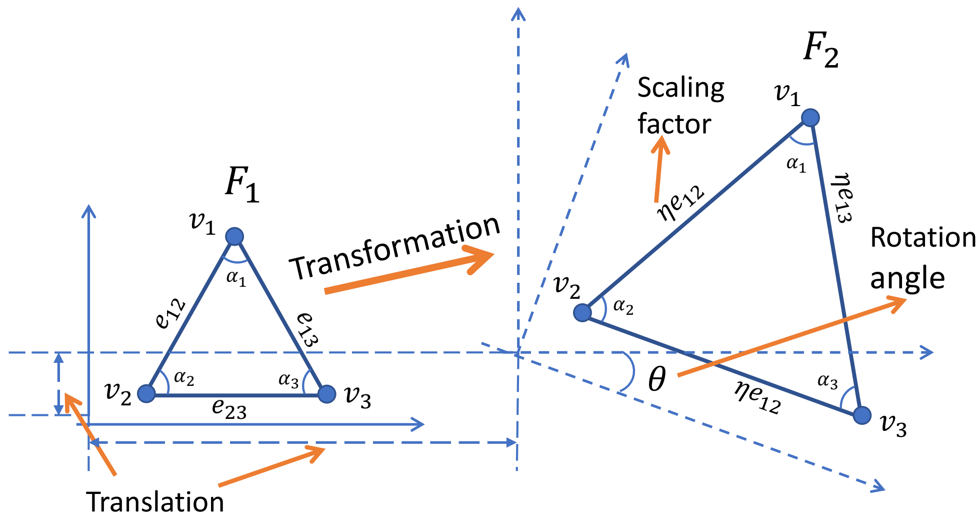

Figure 3.1: The transformation of a MIR framework with three vertices in 2D ($\eta \neq 0$).

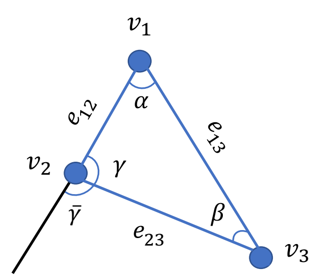

Figure 3.2: A rigid graph of three vertices in 2D.

Corollary 3.1. *For an undirected MIR graph in d-dimensional space where $d \in \{2, 3\}$, a combination of scaling, translation, and rotation does not change the singular value of the normalized rigidity matrix.*

The proof of this Corollary is similar to Theorem 3.1; hence we skip the proof here.

Example 3.1. *This example demonstrates the Corollary 3.1 in 2D. The smallest singular value of a rotated framework (F_2) is the same as the smallest singular value of the normalized rigidity matrix for a MIR graph (F_1) in 2D, as shown in Figure 3.1.*

3.3 Main Results on the Normalized Rigidity Matrix for Triangular Formations

We establish two spectral properties of the normalized rigidity matrix for a rigid triangular formation in 2D: (i) the largest singular value; and (ii) the maximum smallest singular value.

Theorem 3.4. *For a rigid graph of three vertices in 2D, the largest singular value of the normalized rigidity matrix is* $\sqrt{3}$*.*

Proof. We show that (i) one of the eigenvalues of the matrix of $\bar{R}$ has the value of *three*, and (ii) this is the largest eigenvalue of $\bar{R}$. As a result, $\sqrt{3}$ is the largest singular value of the normalized rigidity matrix.

(i) Consider an arbitrary triangular formation shown in Figure 3.2, where α, β, and γ are angles between the edges. From Theorem 3.1, the diagonal elements of $\bar{R}$ have a value of *two*. Moreover, one can show that the off-diagonal elements have absolute values of less than or equal to *one*.

The positive definite matrix $\bar{R} = \bar{R}_p \bar{R}_p^T$ can be written as

$$\bar{R} = \begin{bmatrix} 2 & \frac{p_{12}^T p_{13}}{||p_{12}||\,||p_{13}||} & -\frac{p_{12}^T p_{23}}{||p_{12}||\,||p_{23}||} \\ * & 2 & \frac{p_{13}^T p_{23}}{||p_{13}||\,||p_{23}||} \\ * & * & 2 \end{bmatrix} = \begin{bmatrix} 2 & \cos(\alpha) & -\cos(\bar{\gamma}) \\ * & 2 & \cos(\beta) \\ * & * & 2 \end{bmatrix}. \tag{3.4}$$

As $\bar{R}$ is a symmetric matrix, we only show the upper triangular elements. The eigenvalues of $\bar{R}$ are roots of the following equation

$$(\lambda_i - 2)^3 - (\lambda_i - 2)(a^2 + b^2 + c^2) - 2(abc) = 0, \tag{3.5}$$

where $a = \cos(\alpha)$, $b = -\cos(\bar{\gamma}) = -\cos(\alpha + \beta)$ and $c = \cos(\beta)$. Substitute $\lambda_1 = 3$ in (3.5) and recall that the following is valid

$$1 - (\cos^2(\alpha) + \cos^2(\beta) + \cos^2(\gamma)) - 2\cos(\alpha)\cos(\beta)\cos(\gamma) = 0. \tag{3.6}$$

One can conclude that $\lambda_1 = 3$ is a root of (3.5).

(ii) Here we show that the matrix $\bar{\lambda} I_3 - \bar{R}$ is a positive semi-definite matrix, where $\bar{\lambda}$ is the maximum eigenvalue of $\bar{R}$. Consequently, $\bar{\lambda} = 3$ is the maximum eigenvalue of $\bar{R}$.

One can show that the leading principal minors are either positive or zero, which implies $\bar{\lambda} I_3 - \bar{R}$ to be a positive semi-definite matrix. The matrix $\bar{R}$ is a positive symmetric matrix; therefore, all of the eigenvalues are real and positive. As matrix $\bar{\lambda} I_3 - \bar{R} \geq 0$, there is no eigenvalue of $\bar{R}$ that has a value greater than $\bar{\lambda}$; thus, $\bar{\lambda}$ is the maximum eigenvalue of $\bar{R}$ and $\sqrt{\bar{\lambda}}$ is the largest singular value of the normalized rigidity matrix. $\square$

Remark 3.1. *From Lemma 3.1, one can conclude that the* $rank(\bar{R}) = 3$, $\lambda_1 = 3$, *and* $\sum \lambda_i = 6,\ i = 1, 2, 3$. *Thus, one has* $\lambda_2 + \lambda_3 = 3$, *implying* $\lambda_2 < 3$ *and* $\lambda_3 < 3$. *Thus, the eigenvalue* $\bar{\lambda}$ *is the maximum eigenvalue of the positive definite matrix* $\bar{R}$.

Remark 3.2. *Theorem 3.4 provides the largest singular value of the normalized rigidity matrix for rigid frameworks with three vertices in 2D, while Theorem 3.2 establishes an upper bound.*

The necessary and sufficient conditions to reach the maximum smallest singular values for three vertices in 2D are given next.

Theorem 3.5. *Every rigid framework of three agents in 2D satisfies* $\underline{\sigma}(\bar{R}_p) \leq \sqrt{3/2}$, *with the smallest singular value of the normalized rigidity matrix reaching the limit if and only if the framework is an equilateral triangle.*

Proof. Let us define auxiliary variables $x = \lambda - 2$ and $y = a^2 + b^2 + c^2$. From Theorem 3.4 and (3.6), one can write (3.5) as

$$x^3 - xy + y - 1 = (x - 1)(x^2 + Ax + B), \tag{3.7}$$

where $A = 1$ and $B = 1 - y$. Thus, two other eigenvalues of $\bar{R}$ can be obtained as follows:

$$\lambda_{2,3} = 2 + \frac{-1 \pm \sqrt{4y - 3}}{2}. \tag{3.8}$$

From (3.8), it is evident that the smallest eigenvalue of $\bar{R}$ has a value of less than $\frac{3}{2}$. Therefore, $\sqrt{\frac{3}{2}}$ is an upper bound for the smallest singular value of the normalized rigidity matrix for a rigid

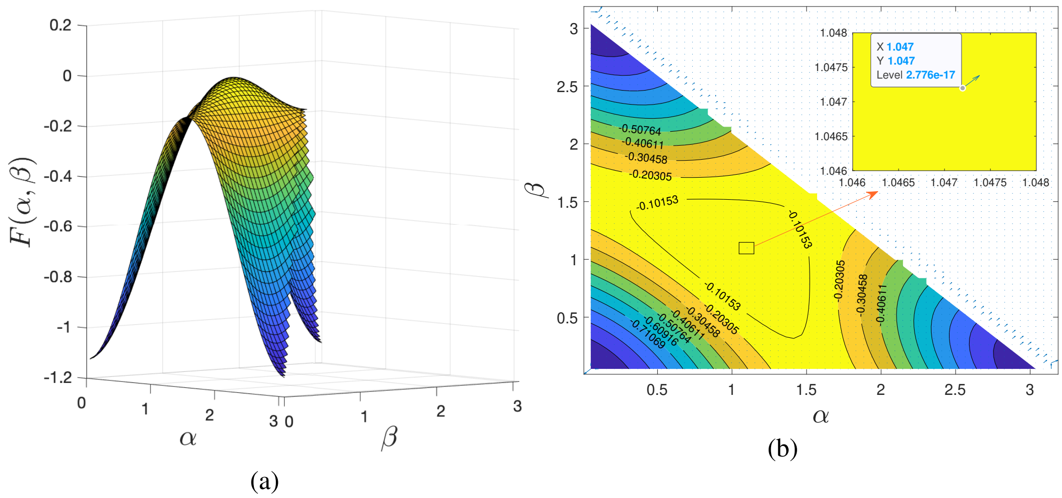

Figure 3.3: (a) Function of $F(\alpha, \beta)$ on $\alpha\beta$-plane; (b) Contour plot and gradient of $F(\alpha, \beta)$ on $\alpha\beta$-plane.

framework with three vertices in 2D. One can show that $\alpha = \beta = \gamma = \frac{\pi}{3}$ yields $y = \frac{3}{4}$, and thus the smallest singular value of $\sqrt{\frac{3}{2}}$ is achieved. As a result, all the edges have the same length. We have shown that for a rigid graph of three vertices (agents) in 2D if the lengths of edges are equal, the maximum smallest singular value of the normalized rigidity matrix is reached. Now we show that the maximum smallest singular value ($\sqrt{\frac{3}{2}}$) of the normalized rigidity matrix of three vertices in 2D is reached only for equilateral triangular frameworks.

Consider Figure 3.3, where eigenvalues of $\bar{R}$ are $\lambda_1 = 3$ and $\lambda_{2,3} = 2 + \frac{-1 \pm \sqrt{4y-3}}{2}$. The maximum smallest singular value of the normalized rigidity matrix implies $y = \frac{3}{4}$. Setting $y = \frac{3}{4}$ implies

$$\cos(\alpha)\cos(\beta)\cos(\gamma) = 1/8. \tag{3.9}$$

Let us write (3.9) in the form

$$f(\alpha, \beta, \gamma) = \cos(\alpha)\cos(\beta)\cos(\gamma) - 1/8. \tag{3.10}$$

Function $f(\alpha, \beta, \gamma)$ achieves its maximum over the set $S = \{\alpha, \beta, \gamma \mid \alpha + \beta + \gamma = \pi\}$, at 0 for $\alpha = \beta = \gamma = \frac{\pi}{3}$. To find the maximum value of the function $f(\alpha, \beta, \gamma)$ over the set S, let us define the Lagrangian function of $\mathcal{L}(\alpha, \beta, \gamma, \lambda)$ as follows:

$$\mathcal{L}(\alpha, \beta, \gamma, \lambda) = f(\alpha, \beta, \gamma) + \lambda(\pi - \alpha - \beta - \gamma), \tag{3.11}$$

where λ is the Lagrange multiplayer. Taking the partial derivatives of $\mathcal{L}$ and setting zero, one can obtain

$$\frac{\partial \mathcal{L}}{\partial \alpha} = -\sin(\alpha)\cos(\beta)\cos(\gamma) - \lambda = 0, \tag{3.12}$$

$$\frac{\partial \mathcal{L}}{\partial \beta} = -\cos(\alpha)\sin(\beta)\cos(\gamma) - \lambda = 0, \tag{3.13}$$

$$\frac{\partial \mathcal{L}}{\partial \gamma} = -\cos(\alpha)\cos(\beta)\sin(\gamma) - \lambda = 0, \tag{3.14}$$

$$\frac{\partial \mathcal{L}}{\partial \lambda} = \alpha + \beta + \gamma = \pi. \tag{3.15}$$

Subtracting (3.12) from (3.13), one can conclude

$$\sin(\alpha - \beta)\cos(\gamma) = 0, \tag{3.16}$$

implying $\alpha = \beta$ or $\gamma = 0$. Excluding $\gamma = 0$ (implies $\lambda = 0$) yields $\alpha = \beta$. Similarly, one can show that $\alpha = \gamma$ and $\beta = \gamma$. Considering (3.15), one has $\alpha = \beta = \gamma = \frac{\pi}{3}$, which implies the equilateral triangular framework. □

For a rigid framework of three vertices in 2D, (3.11) can be written as

$$F(\alpha, \beta) = \cos(\alpha)\cos(\beta)\cos(\pi - (\alpha + \beta)) - 1/8, \tag{3.17}$$

which is shown in Figure 3.3(a). As the singular values of a real symmetric matrix are real, one can show that $y \geq \frac{3}{4}$, implying $F(\alpha, \beta) \leq 0$. The gradient of $F(\alpha, \beta)$ is shown in Figure 3.3(b) in $\alpha\beta$-plane (x- and y-axis are α and β, respectively). Figure 3.3(b) illustrates that the pair of $(\alpha, \beta) = [\frac{\pi}{3}, \frac{\pi}{3}]$ is the location of the maximum smallest singular value for three vertices in 2D (it can be shown that the gradient is zero at this point).

Remark 3.3. *The proof of Theorem 3.5 can alternatively be based on Cardano Method to solve a*

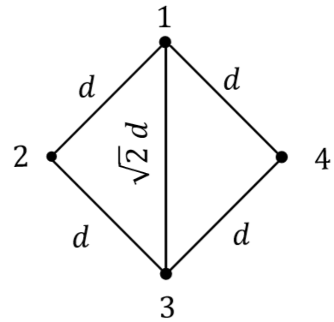

Figure 3.4: Formation of a MIR framework with four agents in 2D.

depressed cubic equation.

Example 3.2. *The maximum smallest singular value of a normalized rigidity matrix for a MIR square framework in 2D (Figure 3.4) is* $\sqrt{2-\sqrt{2}}$.

3.4 Simulation Results

Here we provide numerical simulation results in order to verify and validate the theoretical results.

Example 3.3. *Consider a nonlinear multi-agent system with three agents in a plane, where the dynamics of each agent is given by [28]*

$$\begin{aligned} \dot{p}_i(t) =& v_i(t), \\ \dot{v}_i(t) =& \begin{pmatrix} a_{i1}v_{i2}(t)v_{i1}(t) + \sin(a_{i2}p_{i1}(t)) \\ b_{i1}p_{i2}(t)v_{i2}(t) + \cos(b_{i2}p_{i2}(t)) \end{pmatrix} + u_i(t) + \begin{pmatrix} c_{i1}\cos(1.5t) \\ c_{i2}\sin(t) \end{pmatrix}, \quad i = 1,2,3, \end{aligned} \tag{3.18}$$

where p_i *and* v_i *denote the position and velocity, respectively, in 2D. We used the control law in [39] to achieve the desired formation (*$||p_i - p_j|| \to d_{ij}$ *),* $\forall(i,j), \in E,\ d_{ij} = 1$. *From [39], the parameters that we selected for simulation are given next. The control gains are* $c = 30$, $k_v = 1$. *The radial RBFNN is selected with 9 neurons, centers* μ_j*'s are evenly spaced for each agent, and the values of constants are:* $\kappa = 0.5$, $F_i = I_9$, $b = 3$, $k_r = 2$, $v_r = [0.5, 0.5\cos(t/2)]^T$, $p_r(0) =$

Table 3.1: Parameters $a_{i1}, a_{i2}, b_{i1}, b_{i2}, c_{i1}, c_{i2}$, for the i-th agent.

i	a_{i1}	a_{i2}	b_{i1}	b_{i2}	c_{i1}	c_{i2}
1	0.3	-0.2	0.2	-0.3	1	-1
2	0.7	-0.8	0.4	0.7	2.1	-2.2
3	-0.6	0.4	-0.5	0.3	-1	0.2

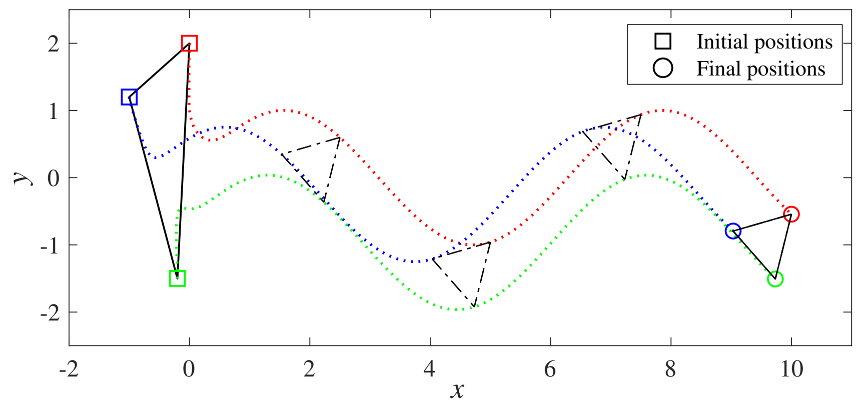

Figure 3.5: Performance of a multi-agent system with three agents using the proposed distance-based control method in [39] with desired distance ($d_{ij} = 1$).

$[0, 0]^T$. *The initial conditions for each agent are* $p_1 = [0, 2]^T$, $v_1 = [0.5, 0.5]^T$, $p_2 = [-1, 1.2]^T$, $v_2 = [-1, 0.8]^T$, $p_3 = [-0.2, -1.5]^T$, *and* $v_3 = [-0.3, 0.5]^T$. *The parameters of each agent are given in Table 3.1.*

We showed that if the formation reaches the condition given in Theorem 3.5, then the smallest singular value of the normalized rigidity matrix reaches the value of $\sqrt{\frac{3}{2}}$.

Figure 3.5 shows the distance-based formation of three agents in 2D with the desired distance ($d_{ij} = 1$)*. In this simulation, the initial conditions do not satisfy the necessary conditions of the Theorem 3.5; therefore, the smallest singular value of the normalized rigidity matrix has a value less than* $\sqrt{\frac{3}{2}}$. *This value is shown in Figure 3.6, and it can be seen as the framework satisfies the sufficient condition of Theorem 3.5, and it converges to the desired formation.*

Example 3.4. *We used CoppeliaSim software to verify the presented theoretical results in this example. The CoppeliaSim (formerly V-REP) [40], is a virtual robot experimentation platform. It is used to validate the theoretical results of the chapter. The simulation software CoppeliaSim enables us to simulate real-world physics and object interactions. We considered a simulation of three*

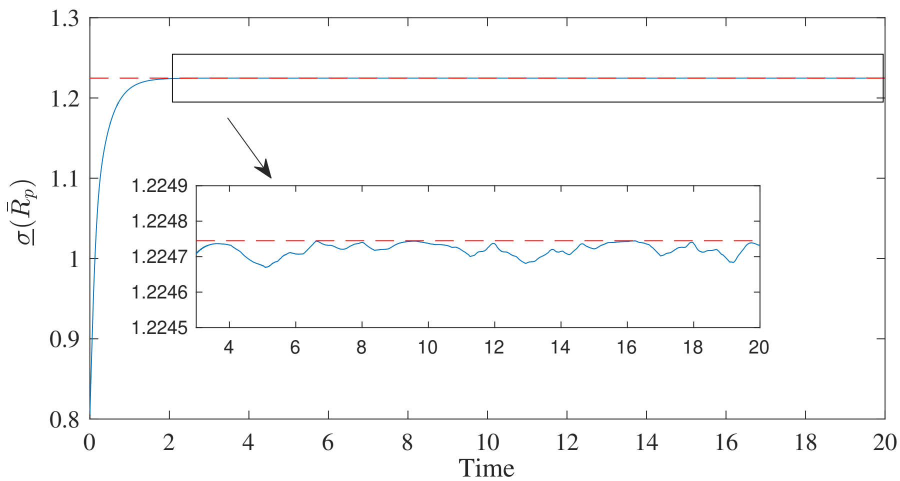

Figure 3.6: The smallest singular value of the framework and the maximum smallest singular value in Theorem 3.5 (dashed line).

nonholonomic mobile robots (Pioneer P3-DX), which are modeled by single-integrator dynamics similar to [41]. The control inputs are the robots' right and left wheels' speeds in Figure 3.7. The driving wheel motor of each nonholonomic mobile robot is configured to produce a maximum of $3Nm$ *of torque. Also, the maximum speed of the wheels is limited by* $1.5rad/s$*. Synchronous with the simulation loop, the controller is implemented in the remote API client and runs at 10Hz. We implemented the controller proposed by [8], where the control gain is* $k_v = 0.1$*. The control goal is to achieve a distance-based formation between all three agents while the distance between every two agents is set to be* $2.5m$*. The framework maintains the formation and maneuvers with the speed of* $0.2rad/s$ *along the* x*-axis and* $0rad/s$ *on the* y*-axis. The simulation is run for less than two minutes, and the simulator's real-time factor is selected to get accurate results. The video of the simulation can be found here*[1].

Simulation results are shown in Figure 3.8 and Figure 3.9. Figure 3.8 represents formation errors between agents and the smallest singular value of the normalized rigidity matrix of the formation. One can see from Figure 3.8 that as all edges converge to the desired distance (condition of Theorem 3.5), the maximum smallest singular value is reached for the triangular formation. Figure 3.9 shows the velocities of robots' left and right wheels, which converge to the desired velocity.

[1] https://www.dropbox.com/s/uf12r2rtuog5j2t

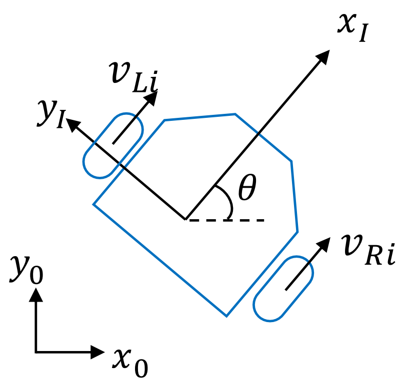

Figure 3.7: An illustration of the i-th differential drive robot.

3.5 Conclusion

We have investigated the spectral properties of the normalized rigidity matrix for a framework in 2D and 3D spaces. The upper bounds of the normalized rigidity matrix singular value have been derived for a MIR graph in 2D and 3D. We have shown that the normalized rigidity matrix spectrum is invariant under the framework's translation, rotation, and uniform scaling transformations. For a rigid framework with three vertices in 2D space, the necessary and sufficient conditions were given to reach the maximum smallest singular value of the normalized rigidity matrix. The numerical simulation for multi-agent systems in 2D validated the theoretical results.

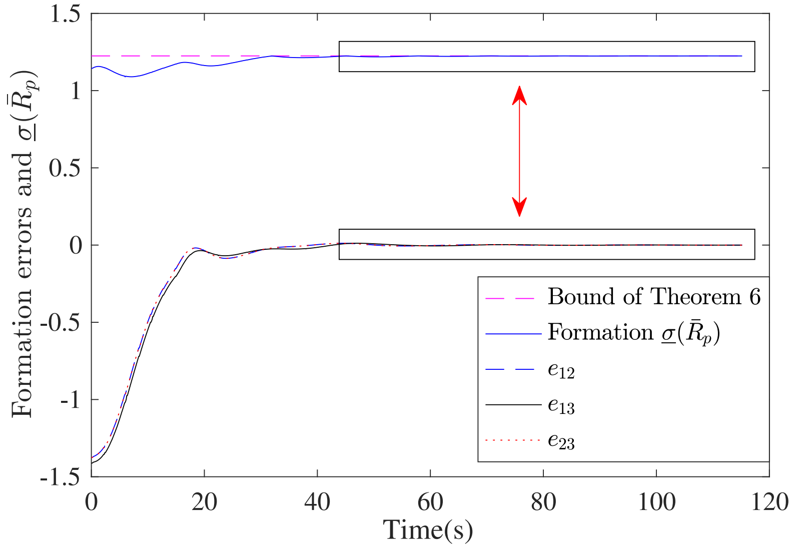

Figure 3.8: Distance-based formation of three agents in 2D with the desired distance ($d_{ij} = 2.5$m). This figure shows that as the inter-agent distance error converges to zero, the smallest singular value converges to its maximum value provided by Theorem 3.5.

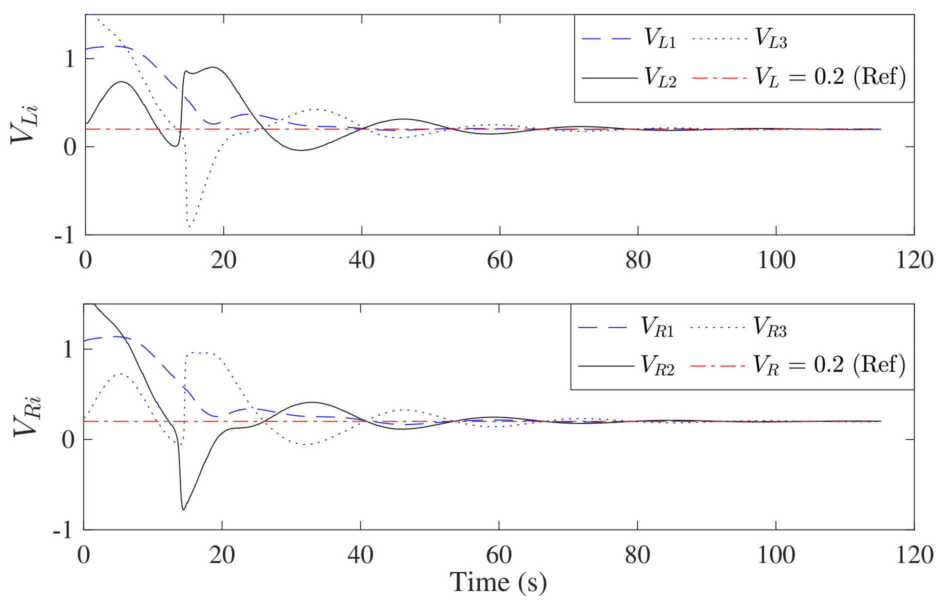

Figure 3.9: Velocities of right and left wheels of each robot.

Chapter 4

Undirected Formation Control Using Inter-Agent Distance for Second-Order Nonlinear Multi-Agent Systems

4.1 Introduction

This chapter focuses on the formation control of input-affine, nonlinear multi-agent systems using inter-agent distance with unknown nonlinearity. Directed or undirected graphs can model the relations among agents. Most developed control methods focus on the undirected graph topology for single-integrator multi-agent systems [42–45]. However, in recent studies, double-integrator multi-agent systems have become more commonly used due to their practical applications. Distance-based formation control of double-integrator systems with undirected graph topology was studied in [7, 17, 46]. Unlike these results, we establish a new control method to address distance-based formation and target tracking of nonlinear multi-agent systems.

4.1.1 Related Works on Formation Control of Nonlinear Multi-Agent Systems

Graph theory, and in particular graph rigidity, is used in distance-based control, where each agent measures distances from its neighboring agents instead of their exact locations in the global coordinate frame [47]. In [7], authors studied single- and double-integrator multi-agent systems over undirected graphs. Directed graph formations of single- and double-integrator systems through distance-based control were studied in [48], where leaders can sense their positions in a global reference framework, while the followers can only sense their neighbors' relative positions with regard to their own local reference frames.

In [49], authors considered double-integrator dynamics of agents for the leader-follower consensus problem. The distance-based formation control was studied in [50], where a discrete-time control algorithm was designed to achieve velocity consensus. Related to our work, the authors in [51] used the backstepping design to solve the formation control problem for double-integrator agents. Distance-based formation control for single-integrator dynamics was addressed in [52], where collision avoidance and desired formation are achieved using the angular information between the agents. Authors in [26] addressed the distance-based formation control for single- and double-integrator dynamics with energy constraints where normalized rigidity is used to asymptotically minimize energy consumption.

NN-based control methods have widely been used in literature to approximate unknown nonlinearities of nonlinear multi-agent systems [14, 28, 53–57]. In [53], an adaptive NN control method for a class of first-order nonlinear multi-agent systems with state time delay was proposed, where an undirected graph models the communication among the agents.

In [54], a self-structuring adaptive NN controller for multi-agent systems with second-order nonlinear dynamics was presented where the control goal is to achieve a leader-following formation over a directed connected graph. In [14], a cooperative adaptive consensus controller was designed based on the NN approximation method for a set of second-order nonlinear multi-agent systems. In [55], particle tracking formation of second-order multi-agent systems using an adaptive NN control with multiple leaders was presented. In [28], a consensus control based on graph Laplacian for a second-order nonlinear multi-agent system was presented. The Frobenius norm of the NN weights is tuned, reducing the proposed approach's computation complexity. In [56], an adaptive NN-based distributed containment controller was designed to reach a leader-follower synchronization where an NN is utilized to approximate the uncertain dynamics of a second-order nonlinear multi-agent system.

We study a general type of nonlinear multi-agent system where the objective is to keep agents, modeled by second-order nonlinear systems, at pre-specified distances from each other and to track a target within the bounded trajectory. We also prove that the tracking error is uniformly ultimately bounded (UUB) and demonstrate extensive simulation results in order to validate and verify the efficiency of the proposed method. We introduce a performance index to demonstrate the advantages of the proposed method in comparison with the displacement-based control methods.

We propose a control design for the nonlinear multi-agent systems using the backstepping control technique to achieve the control objectives. The unknown nonlinear part of the system dynamics is compensated using an RBFNN similar to [28], where authors used the norm of the NN weights matrix. The leader follows the target while the rest of the agents maintain the desired formation and follow the leader [8]. Our results are based on a MIR graph, while displacement-based methods usually rely on the graph Laplacian [2].

The novelties are a rigorous analysis and proof of formation stability control using NNs for second-order nonlinear multi-agent systems in the presence of disturbance. The main contributions of this chapter are:

(1) Compared with existing distance-based formation control methods [7, 42–46, 52, 58], which considered single- or double-integrator dynamics for agents, we assume that agents are modeled as the second-order nonlinear systems with unknown nonlinearity and disturbance. We provided a rigorous Lyapunov stability analysis for the formation control and target tracking for such a system.

(2) In contrast with existing methods [14, 28, 53–55, 59], that use the Laplacian matrix to model relations among the agents and addressed the displacement-based formation problem, we applied the rigid graph theory to address the problem of target tracking and distance-based formation control for input-affine, nonlinear multi-agent systems.

4.2 Problem Formulation

Consider a nonlinear multi-agent dynamical system with agents modeled by

$$\begin{aligned} \dot{p}_i &= v_i, \\ \dot{v}_i &= f_i(p_i, v_i) + g_i(p_i, v_i)u_i(t) + w_i(t), \;\; i \in \{1, 2, ..., N\}, \end{aligned} \tag{4.1}$$

where the vectors $p_i \in \mathbb{R}^2$ and $v_i \in \mathbb{R}^2$ represent the position and velocity of each agent, respectively. Let us define $\check{\mathbf{x}}_i = [p_i^T, v_i^T]^T \in \mathbb{R}^4$. The nonlinear function $f_i(\check{\mathbf{x}}_i) \in \mathbb{R}^2$ is the unknown function and considered to be continuously differentiable, $g_i(\check{\mathbf{x}}_i) \in \mathbb{R}^{2\times 2}$ is the input gain matrix function, $u_i \in \mathbb{R}^2$ is the control input, $w_i \in \mathbb{R}^2$ is a disturbance affecting each agent, and N represents the number of the agents.

The overall dynamics of the multi-agent system is given by

$$\begin{aligned} \dot{\mathbf{x}}_1 =& \mathbf{x}_2, \\ \dot{\mathbf{x}}_2 =& f(\mathbf{x_1}, \mathbf{x_2}) + g(\mathbf{x_1}, \mathbf{x_2})u + w, \end{aligned} \tag{4.2}$$

where $\mathbf{x}_1 = [p_1^T, p_2^T, ..., p_N^T]^T \in \mathbb{R}^{2N}$ and $\mathbf{x}_2 = [v_1^T, v_2^T, ..., v_N^T]^T \in \mathbb{R}^{2N}$ are defined as overall positions and velocities of all agents, respectively. The vector $\mathbf{x} = [\mathbf{x}_1^T, \mathbf{x}_2^T]^T$, $f(\mathbf{x}) = [f_1^T(\check{\mathbf{x}}_1), f_2^T(\check{\mathbf{x}}_2),$ $..., f_N^T(\check{\mathbf{x}}_N)]^T \in \mathbb{R}^{2N}$ is the nonlinear vector function of the whole system, $g(\mathbf{x}) = diag(g_1(\check{\mathbf{x}}_1), g_2(\check{\mathbf{x}}_2),$ $..., g_N(\check{\mathbf{x}}_N)) \in \mathbb{R}^{2N\times 2N}$, the control input vector is $u = [u_1^T, u_2^T, ..., u_N^T]^T \in \mathbb{R}^{2N}$, and the disturbance vector is $w = [w_1^T, w_2^T, ..., w_N^T]^T \in \mathbb{R}^{2N}$.

We establish some standard assumptions [14, 60].

Assumption 4.1. *The unknown matrix $g_i(\check{\mathbf{x}}_i)$ is a positive-definite, symmetric matrix, with eigenvalues satisfying $0 < \underline{g}_i \leq \lambda_1(g_i(\check{\mathbf{x}}_i)) \leq \lambda_2(g_i(\check{\mathbf{x}}_i)) < \infty$, and $\underline{g}_i$ being a constant lower bound of $g_i(\check{\mathbf{x}}_i)$.*

Assumption 4.1 is needed for the controllability of the system (4.1), which is a standard assumption in most NN-based controller designs [28, 35, 60, 61]. A large class of nonlinear systems described by Euler–Lagrange formulation satisfies this assumption [27, 32]. Let us define $\underline{g} = min(\underline{g}_i)$.

Assumption 4.2. *Disturbance $w_i(t)$ is unknown and bounded with a fixed bound, i.e., $||w_i|| \leq w_M$.*

The objective of the control law is to ensure that the distance between neighboring agents i and j converges to the desired distance d_{ij}: $\|p_i - p_j\| \to d_{ij}, \forall (i,j) \in E$.

Assumption 4.3. *Desired distances between agents are bounded by $||d_{ij}|| < D, \forall (i,j) \in E$, with a fixed bound D.*

Consider points $p_1, p_2 \in \mathbb{R}^2$ and a set $\mathcal{S}_p$. The distance between point p_1 and the set $\mathcal{S}_p$ is defined as $\mathrm{d}(p_1, \mathcal{S}_p) \triangleq \inf_{p_2 \in \mathcal{S}_p} ||p_1 - p_2||$. Let the initial conditions belong to the set $\mathcal{S}$ given by

$$\mathcal{S} = \{\mathbf{x}_1 \in \mathbb{R}^{2N} | \sum_{(i,j) \in E^*} (||p_{ij}||^2 - d_{ij}^2)^2 \leq \delta, \mathrm{d}(\mathbf{x}_1, \mathrm{Iso}(F^*)) < \mathrm{d}(\mathbf{x}_1, \mathrm{Amb}(F^*))\}. \tag{4.3}$$

where δ is a positive constant, [8, 21, 62]. For initial conditions belonging to $\mathcal{S}$, the convergence of the formation to Iso(F^*) and avoidance of getting stuck in Amb(F^*) are guaranteed [21]. While the precise determination of δ is difficult when the number of agents increases [8], the sufficient condition to satisfy the inequality is given in [7]. The interested reader is invited to see [7, 8, 62] and references therein.

For target tracking, we consider the first agent to be the leader that tracks the target, while the remaining agents follow the leader and retain the desired formation, see Figure 4.1.

Let us define the tracking error between the leader and the target as [8]:

$$e_r = p_r - p_1, \tag{4.4}$$

$e_r(t) = [e_{r1}, e_{r2}]^T$, and components e_{r1} and e_{r2} represent the leader's tracking errors in x and y directions, respectively. Vectors $p_r, p_1 \in \mathbb{R}^2$ denote positions of the target and the leader, respectively, while $v_r \triangleq \dot{p}_r$ is the target (reference) velocity.

Assumption 4.4. *The variables $p_r, \dot{p}_r, \ddot{p}_r$ are bounded.*

Let us define a compact set [63] such that

$$\Omega_T = \{p_r, \dot{p}_r, \ddot{p}_r \mid ||p_r|| \leq \bar{P}_r, ||\dot{p}_r|| \leq \bar{V}_r, ||\ddot{p}_r|| \leq \bar{A}_r\}, \tag{4.5}$$

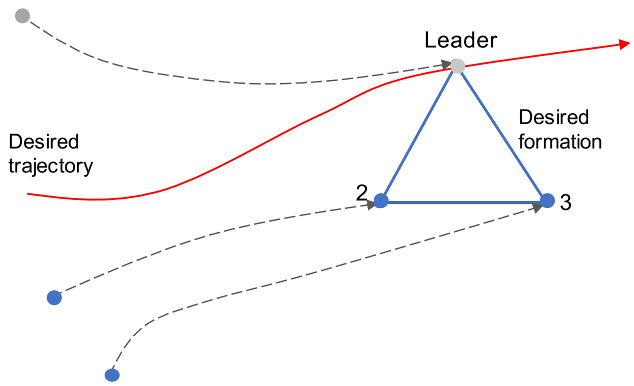

Figure 4.1: Target tracking and formation control problems.

where $\bar{P}_r$, $\bar{V}_r$ and $\bar{A}_r$ are positive constants.

Assumption 4.5. *The signals $p_r - p_1, \dot{p}_r - \dot{p}_1$, as well as v_r, are known signals and can be broadcasted to the followers [8].*

Remark 4.1. *We assume that the leader can approximate the position and velocity of the moving target using, for example, the proposed technique in [64], where a moving target is detected. Furthermore, its 2D velocity is estimated through a moving target indication method [65] based on back projection and velocity synthetic aperture radar (VSAR) [64]. Moreover, the leader can distribute the relative position and velocity of the target to the followers [8, 63].*

In the following, we study the formation control and target tracking of multi-agent systems described by second-order nonlinear dynamics.

4.3 Controller Design

Consider a multi-agent system (4.1) that is modeled by an undirected graph. The distance error is given by

$$e_{ij} = ||\tilde{p}_{ij}|| - d_{ij}, \tag{4.6}$$

where $\tilde{p}_{ij} = p_i - p_j$. From (4.3), the distance error dynamics is

$$\dot{e}_{ij} = \tfrac{\tilde{p}_{ij}^T(\dot{p}_i - \dot{p}_j)}{||\tilde{p}_{ij}^T||} = \tfrac{\tilde{p}_{ij}^T(v_i - v_j)}{e_{ij} + d_{ij}}. \tag{4.7}$$

Define $\mathbf{e} = [..., e_{ij}, ...]^T \in \mathbb{R}^{|E|}$, auxiliary variable q_{ij} as

$$q_{ij} = e_{ij}(e_{ij} + 2d_{ij}), \tag{4.8}$$

and the energy function as $M_1(\mathbf{e}) = \sum_{(i,j)\in E} M_{ij}(e_{ij})$ [7], where

$$M_{ij}(e_{ij}) = \frac{1}{4}q_{ij}^2 = \frac{1}{4}e_{ij}^2(e_{ij} + 2d_{ij})^2. \tag{4.9}$$

Considering (4.6) and (4.9), $\dot{M}_1(\mathbf{e})$ is given by

$$\dot{M}_1(\mathbf{e}) = \sum \tfrac{\partial M_{ij}}{\partial e_{ij}} \tfrac{\tilde{p}_{ij}^T(v_i - v_j)}{e_{ij}+d_{ij}}. \tag{4.10}$$

Let us define $\beta(\mathbf{e})$ as

$$\beta(\mathbf{e}) = (..., \tfrac{\frac{\partial M_{ij}}{\partial e_{ij}}}{e_{ij}+d_{ij}}, ...) = (..., e_{ij}(e_{ij} + 2d_{ij}), ...), \tag{4.11}$$

where pair $(i, j) \in E$ and $\beta(\mathbf{e}) \in \mathbb{R}^{|E|}$. As shown in [62], it follows from (4.7) and (4.10) that

$$\dot{M}_1 = \beta^T(\mathbf{e})R_p\mathbf{x}_2. \tag{4.12}$$

Using the backstepping technique [7], we define $\mathbf{s} = [s_1^T, ..., s_N^T]^T \in \mathbb{R}^{2N}$ as

$$\mathbf{s} = \mathbf{x}_2 - \tau. \tag{4.13}$$

The auxiliary variable τ is given by

$$\tau = u_s + \mathbf{1}_N \otimes (v_r + k_r e_r), \tag{4.14}$$

where $\tau = [\tau_1^T, ..., \tau_N^T]^T \in \mathbb{R}^{2N}$ and $u_s = -k_v R_p^T \beta(\mathbf{e}) \in \mathbb{R}^{2N}$, k_r and k_v are positive constants. One can express u_s element-wise as $u_s = [u_{s_1}^T, ..., u_{s_N}^T]^T \in \mathbb{R}^{2N}$. The first term in (4.14) is responsible for achieving the desired formation of agents, while the second term is used for tracking

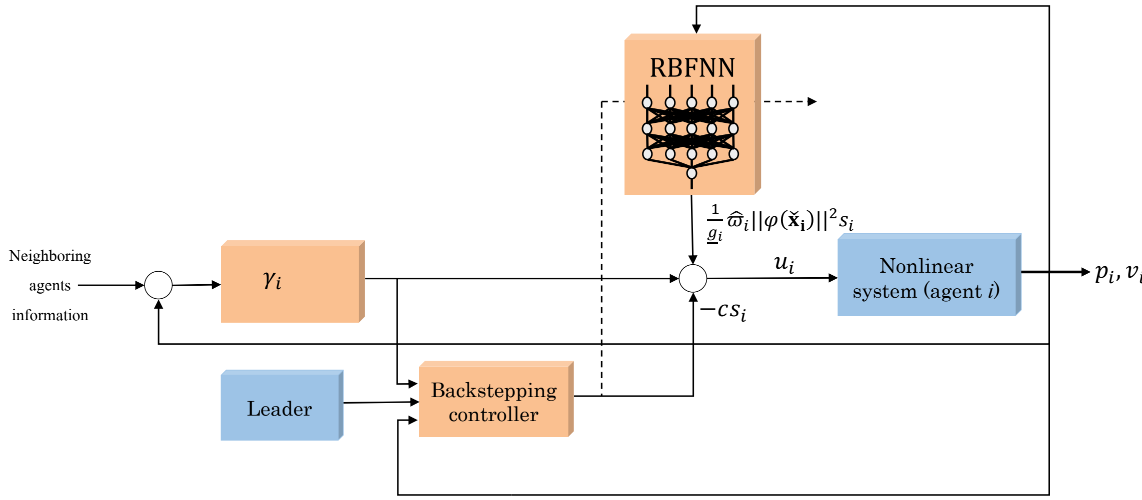

Figure 4.2: Block diagram of the proposed control scheme for each agent.

the target by the leader and other agents. Define the potential function

$$M_2 = M_1(\mathbf{e}) + \tfrac{1}{2}\mathbf{s}^T\mathbf{s}. \tag{4.15}$$

Taking a time derivative of (4.15), using Lemma 2.3, and (4.2), (4.14), yields

$$\begin{aligned}\dot{M}_2 =&\beta^T(\mathbf{e})R_p\mathbf{x}_2 + \mathbf{s}^T\dot{\mathbf{s}}\\ =&\beta^T(\mathbf{e})R_p\tau + \mathbf{s}^T[f(\mathbf{x}) + g(\mathbf{x})u + w + R_p^T\beta(\mathbf{e}) - \dot{\tau}]\\ =&-k_v\beta^T(\mathbf{e})R_pR_p^T\beta(\mathbf{e}) + \mathbf{s}^T[f(\mathbf{x}) + g(\mathbf{x})u + w + R_p^T\beta(\mathbf{e}) - \dot{\tau}].\end{aligned} \tag{4.16}$$

Using Cauchy–Schwarz inequality, one can write

$$\begin{aligned}\mathbf{s}^Tf(\mathbf{x}) \leq \sum_{i=1}^{N} s_i^T f_i(\check{\mathbf{x}}_i) \leq \sum_{i=1}^{N} s_i^T(W_i^T\varphi_i(\check{\mathbf{x}}_i) + \epsilon_i)\\ \leq \sum_{i=1}^{N}\big(||s_i||\,||W_i||\,||\varphi_i(\check{\mathbf{x}}_i)|| + ||s_i||\,||\epsilon_i||\big).\end{aligned} \tag{4.17}$$

Using the fact that $||.||_F \geq ||.||$, from (2.14) and Young's inequality, one can write (4.17) as

$$\mathbf{s}^Tf(\mathbf{x}) \leq \sum_{i=1}^{N}\Big(\,||W_i||_F^2(||s_i||\,||\varphi_i(\check{\mathbf{x}}_i)||)^2 + \frac{1}{4\varrho_i^2} + ||s_i||^2 + \frac{1}{4\alpha_i^2}||\epsilon_i||^2\Big), \tag{4.18}$$

where $\alpha_i, \forall\, i = 1, ..., N$ is a positive constant. Let us define $\varpi = [\varpi_1, ..., \varpi_N]^T$, where the norm of the NN weights matrix is given as $\varpi_i = ||W_i||_F^2$ for $i = 1, ..., N$, and $\hat{\varpi}_i$ is an estimation of ϖ_i [28]. From Assumption 2.1, it is clear that ϖ_i is bounded by W_M^2. Define the NN weights' norm estimation error as $\tilde{\varpi} = \varpi - \hat{\varpi}$, where $\hat{\varpi} = [\hat{\varpi}_1, ..., \hat{\varpi}_N]^T \in \mathbb{R}^N$. Define $\Xi = R_p^T \beta(\mathbf{e}) \in \mathbb{R}^{2N}$, where vector Ξ can be written as $\Xi = [\Xi_1^T, ..., \Xi_N^T]^T$, with $\Xi_i = \sum_{j \in N_i} p_{ij} q_{ij} \in \mathbb{R}^2$. From Assumption 4.2 and following the same procedure as (4.18), one can obtain the following inequalities

$$
\begin{aligned}
\mathbf{s}^T w &\leq \sum_{i=1}^{N} \big((||s_i||^2 + \frac{1}{4\eta_i^2} w_M^2 \big), \\
\mathbf{s}^T R_p^T \beta(\mathbf{e}) &\leq \sum_{i=1}^{N} \big((||s_i||\, ||\Xi_i||)^2 + \frac{1}{4\Upsilon_i^2} \big), \\
\mathbf{s}^T \dot{\tau} &\leq \sum_{i=1}^{N} \big((||s_i||\, ||\dot{u}_{s_i} + k_r \dot{e}_r||)^2 + \frac{1}{4\psi_i^2} \big) + s_i^T \dot{v}_r \big),
\end{aligned}
\tag{4.19}
$$

where $\Upsilon_i, \psi_i, \eta_i$, for $i = 1, ..., N$ are positive constants. Substituting (4.18), (4.19), in (4.16) one can obtain

$$
\begin{aligned}
\dot{M}_2 =& - k_v \beta^T(\mathbf{e}) R_p R_p^T \beta(\mathbf{e}) + \mathbf{s}^T [f(\mathbf{x}) + g(\mathbf{x})u + w + R_p^T \beta(\mathbf{e}) - \dot{\tau}] \\
\leq& - k_v \beta^T(\mathbf{e}) R_p R_p^T \beta(\mathbf{e}) + \sum_{i=1}^{N} [||s_i||^2 \big(\varpi_i ||\varphi_i(\check{\mathbf{x}}_i)||^2 + ||\Xi_i||^2 + 2 \\
&+ (||\dot{u}_{s_i} + k_r \dot{e}_r||)^2 \big) + s_i^T \dot{v}_r] \\
&+ s_i^T g_i(\check{\mathbf{x}}_i) u_i + \sum_{i=1}^{N} \big(\frac{1}{4\varrho_i^2} + \frac{1}{4\alpha_i^2} ||\epsilon_i||^2 + \frac{1}{4\eta_i^2} w_M^2 + \frac{1}{4\Upsilon_i^2} + \frac{1}{4\psi_i^2} \big).
\end{aligned}
\tag{4.20}
$$

Consider the following energy function

$$
V = M_2 + \frac{1}{2} \tilde{\varpi}^T F^{-1} \tilde{\varpi}, \tag{4.21}
$$

where the matrix $F = \Pi_i I_N \in \mathbb{R}^{N \times N}$ is a positive-definite matrix, i.e., $\Pi_i \in \mathbb{R}^+$, for $i = 1, ..., N$. We propose the following control law:

$$
u_i = -c s_i - \gamma_i - \frac{1}{\underline{g}_i} \hat{\varpi}_i ||\varphi_i(\check{\mathbf{x}}_i)||^2 s_i, \tag{4.22}
$$

where constant c is a positive scalar. Moreover, the term γ_i is given as

$$\gamma_i = \frac{1}{\underline{g}_i}(||\dot{u}_{s_i} + k_r \dot{e}_r||^2 + ||\Xi_i||^2)s_i + \frac{b}{\underline{g}_i}\text{sgn}(s_i), \tag{4.23}$$

with b being a positive constant. The tuning law of $\hat{\varpi}_i$ is given by

$$\dot{\hat{\varpi}}_i = \Pi_i ||\varphi_i(\check{\mathbf{x}}_i)||^2 ||s_i||^2 - \kappa_i \Pi_i \hat{\varpi}_i. \tag{4.24}$$

The control input signal is comprised of tracking error between the leader and the target, a backstepping controller, and an NN-based component to compensate for the unknown nonlinearity of the system dynamics (see Figure 4.2). The controller is developed based on relative positions and velocities of neighboring agents only; therefore, the proposed controller is distributed [8]. The control input signal (4.22) for each agent can be written as follows:

$$\begin{aligned} u_i = &- cs_i - \frac{1}{\underline{g}_i}\hat{\varpi}_i ||\varphi_i(\check{\mathbf{x}}_i)||^2 s_i - ||\sum_{j\in N_i}[k_v(q_{ij}I_2 + 2\tilde{p}_{ij}\tilde{p}_{ij}^T)v_{ij}] - k_r\dot{e}_r||^2 s_i \\ &+ \frac{1}{\underline{g}_i}||\sum_{j\in N_i}\tilde{p}_{ij}q_{ij}||^2 s_i + \frac{b}{\underline{g}_i}\text{sgn}(s_i)\big), \end{aligned} \tag{4.25}$$

with

$$s_i = v_i - v_r - k_r e_r + k_v \sum_{j\in N_i}\tilde{p}_{ij}q_{ij}. \tag{4.26}$$

Remark 4.2. *The control input signal (4.25) includes the relative position and relative velocity vectors between agent i and its neighboring agents j. This over-sensing is necessary for the distance-based formation [8, 66–69] and the volume of the over-sensing can be reduced by considering a minimally rigid framework. The relative position between the agent i and its arbitrary neighboring agent j can be presented by the distance and angle sensing between agents. This angle between agent i and j can be obtained through information such as the heading of the neighboring agent for a rigid framework [70]. The agent can also calculate the relative velocity vector by differentiating the relative position.*

4.3.1 Stability Analysis

In this section, we show that the proposed control law (4.22) can be used for nonlinear multi-agent systems (4.2) with guaranteed stability of agent formation.

Theorem 4.1. *Consider the framework $F = (G, p)$ to be modeled by an undirected MIR graph. Select the control input signals as (4.22) and NN weights' norm tuning law as (4.24). Under Assumptions 2.1,2.2, 4.1-4.5, choose $b \geq \sqrt{2}||\dot{v}_r||_\infty$ and $c > \frac{2}{\underline{g}}$. Then, for initial conditions that belong to the compact set Ω_0 defined by*

$$\Omega_0 = \{\mathbf{x}_1(0), p_r(0) | p_r(0) \in \Omega_T, \mathrm{d}(\mathbf{x}_1, \mathrm{Iso}(F^*)) < \mathrm{d}(\mathbf{x}_1, \mathrm{Amb}(F^*)), \sum_{(i,j)\in E^*} (||p_{ij}||^2 - d_{ij}^2)^2 \leq \delta\}, \tag{4.27}$$

the distance errors and the NN weights' norm estimation errors are UUB. The leader follows the target, and followers maintain the desired formation (F^*) with the leader.

Proof. Note that the closed-loop system with (4.22)-(4.24) has a discontinuity due to $\mathrm{sgn}(s_i)$ in (4.23) at $s_i = \mathbf{0}$. We choose the Lyapunov function candidate as (4.21). Let $\dot{\varsigma}_i = \mathcal{F}_i(\varsigma_i, t)$ be the closed loop system with respect to multi-agent systems with (4.22)-(4.24). Following the procedure in [8, 63], the time derivative of Lyapunov function (4.21) is given by

$$\begin{aligned}\dot{V} &\overset{a.e.}{\in} \sum_{i=1}^{N} \frac{\partial V}{\partial \varsigma_i} K_i[\mathcal{F}_i](\varsigma_i, t) \\ &\subset \dot{M}_2 + \tilde{\varpi}^T F^{-1} \dot{\tilde{\varpi}}.\end{aligned} \tag{4.28}$$

Recall the definition of $\tilde{\varpi}$ and consider the Assumption 2.1. By considering (4.20) and substituting the proposed control input (4.22), using the NN tuning law (4.24), one obtains

$$
\begin{aligned}
\dot{V} \leq &- k_v\beta^T(\mathbf{e})R_pR_p^T\beta(\mathbf{e}) + \sum_{i=1}^{N}[||s_i||^2\big(\,\varpi_i||\varphi_i(\check{\mathbf{x}}_i)||^2 + 2 + ||\Xi_i||^2 + ||\dot{u}_{s_i} + k_r\dot{e}_r||^2\big) + s_i^T\dot{v}_r] \\
&+ \sum_{i=1}^{N}\big(\frac{1}{4\varrho_i^2} + \frac{1}{4\alpha_i^2}||\epsilon_i||^2 + \frac{1}{4\eta_i^2}w_M^2 + \frac{1}{4\Upsilon_i^2} + \frac{1}{4\psi_i^2}\big) + \sum_{i=1}^{N}\tilde{\varpi}_i(-||\varphi_i(\check{\mathbf{x}}_i)||^2||s_i||^2 + \kappa_i\hat{\varpi}_i) \\
&+ \sum_{i=1}^{N}s_i^Tg_i(\check{\mathbf{x}}_i)\big(-cs_i - \frac{b}{\underline{g}_i}\mathrm{sgn}(s_i) - \frac{1}{\underline{g}_i}(||\dot{u}_{s_i} + k_re_r||^2 + ||\Xi_i||^2 + \hat{\varpi}_i||\varphi_i(\check{\mathbf{x}}_i)||^2)s_i\big).
\end{aligned}
\tag{4.29}
$$

From Assumption 4.1, matrix $g_i(\check{\mathbf{x}}_i)$ is a full-rank and positive-definite matrix. Using the fact that $g_i(\check{\mathbf{x}}_i)g_i^{-1}(\check{\mathbf{x}}_i) = I_2$, one can have $\frac{||g_i(\check{\mathbf{x}}_i)||}{\underline{g}_i} \geq 1$. Considering the fact that $s_i^T\mathrm{sgn}(s_i) \geq 0$, the following inequality holds

$$
-\frac{b}{\underline{g}_i}s_i^Tg_i(\check{\mathbf{x}}_i)\mathrm{sgn}(s_i) \leq -bs_i^Tsgn(s_i). \tag{4.30}
$$

From (4.30), and by simplifying and rearranging (4.29), one has

$$
\begin{aligned}
\dot{V} \leq &- k_v\beta^T(\mathbf{e})R_pR_p^T\beta(\mathbf{e}) - \sum_{i=1}^{N}\big((c\underline{g}_i - 2)||s_i||^2 + ||s_i||(\sqrt{2}||\dot{v}_r||_\infty - b)\big) + \sum_{i=1}^{N}\big(\frac{1}{4\varrho_i^2} \\
&+ \frac{1}{4\alpha_i^2}||\epsilon_i||^2 + \frac{1}{4\eta_i^2}w_M^2 + \frac{1}{4\Upsilon_i^2} + \frac{1}{4\psi_i^2}\big) + \sum_{i=1}^{N}\kappa_i\tilde{\varpi}_i(\hat{\varpi}_i).
\end{aligned}
\tag{4.31}
$$

From (4.19) and (4.31), one can notice that the selection of b is important to counteract the effect of the disturbance in the system dynamics. Let us define $\underline{\kappa} = \min(\kappa_1, ..., \kappa_N)$. Applying Young's inequality to the last term yields

$$
\tilde{\varpi}_i\hat{\varpi}_i \leq -\frac{\tilde{\varpi}_i^2}{2} + \frac{\varpi_i^2}{2}. \tag{4.32}
$$

Recalling the definition of $\underline{g}$, using $b \geq \sqrt{2}||\dot{v}_r||_\infty$, and Assumptions 2.1-2.2, one has

$$
\dot{V} \leq -k_v\beta^T(\mathbf{e})R_pR_p^T\beta(\mathbf{e}) - (c\underline{g} - 2)||\mathbf{s}||^2 - \frac{\underline{\kappa}}{2}||\tilde{\varpi}||^2 + q, \tag{4.33}
$$

where q is written as

$$q = \sum_{i=1}^{N} (\frac{1}{4\varrho_i^2} + \frac{1}{4\alpha_i^2}\epsilon_M^2 + \frac{1}{4\eta_i^2}w_M^2 + \frac{1}{4\Upsilon_i^2} + \frac{1}{4\psi_i^2} + \kappa_i\frac{W_M^4}{2}). \tag{4.34}$$

Based on Assumptions 2.1-2.2, 4.1-4.5, the time derivative of Lyapunov function (4.29) is bounded by

$$\dot{V} \leq -k_v\underline{\sigma}(R_p)||\beta(\mathbf{e})||^2 - (c\underline{g} - 2)||\mathbf{s}||^2 - \frac{\kappa}{2}||\tilde{\varpi}||^2 + q, \tag{4.35}$$

or equivalently

$$\dot{V} \leq -\begin{bmatrix} ||\beta(\mathbf{e})|| & ||\mathbf{s}|| & ||\tilde{\varpi}|| \end{bmatrix} \underbrace{\begin{bmatrix} k_v\underline{\sigma}(R_p) & 0 & 0 \\ 0 & c\underline{g} - 2 & 0 \\ 0 & 0 & \frac{\kappa}{2} \end{bmatrix}}_{Q} \begin{bmatrix} ||\beta(\mathbf{e})|| \\ ||\mathbf{s}|| \\ ||\tilde{\varpi}|| \end{bmatrix} + q. \tag{4.36}$$

Defining $z = [||\beta(\mathbf{e})||\ ||\mathbf{s}||\ ||\tilde{\varpi}||]^T$, (4.36) can be rewritten as

$$\dot{V} \leq -z^T Q z + q. \tag{4.37}$$

For $\dot{V} \leq 0$ one requires $Q \geq 0$ and

$$||z||^2 > \frac{q}{\underline{\sigma}(Q)}. \tag{4.38}$$

From (4.21), one can write the following inequality for V

$$
\begin{aligned}
&\frac{1}{2}\begin{bmatrix} ||\beta(\mathbf{e})|| & ||\mathbf{s}|| & ||\tilde{\varpi}|| \end{bmatrix} \overbrace{\begin{bmatrix} \frac{1}{2} & 0 & 0 \\ 0 & 1 & 0 \\ 0 & 0 & \frac{1}{\Pi_{max}} \end{bmatrix}}^{T_1} \begin{bmatrix} ||\beta(\mathbf{e})|| \\ ||\mathbf{s}|| \\ ||\tilde{\varpi}|| \end{bmatrix} \\
&\leq V \leq \\
&\frac{1}{2}\begin{bmatrix} ||\beta(\mathbf{e})|| & ||\mathbf{s}|| & ||\tilde{\varpi}|| \end{bmatrix} \underbrace{\begin{bmatrix} \frac{1}{2} & 0 & 0 \\ 0 & 1 & 0 \\ 0 & 0 & \frac{1}{\Pi_{min}} \end{bmatrix}}_{T_2} \begin{bmatrix} ||\beta(\mathbf{e})|| \\ ||\mathbf{s}|| \\ ||\tilde{\varpi}|| \end{bmatrix},
\end{aligned}
\tag{4.39}
$$

where $\underline{\sigma}(T_1) = min(\frac{1}{2}, \frac{1}{\Pi_{max}})$ and $\bar{\sigma}(T_2) = max(1, \frac{1}{\Pi_{min}})$. Therefore, one has

$$\tfrac{1}{2}\underline{\sigma}(T_1)||z||^2 \leq V \leq \tfrac{1}{2}\bar{\sigma}(T_2)||z||^2. \tag{4.40}$$

From (4.40), we conclude that

$$V \geq \frac{\underline{\sigma}(T_1)}{2\underline{\sigma}(Q)}q, \tag{4.41}$$

implies (4.38), and therefore, $z(t)$ is UUB [71]. As for any vector z, one has $||z||_1 \geq ||z||_2 \geq ... \geq ||z||_\infty$, and sufficient conditions for (4.38) are [14]

$$||\beta(\mathbf{e})|| > \sqrt{\tfrac{q}{\underline{\sigma}(Q)}}, \tag{4.42}$$

or

$$||\mathbf{s}|| > \sqrt{\tfrac{q}{\underline{\sigma}(Q)}}, \tag{4.43}$$

or

$$||\tilde{\varpi}|| > \sqrt{\tfrac{q}{\underline{\sigma}(Q)}}. \tag{4.44}$$

This shows that $||\beta(\mathbf{e})||, ||\mathbf{s}||, ||\tilde{\varpi}||$ are UUB. Using (4.37) and (4.40), one can write

$$\dot{V} \leq -a_1 V + a_2, \tag{4.45}$$

with $a_1 \triangleq 2\underline{\sigma}(Q)/\bar{\sigma}(T_2)$ and $a_2 \triangleq q$. From (4.45), it follows that

$$\begin{aligned} V(t) \leq & V(0)e^{-a_1 t} + \frac{a_2}{a_1}(1 - e^{-a_1 t}) \\ \leq & V(0) + \frac{a_2}{a_1}. \end{aligned} \tag{4.46}$$

Using (4.40), one has

$$\begin{aligned} & ||\beta(\mathbf{e})|| \leq ||z(t)|| \\ & \qquad \leq \sqrt{\frac{\bar{\sigma}(T_2)}{\underline{\sigma}(T_1)}(||\beta(e(0))||^2 + ||\mathbf{s}(0)||^2 + ||\tilde{\varpi}(0)||^2)} + \sqrt{\frac{\bar{\sigma}(T_2)q}{\underline{\sigma}(T_1)\underline{\sigma}(Q)}} \triangleq \rho, \end{aligned} \tag{4.47}$$

and

$$||\mathbf{s}|| \leq ||z(t)|| \leq \rho, \tag{4.48}$$

and

$$||\hat{\varpi}|| \leq ||z(t)|| \leq \rho. \tag{4.49}$$

From (4.47), we have

$$||\beta(\mathbf{e})|| = \sqrt{\textstyle\sum_{(i,j)\in E}(e_{ij}^2 + 2d_{ij}e_{ij})^2} \leq \rho. \tag{4.50}$$

By substituting e_{ij} in (4.50), one has

$$||\beta(\mathbf{e})|| = \sqrt{\textstyle\sum_{(i,j)\in E}((||\tilde{p}_{ij}|| - d_{ij})^2(||\tilde{p}_{ij}|| + d_{ij})^2)} \leq \rho. \tag{4.51}$$

From (4.51), for the edge $(i,j) \in E$ one can write

$$||\tilde{p}_{ij}||^2 - d_{ij}^2 \leq \rho. \tag{4.52}$$

Using Assumption 4.3, the upper bound is given by

$$||\tilde{p}_{ij}|| \leq \sqrt{\rho + D^2}. \tag{4.53}$$

As desired distances d_{ij}'s are considered bounded, the inequality (4.53) implies boundedness of the distance error dynamics (e_{ij}) for all $(i, j) \in E$. Thus, inter-agent distance error, as well as NN weights' norm estimation error remain bounded. □

Lemma 4.1. *Given the bounded initial conditions for $p_r(0)$ and $p_1(0)$, the tracking error between the leader and the target is bounded by $||e_r(t)|| \leq \bar{\xi}$, with the bound*

$$\bar{\xi} = ||e_r(0)|| + \frac{\sqrt{2}\rho}{k_r}(1 + k_v\bar{\sigma}(R_p)). \tag{4.54}$$

Proof. From (4.13) and (4.14) the velocity of the leader (first agent) can be written as

$$v_1 = \tau_1 + s_1 = u_{s1} + v_r + k_r e_r + s_1. \tag{4.55}$$

The target tracking error dynamics is

$$\dot{e}_r = v_r - v_1 = -k_e e_r - (s_1 - u_{s_1}). \tag{4.56}$$

From (4.48) and (4.49), it follows that

$$\dot{e}_r \leq -k_r e_r + \rho(1 + k_v\bar{\sigma}(R_p)) \otimes \mathbf{1}_2. \tag{4.57}$$

Multiplying both sides by $e^{k_r t}$ yields

$$\frac{d}{dt}(e_r e^{k_r t}) \leq \rho(1 + k_v\bar{\sigma}(R_p))e^{k_r t} \otimes \mathbf{1}_2. \tag{4.58}$$

By taking integral over $[0, t]$, we have

$$e_r(t) \leq [e_r(0) - (\frac{\rho(1 + k_v\bar{\sigma}(R_p))}{k_r})]e^{-k_r t} \otimes \mathbf{1}_2 + (\frac{\rho(1 + k_v\bar{\sigma}(R_p))}{k_r}) \otimes \mathbf{1}_2. \tag{4.59}$$

We can conclude that

$$e_r(t) \leq e_r(0) + (\frac{\rho(1 + k_v\bar{\sigma}(R_p))}{k_r}) \otimes \mathbf{1}_2. \tag{4.60}$$

Equivalently, $||e_r(t)|| \leq \bar{\xi}$. □

We provide a bound over the states of second-order nonlinear multi-agent systems defined by (4.1). From (4.4) it follows that

$$||p_1|| = ||p_r - e_r|| \leq ||p_r|| + ||e_r||, \tag{4.61}$$

which yields

$$||p_1|| \leq \bar{P}_r + \bar{\xi}. \tag{4.62}$$

As the framework is considered a MIR graph, there exists at least one neighbor of the leader, say agent j. Therefore, from triangle inequality and (4.53), we have

$$\exists\, j \in N_1 \mid ||\tilde{p}_{j1}|| = ||p_j - p_1|| \geq ||p_j|| - ||p_1||. \tag{4.63}$$

From (4.53) and (4.63), we can write

$$\begin{aligned} ||p_j|| - ||p_1|| &\leq \sqrt{\rho + D^2}, \\ ||p_j|| &\leq ||p_1|| + \sqrt{\rho + D^2}, \\ ||p_j|| &\leq \bar{P}_r + \bar{\xi} + \sqrt{\rho + D^2}. \end{aligned} \tag{4.64}$$

Since the framework is rigid, there exists another vertex $k \in N_j$. Using (4.53) and (4.64) we have

$$||p_k|| \leq \bar{P}_r + \bar{\xi} + 2\sqrt{\rho + D}. \tag{4.65}$$

Thus, for all positions there is a bound ($\forall i \in V,\ \exists \bar{P}_i \mid ||p_i|| \leq \bar{P}_i$); equivalently, $||\mathbf{x}_1|| \leq ||\bar{P}||$, where $\bar{P} = [\bar{P}_1, ..., \bar{P}_N]^T$. From (4.13), and using triangle inequality, we have

$$\begin{aligned} ||\mathbf{x}_2|| &\leq ||\mathbf{s}|| + ||\tau||, \\ ||\mathbf{x}_2|| &\leq ||\mathbf{s}|| + ||u_s + \mathbf{1}_N \otimes (v_r + k_r e_r)||. \end{aligned} \tag{4.66}$$

Using inequalities (4.40), (4.48), and $||e_r(t)|| \leq \bar{\xi}$ we conclude

$$||\mathbf{x}_2|| \leq \rho(1 + k_v \bar{\sigma}(R_p)) + \sqrt{N}(\bar{V}_r + k_r \bar{\xi}) \triangleq \bar{V}. \tag{4.67}$$

Since the velocity of the target is considered to be bounded (Assumption 4.4), for $t \geq 0$ there exists a compact set of Ω where $\Omega = \{\mathbf{x} \mid ||\mathbf{x}_1|| \leq \bar{P}, ||\mathbf{x}_2|| \leq \bar{V}\}$.

The results presented below are a specific case of the main theorem, which pertains to Brunovsky form nonlinear multi-agent systems [39].

Corollary 4.1. *Let the required framework be modeled by an undirected MIR graph where each agent is described by a second-order nonlinear system in Brunovsky form as follows:*

$$\begin{aligned} \dot{p}_i &= v_i, \\ \dot{v}_i &= f_i(p_i, v_i) + u_i(t) + w_i(t), \quad i = 1, 2, ..., N. \end{aligned} \tag{4.68}$$

Select the control input signals as (4.22) and NN weights' norm tuning law as (4.24), under Assumptions 2.1, 2.2, 4.2 -4.5, choose $b \geq \sqrt{2}||\dot{v}_r||_\infty$, $c > 2$, and $\underline{g}_i = 1$. Then, for the initial conditions belonging to the compact set Ω_0, the NN weights' norm estimation and inter-agent distance errors are UUB. The leader tracks the target, and other agents maintaining the desired formation follow the leader.

Proof. Set $\underline{g}_i = 1$, then it is not difficult to see the proof of Theorem 4.1 still holds for a class of nonlinear multi-agent systems given as (4.68). □

Remark 4.3. *Inequalities (4.47) and (4.49) provide bounds for inter-agent distance errors and the NN weights' norm estimation errors. As the leader (first agent) tracks the moving target within a bounded trajectory, the leader's position remains bounded by (4.62). The control law guarantees the boundedness of inter-agent distance errors, and other agents remain in their desired formation.*

It has been shown that the velocities of agents remain bounded as the velocity of the target is bounded. Using the proposed control, and based on Assumptions 4.3-4.5, all positions and velocities of the agents remain bounded. We use this bounded region to form a compact set Ω where the NN approximation property holds.

Remark 4.4. *Signal γ_i in (4.23) has a discontinuous right-hand side part. Therefore, the existence of a general solution should be checked through differential inclusions. As the sign function is a bounded function, the Filippov solution exists, [8, 72]. Consequently, the time derivative of the Lyapunov function (4.21) belongs to a closed, upper semi-continuous set-valued map [73]. Thus, the Lyapunov function is continuously differentiable, and the proof is valid. Moreover, a hyperbolic tangent can be used in practical applications to alleviate the undesired chattering effect caused by the sign function.*

Remark 4.5. *The proposed control law guarantees that the multi-agent system (4.1) converges to the equilibrium within the set Ω_0. Thus, the distance errors remain in the invariant set Ω_0 [8] and $\tilde{p}_{ij} \neq 0$. Moreover, the multi-agent system (4.1) converges to the equilibrium inside this invariant set, thus preventing the flip ambiguity.*

4.4 Simulation Results

We conducted multiple simulations in order to evaluate the performance of the proposed method for distance-based formation control applied to second-order nonlinear multi-agent systems. In each example, the results of the proposed distance-based method are compared with the results of existing displacement-based methods. Also, to evaluate and quantify the performance of each method, a performance index is introduced.

Example 4.1. *Consider a nonlinear multi-agent system with $N = 5$ agents in a plane where the dynamics of each agent is given by*

$$\begin{aligned} \dot{p}_i(t) &= v_i(t), \\ \dot{v}_i(t) &= \begin{pmatrix} c_{i1} v_{i1}(t) sin(d_{i1} p_{i1}(t)) \\ c_{i2} v_{i2}(t) cos(d_{i2} p_{i2}(t)) \end{pmatrix} + u_i(t) + w_i(t) \quad i = 1, 2, ..., 5. \end{aligned} \tag{4.69}$$

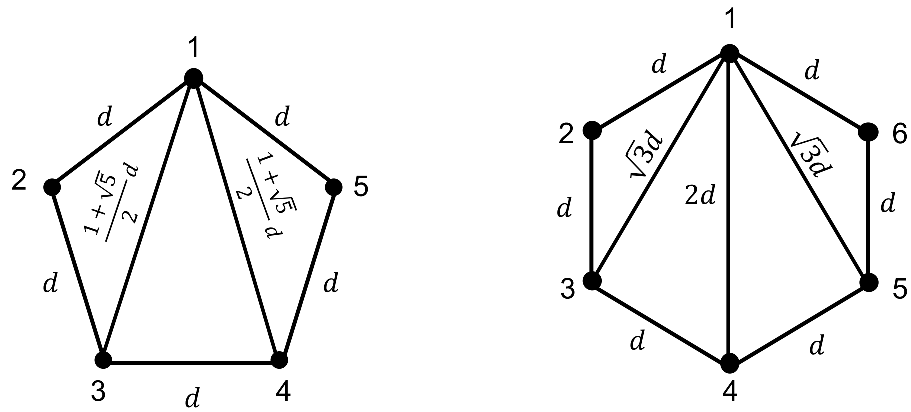

Figure 4.3: Communication topology and desired distances of multi-agent systems: MIR frameworks of five agents (left) and six agents (right) in 2D.

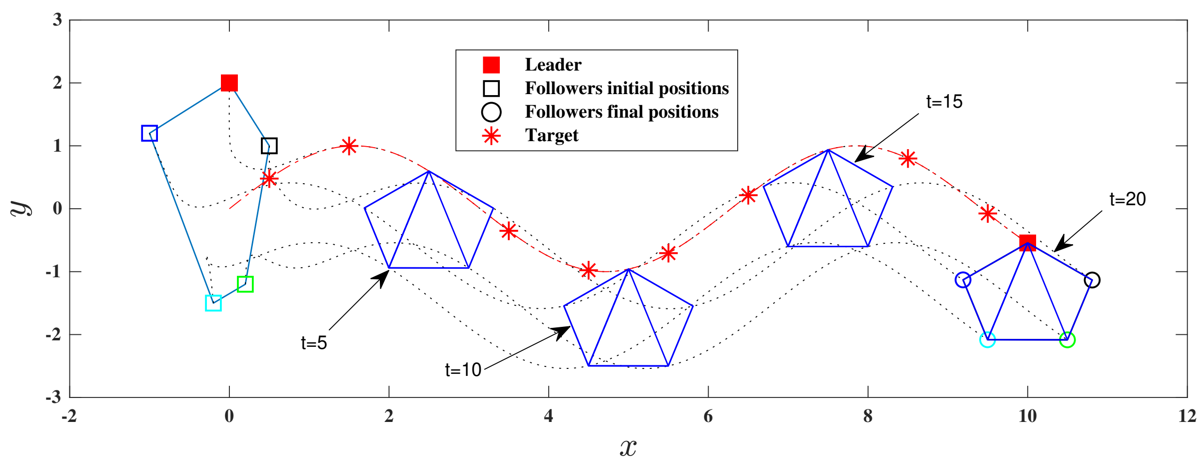

Figure 4.4: Desired formation of equilateral pentagon with side length $d = 1$.

The goal is to form the desired formation, shown in Figure 4.3 (left), while the agents follow the leader which is tracking a target within a bounded trajectory. To this end, the proposed control law in Corollary 4.1 is applied.

Vectors $p_i(t) = [p_{i1}, p_{i2}]^T$ *and* $v_i(t) = [v_{i1}, v_{i2}]^T$ *represent the location and velocity of* i*-th agent in* x *and* y *directions, respectively. Parameters* c_{i1}, c_{i2}, d_{i1}, d_{i2} *of each agent are given in Table 4.1. The initial conditions for these five agents are:* $p_1(0) = (0, 2.1)^T$, $v_1(0) = (0.5, 0.5)^T$, $p_2(0) = (-1, 1.2)^T$, $v_2(0) = (-1, 0.8)^T$, $p_3(0) = (-2, -1.5)^T$, $v_3(0) = (0.3, 0.5)^T$, $p_4(0) = (0.2, -1.2)^T$, $v_4(0) = (0.5, 1)^T$, $p_5(0) = (0.5, 1)^T$, $v_5(0) = (-1, -1)^T$. *The disturbance* $w_i = 0.1cos(t)\delta(t)$, *where* $\delta(t) \in \mathbb{R}^2$ *is a random variable with the normal distribution* $\mathcal{N}(0, 1)$ *borrowed*

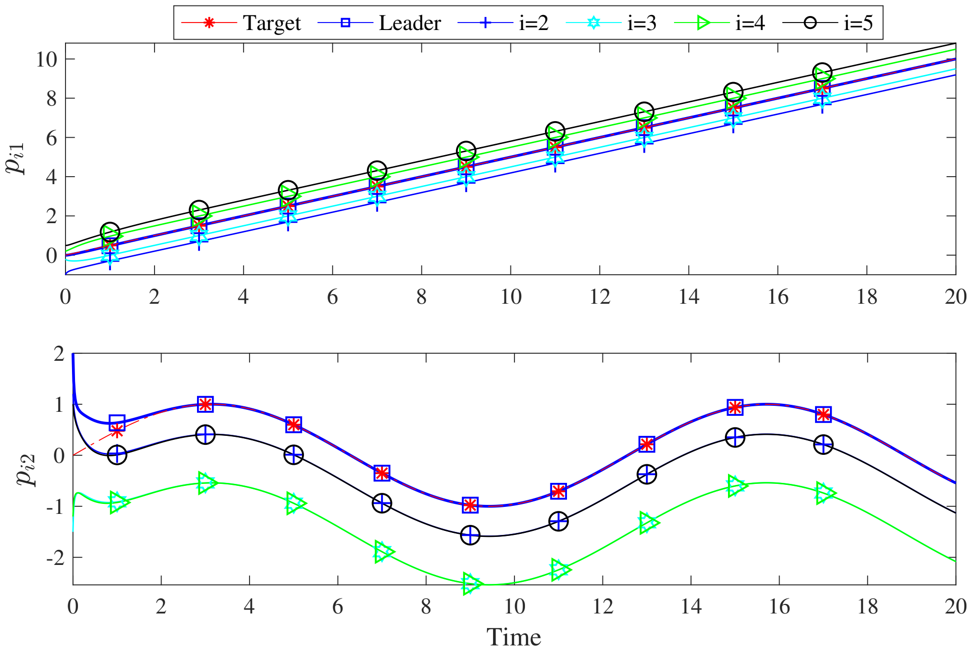

Figure 4.5: Trajectories of agents and the target along x and y directions.

from [15, 74]. The target velocity and initial position are $v_r = [0.5, 0.5cos(t/2)]^T$ and $p_r(0) = [0, 0]^T$ respectively.

We selected constants $b = 3$ and $k_r = 2$. RBFNN is selected with 9 neurons, centers μ_j's are evenly spaced for each agent, and the values of constants are: $\kappa = 0.5$, $F_i = I_9$, $c = 5$, $k_v = 0.5$. The desired distances and communication topology are given in Figure 4.3 (left) with $d = 1$. Figures 4.4-4.8 show results of the proposed control law. Figure 4.4 shows how agents form an equilateral pentagon where each side is equal to the desired distance. Figure 4.5 represents the trajectories of each agent and the target in x and y directions. The velocity of each agent and the target in x and y directions are shown in 4.6.

In order to compare the results with a displacement-based method, the modified version of [14] is simulated. We selected the following parameter for the proposed controller [14]: number of neurons is 9, $\varphi_m = 1$, $\kappa = 0.5$ and $c = 91.21$. We compared distance (edge) errors in Figure 4.7 and the target tracking errors of the leader along x and y directions and its time derivative in

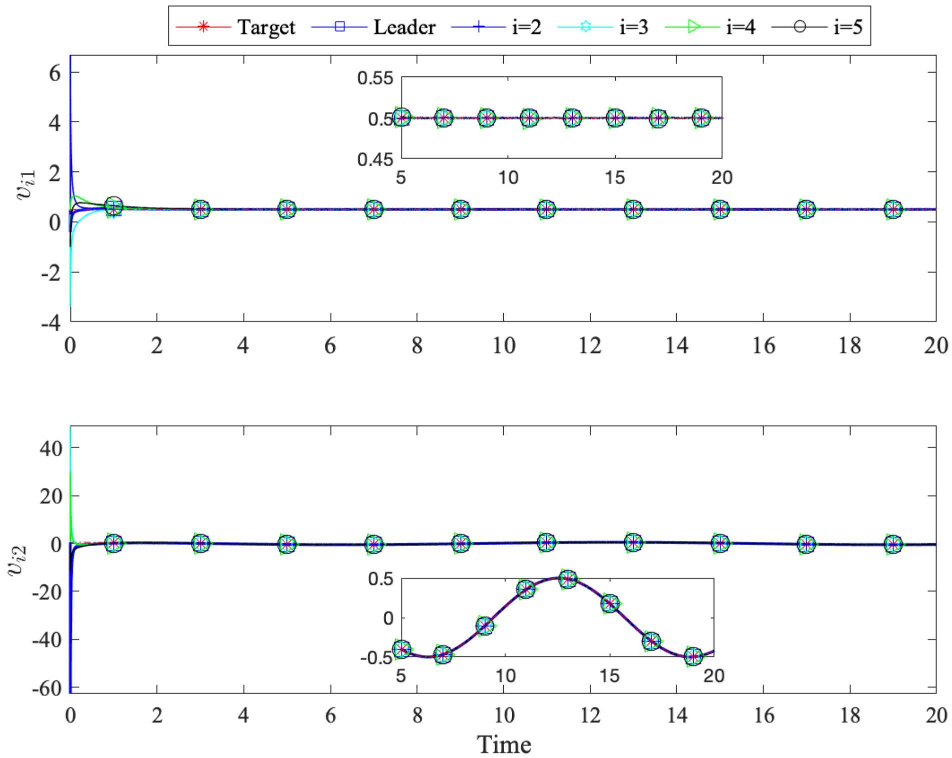

Figure 4.6: Speeds of agents and the target along x and y directions.

Figure 4.8. We use an average absolute formation distance error (AFDE) $\zeta(t)$ function [63]:

$$\zeta(t) = \frac{1}{|E|} \sum_{(i,j)\in E} |(||\tilde{p}_{ij}|| - d_{ij})|, \tag{4.70}$$

which is plotted in Figure 4.9. The proposed method has an improved AFDE compared to the displacement method.

Table 4.1: Values of c_{i1}, c_{i2} and d_{i1}, d_{i2} in the $i - th$ agent.

i	1	2	3	4	5
c_{i1}	0.2	0.4	-0.6	0.7	-0.8
c_{i2}	-0.3	0.6	0.5	0.5	0.6
d_{i1}	0.4	0.7	0.3	-0.4	-0.7
d_{i2}	0.3	-0.4	0.4	0.8	-0.5

Example 4.2. *Consider a multi-agent system consisting of $N = 6$ two-link robot arms. The goal is*

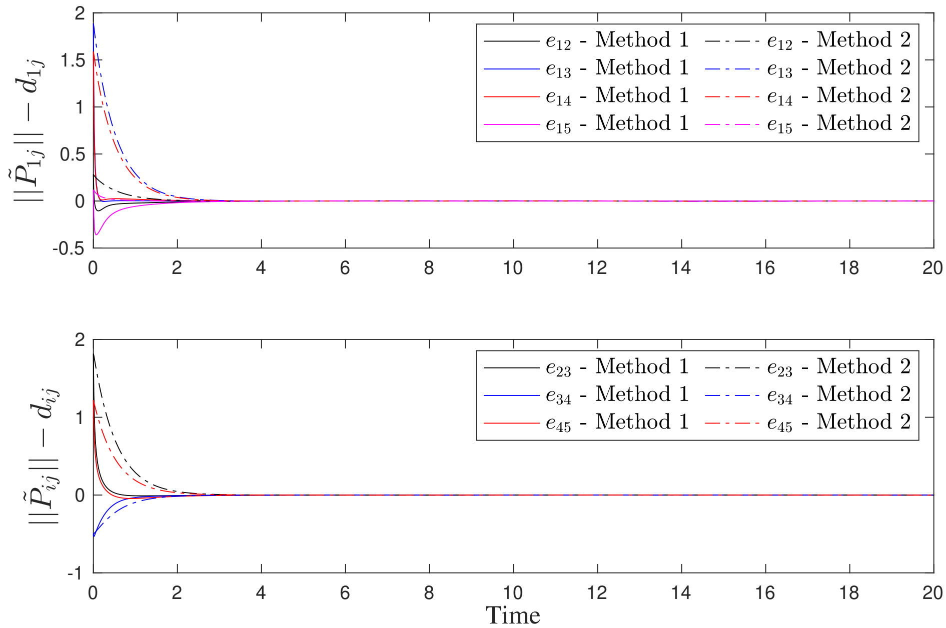

Figure 4.7: The distance errors $e_{ij},\ (i,j) \in E$ of the proposed method (Method 1) and the modified displacement-based method (Method 2) [14].

to form the desired formation, shown in Figure 4.3 (right), while the agents follow the leader that tracks a target within a bounded trajectory. The dynamics of each robot arm is given by [60]

$$\begin{aligned} &\dot{q}_{i1} = q_{i2}, \\ &M_i(q_{i1})\dot{q}_{i2} + V_i(q_{i1}, q_{i2})q_{i2} + G_i(q_{i1}) + \tau_{id} = \tau_i, \\ &i = 1, 2, ..., 6, \end{aligned} \tag{4.71}$$

where the vector $q_{i1} = [q_{i11}, q_{i12}]^T \in R^2$ and $q_{i2} = [q_{i21}, q_{i22}]^T \in R^2$ represent the position and velocity in x and y directions respectively. The dynamics of a two-link robot arm can be described as (4.71) where inertia matrix $M_i(q_{i1})$, centripetal and Coriolis matrix $V_i(q_{i1}, q_{i2})$ and gravitational vector $G_i(q_{i1})$ are defined as follows [27]:

$$M_i(q_{i1}) = \begin{bmatrix} M_{i11} & M_{i12} \\ M_{i21} & M_{i22} \end{bmatrix} \in R^{2\times 2}, \tag{4.72}$$

where

$M_{i11} = (m_{i1} + m_{i2})r_{i1}^2 + 2m_{i2}r_{i1}r_{i2}cos(q_{i12}),$

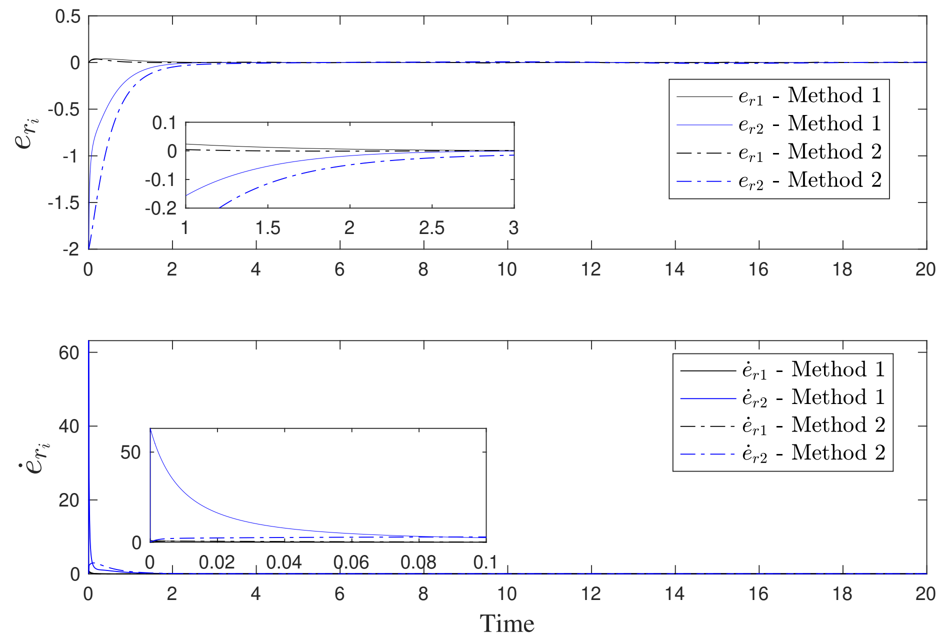

Figure 4.8: The target tracking error of the leader and its time derivative for the proposed method and the modified displacement-based method [14] along x and y directions.

$M_{i12} = M_{i21} = m_{i2}r_{i2}^2 + m_{i2}r_{i1}r_{i2}cos(q_{i12}),$

$M_{i22} = m_{i12}r_{i12}^2.$

$$V_i(q_{i1}, q_{i2}) = \begin{bmatrix} V_{i11} & V_{i12} \\ V_{i21} & V_{i22} \end{bmatrix} \in R^{2\times 2}, \tag{4.73}$$

where

$V_{i11} = -m_{i2}r_{i1}r_{i2}sin(q_{i12})q_{i22},$

$V_{i12} = -m_{i2}r_{i1}r_{i2}sin(q_{i12})q_{i22} - m_{i2}r_{i1}r_{i2}sin(q_{i12})q_{i21},$

$V_{i21} = m_{i2}r_{i1}r_{i2}sin(q_{i12})q_{i22},$

$V_{i22} = 0.$

$$G_i(q_{i1}, q_{i2}) = (G_{i11}, G_{i12})^T \in R^2. \tag{4.74}$$

where $G_{i11} = (m_{i1}+m_{i2})gr_{i1}cos(q_{i11}) + m_{i2}gr_{i2}cos(q_{i11}+q_{i22})$*, and* $G_{i12} = m_{i2}gr_{i2}cos(q_{i21}+q_{i12})$*. In (4.71), the variable* τ_{id} *represents a constant bounded disturbance in the dynamics of each two-arm robot. The parameters of the each robot arm are* $g = 9.8m/s^2$*,* $r_{i1} = 1m$*,* $r_{i1} = 1m$*,* $m_{i2} = 1kg$*, and* $m_{i2} = 1kg$*,* $\tau_{id} = [0.1, 0.1]^T$ $(i = 1, ..., 6)$*. The initial conditions of all agents are*

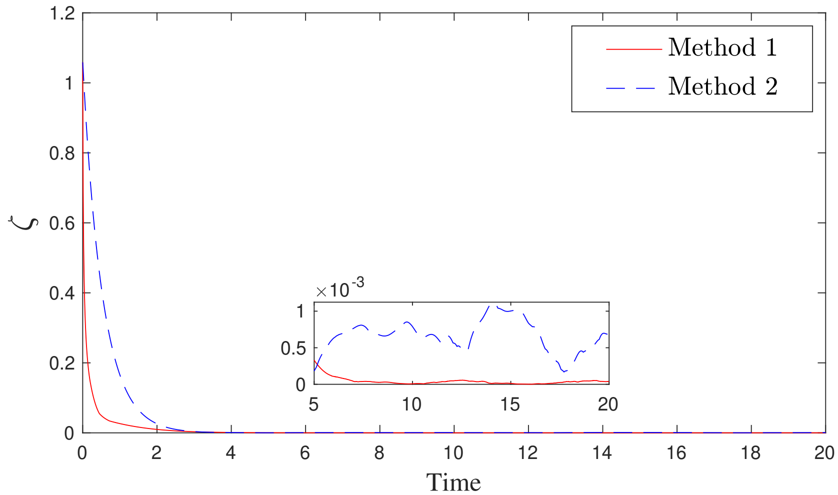

Figure 4.9: Performance comparison (AFDE) between the proposed distance-based method and the modified displacement-based method [14].

given in Table 4.2. The target velocity and initial position are $v_r = [\frac{1}{2\pi}cos(\frac{1.5\pi}{20}t), \frac{1}{2\pi}sin(\frac{1.5\pi}{20}t)]^T$ *and* $p_r(0) = [0, 0]^T$*, respectively. We selected* $b = 2$ *and* $k_r = 1$.

Table 4.2: Initial values of q_{i1}, q_{i2} in the i-th agent

i	1	2	3	4	5	6
q_{i11}	0	2.5	2	0.7	-1.7	-1.9
q_{i12}	2.1	0	-1.1	-1.8	-1	1
q_{i21}	0.3	0.8	0	-0.5	0.5	0.4
q_{i22}	0.3	0	0.7	-1	1	-0.5

We applied an RBFNN with 81 neurons and activation function centers, μ_j*, evenly spaced for each agent. One can obtain* $\underline{g}_i = 1/[(m_{i1}+m_{i2})r_{i1}^2 + 2m_{i2}r_{i2}^2 + 3m_{i2}r_{i1}r_{i2}]$ *for* $\forall i = 1, ..., 6$ *[27]. The values of the constants are* $\kappa = 0.2, \Pi_i = 1, c = 20, k_v = 0.3$*, and the desired distance is* $d = 1.6$ *for all edges. Figures 4.10-4.14 show the simulation results of the proposed control law (4.22) applied to a nonlinear multi-agent system. Figure 4.10 indicates how these agents form an equilateral hexagon where the desired distance for each side is* $d = 1.6$*. Figure 4.11 represents the trajectories of each agent and the target in* x *and* y *directions. The velocity of each agent and the target in* x *and* y *directions are shown in Figure 4.12.*

To compare the results with the displacement-based method, the modified version of [28] has

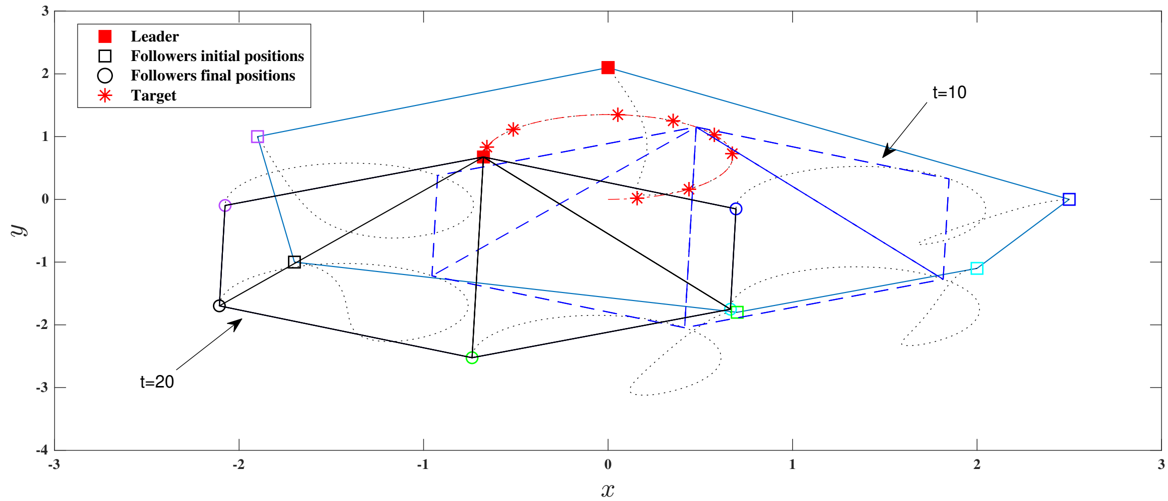

Figure 4.10: Desired formation of equilateral hexagon in 2D with side length $d = 1.6$.

been simulated. By applying this method and adding constant displacements of the desired positions [20, p. 127] to the formation control problem, we obtain a shape-based control with distance errors shown in Figure 4.13. We selected the following parameter for the used controller in [28]: number of neurons is 81, $\varphi_m = 1$, $\kappa = 0.3$ *and* $k_i = 650$, $\kappa = 0.7$ *and* $\sigma_i = 0.3$.

Also, target tracking errors of the leader along x *and* y *coordinates and time derivatives for both methods are shown in Figure 4.14. We use AFDE to compare our results with [28], as shown in Figure 4.15. It can be seen that the proposed control method improves the AFDE when applied to an input-affine, nonlinear multi-agent system.*

4.5 Conclusion

In this chapter, we proposed a control method for distance-based formation control and target tracking for nonlinear multi-agent systems with unknown dynamics and disturbance. We considered second-order nonlinear agents that are connected through an undirected graph network. An RBFNN compensated for the agent's unknown dynamics. The proposed control law was based on the target tracking backstepping controller and is paired with a stable NN tuning law that ensures the stability of the obtained formation. The stability results showed that distance error dynamics and NN weights' norm estimation error were UUB. Simulation results were provided to illustrate the performance and effectiveness of the proposed method. The performance index has been introduced to

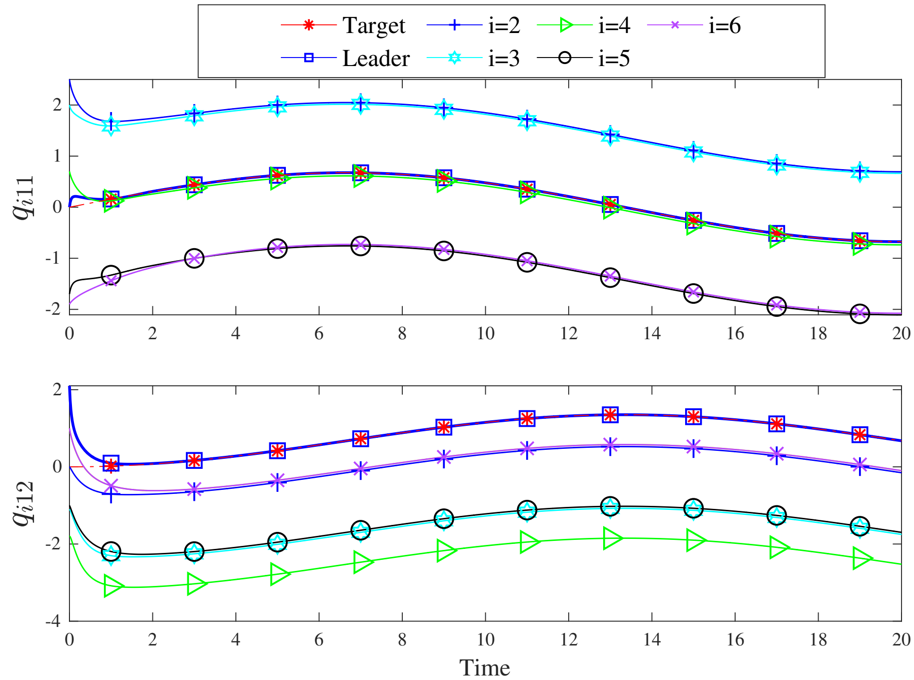

Figure 4.11: Trajectories of the agents and the target along x and y directions.

quantify the comparison with two existing displacement control methods. We demonstrated that the proposed method improves the system performance compared with two other displacement-based methods.

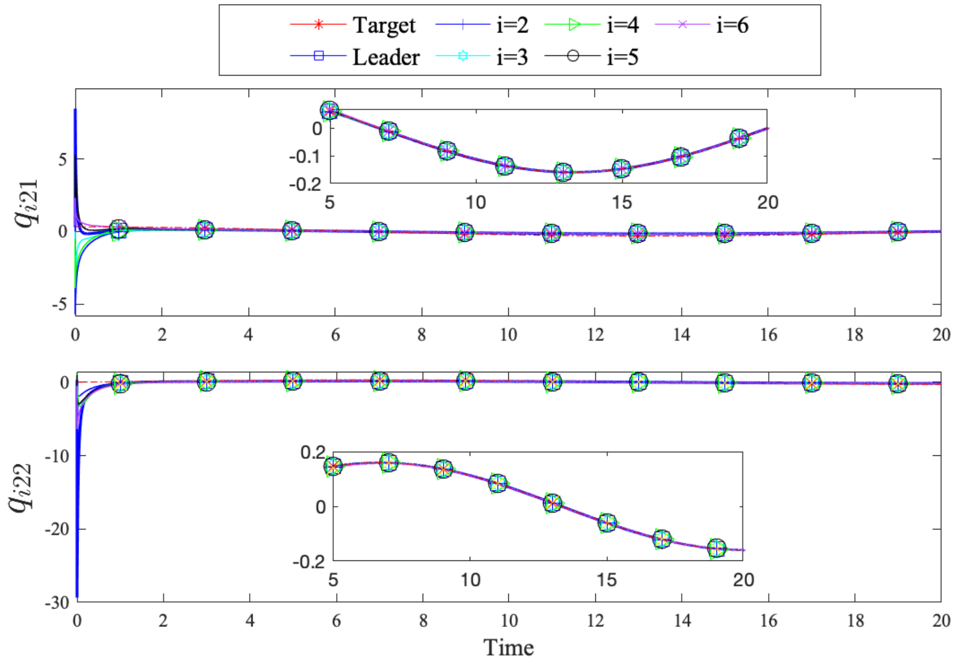

Figure 4.12: Velocities of the agents and the target along x and y directions.

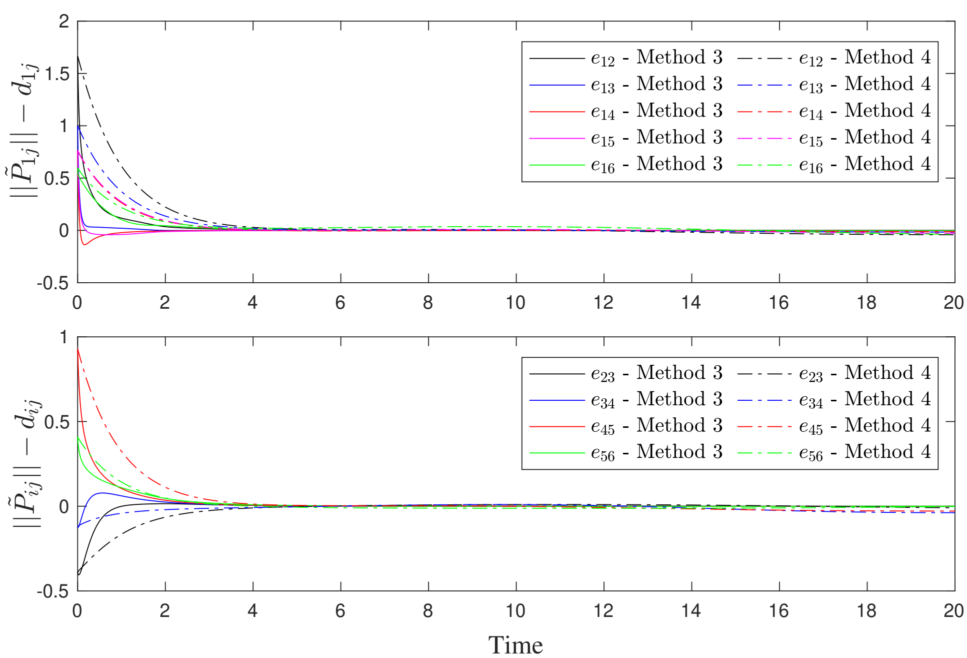

Figure 4.13: The distance errors $e_{ij},\ (i,j) \in E$ of the proposed method in Theorem 4.1 (Method 3) and the modified displacement-based method (Method 4) [28].

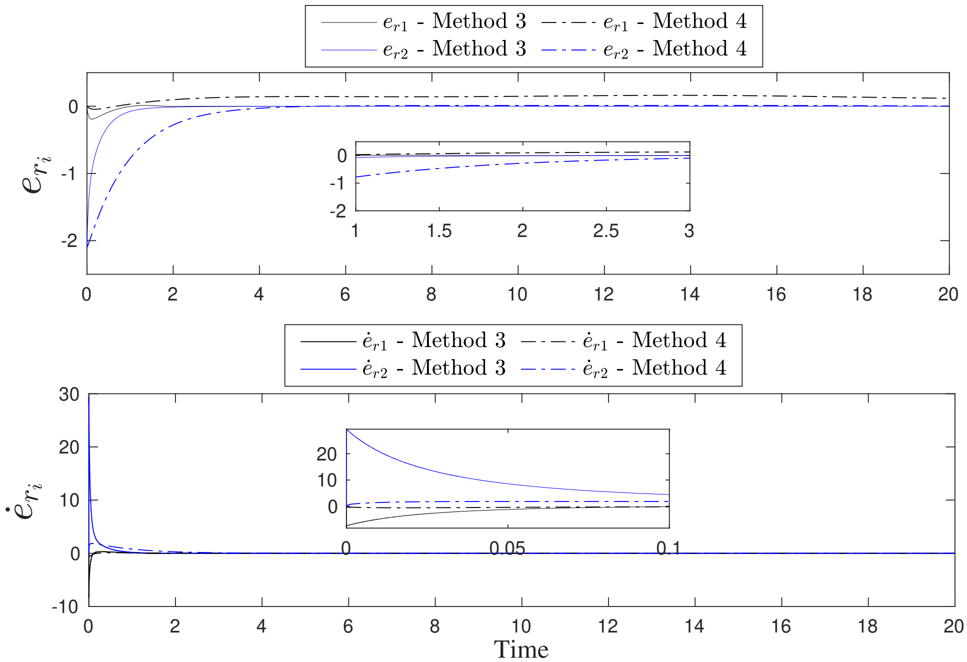

Figure 4.14: Target tracking error of the leader and its time derivative of the proposed method in Theorem 4.1 (Method 3) and the modified displacement-based method (Method 4) [28] along x and y directions.

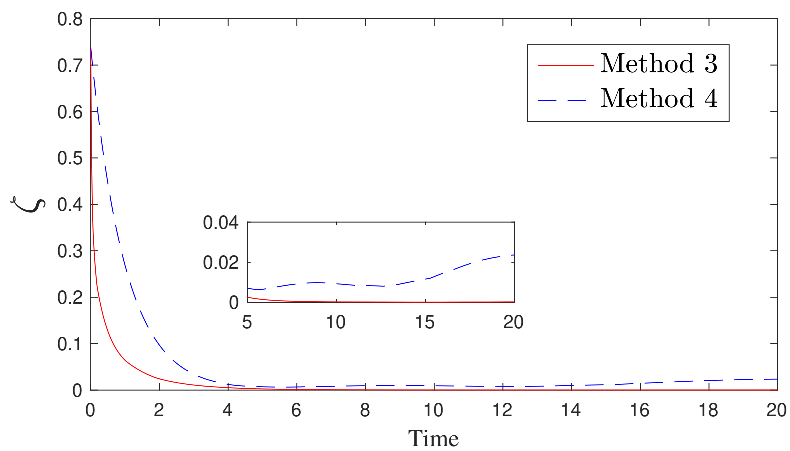

Figure 4.15: Performance comparison (AFDE) between the proposed method in Theorem 4.1 (Method 3) and the modified displacement-based method (Method 4) [28].

Chapter 5

Undirected Formation Control of Second-Order Nonlinear Multi-agent Systems With State Time Delay

5.1 Introduction

This chapter focuses on the formation control of a general class of input-affine nonlinear multi-agent systems using inter-agent distance with unknown nonlinearity, time delay on the dynamical states, and disturbance. To compensate for the time-delayed function, there is a time-dependent control gain, which differs from the control design in Chapter 4. Moreover, the disturbance as well as the assumption for the boundedness of the disturbance are state-dependent. A normalized rigidity matrix is utilized in controller design.

5.1.1 Related Works on Formation Control of Nonlinear Multi-Agent Systems with State Time Delay

Existing distance-based methods, such as [7, 46, 58], use single- or double-integrator dynamics for the system. We consider nonlinear dynamics to model each agent. The formation control problem of nonlinear multi-agent systems with a state time delay function was studied in [53, 60, 75, 76], where the authors considered a bounded time delay for a nonlinear multi-agent system. In contrast with these methods, where the Laplacian matrix has been used to express the relation among the agents, our technique is based on rigid graph theory. While the formation control problems can be modeled with standard graph theory, a rigid graph theory offers modeling that minimizes the number of edges/distances one needs to control to achieve the desired formation.

The objectives are to keep agents, modeled by second-order nonlinear systems and state time delay, at pre-specified distances from each other and to track the target within a bounded trajectory. To achieve this, we propose a new control design for the nonlinear multi-agent systems relying on the backstepping control and rigid graph theory. The unknown nonlinear part of the system dynamics and the disturbance are approximated using NN, where an RBFNN is used to estimate the unknown dynamics. To achieve target tracking, the leader tracks a target within a bounded trajectory while the rest of the agents maintain the desired formation and follow the leader. The main contributions are:

(i) The Lyapunov function is selected for the formation control problem and target tracking of second-order nonlinear multi-agent systems. This chapter is the first contribution proposing a formation control using inter-agent distance for nonlinear multi-agent systems with state time delay and disturbance to the best of the author's knowledge. Compared with existing methods in [53, 60], the system's dynamics is not limited to first-order nonlinear systems.

(ii) Compared with the existing methods [53, 60, 75, 76], which use the Laplacian matrix to express the interactions among the agents, we use rigid graph theory to represent those relations for a general class of nonlinear multi-agent systems.

(iii) The smallest singular value of the normalized rigidity matrix for a MIR framework is utilized to design the neuro-adaptive controller using the backstepping technique to address the formation control problem of nonlinear multi-agent systems.

5.2 Problem Formulation

Consider a second-order nonlinear multi-agent system consisting of N agents. The dynamics of the i-th agent is given by

$$\begin{aligned} \dot{p}_i =& v_i, \\ \dot{v}_i =& f_i(p_i, v_i) + g_i(p_i, v_i)u_i(t) + h_i(p_i(t-\tau_i), v_i(t-\tau_i)) + w_i(p_i, v_i, t), \end{aligned} \tag{5.1}$$

where the vectors $p_i \in \mathbb{R}^2$, $v_i \in \mathbb{R}^2$ represent the position and velocity of each agent respectively, $f_i(.) \in \mathbb{R}^2$, $h_i(.) \in \mathbb{R}^2$ are the unknown smooth vector functions considered to be continuously differentiable and locally Lipchitz, τ_i is an unknown time delay, $u_i \in \mathbb{R}^2$ is the control input, and $w_i(.) \in \mathbb{R}^2$ is a disturbance affecting each agent. Matrix $g_i(p_i, v_i), \mathbb{R}^4 \to \mathbb{R}^{2\times 2}$ is an unknown matrix.

In target tracking, we consider the *first* agent to be the leader, while the remaining agents are followers. The control objectives are: (i) the leader tracks the target; (ii) the distance between neighboring agents i and j converges to desired distance d_{ij}:

$$||p_i - p_j|| \to d_{ij} \quad as\, t \to \infty, (i,j) \in E, \tag{5.2}$$

where the d_{ij}'s are positive and bounded by $\max(d_{ij}) < D, \forall (i,j) \in E$, with a fixed bound D.

We establish standard assumptions [14, 35, 60, 76] as follows.

Assumption 5.1. *The vector function $h_i(.)$ is considered to be bounded, i.e., there exists a known function Υ_i such that $||h_i(x_i(t))|| \leq \Upsilon_i(x_i(t))$.*

Assumption 5.2. *Disturbance $w_i(x_i(t), t)$ is an unknown vector function that satisfies $||w_i(x_i, t)|| \leq \rho_i(x_i(t))$, where $\rho_i(x_i(t))$ is a positive smooth function.*

Assumption 5.3. *Time-invariant delay τ_i is unknown and bounded by $||\tau_i|| \leq \tau_M$, with a fixed bound τ_M for $i = 1, ..., N$.*

Note that we consider the Assumptions 2.1,2.2, 4.1, and 4.3-4.5 are also valid here.

5.3 Controller Design

The distance error for the multi-agent system (5.1), modeled by an undirected graph, is given by $e_{ij} = ||p_{ij}|| - d_{ij}$. The distance error dynamics can be derived as (4.7). Let us define an energy function

$$M_1(e) = \frac{1}{2} \sum_{(i,j)\in E} e_{ij}^2. \tag{5.3}$$

Considering (4.10), Definition 2.5, and by taking a time derivative of (5.3), $\dot{M}_1$ is given by

$$\dot{M}_1 = \sum e_{ij} \frac{p_{ij}^T (v_i - v_j)}{||p_{ij}||} = \beta^T(e) \bar{R}_p \mathbf{x}_2, \tag{5.4}$$

where $\beta(e) = (..., e_{ij}, ...) \in \mathbb{R}^{|E|}$ for $(i,j) \in E$. Moreover, $\mathbf{x}_1 = [p_1^T, ..., p_N^T]^T$ and $\mathbf{x}_2 = [v_1^T, ..., v_N^T]^T \in \mathbb{R}^{2N}$ is defined as an overall velocity vector for all agents. Note that $\bar{R}_p$ is the normalized rigidity matrix explained in Section 2.3.1. Using the backstepping technique [7], we define $\mathbf{s} = [s_1^T, ..., s_N^T]^T \in \mathbb{R}^{2N}$, $\mathbf{s} = \mathbf{x}_2 - \nu$, where ν is an auxiliary variable given by

$$\nu = u_s + \mathbf{1}_N \otimes (v_r + k_r e_r), \tag{5.5}$$

with $u_s = -k_v \bar{R}_p^T \beta(e)$ and k_v being a positive constant. From (5.5), one has

$$\begin{aligned} \nu_i &= -k_v \sum_{j\in N_i} (\frac{p_{ij}}{||p_{ij}||} e_{ij}) + (v_r + k_r e_r), \\ s_i &= v_i + k_v \sum_{j\in N_i} (\frac{p_{ij}}{||p_{ij}||} e_{ij}) - (v_r + k_r e_r). \end{aligned} \tag{5.6}$$

Achieving the desired formation in (5.5) relies on u_s, while $\mathbf{1}_N \otimes (v_r + k_r e_r)$ is the term for tracking of the target by the leader and other agents.

Let us define the potential function $V_1 = M_1 + M_2$, where $M_2 = \frac{1}{2}\mathbf{s}^T\mathbf{s} = \frac{1}{2}\sum_{i=1}^N s_i^T s_i$. Taking time-derivative of V_1 and (5.5), one has

$$\dot{V}_1 = \beta^T(e)\bar{R}_p\mathbf{x}_2 + \mathbf{s}^T\dot{\mathbf{s}} = \beta^T(e)\bar{R}_p\nu + \mathbf{s}^T[\dot{\mathbf{x}}_2 + \bar{R}_p^T\beta(e) - \dot{\nu}]$$
$$= -k_v\beta^T(e)\bar{R}_p\bar{R}_p^T\beta(e) + \sum_{i=1}^{N} s_i^T[f_i(x_i) + g_i(x_i)u_i + h_i(x_i(t-\tau_i)) + w_i(x_i,t) \tag{5.7}$$
$$+ \sum_{j\in N_i}(\frac{p_{ij}}{||p_{ij}||}e_{ij}) - \dot{\nu}_i],$$

where $x_i = [p_i^T, v_i^T]^T$. Using Assumptions 5.1-5.2, and applying Cauchy's and Young's inequalities one has

$$\begin{aligned} s_i^T h_i(x_i(t-\tau_i)) &\leq \frac{||s_i||^2}{2} + \frac{\Upsilon_i^2(x_i(t-\tau_i))}{2}, \\ s_i^T w_i(x_i,t) &\leq \frac{1}{2} + \frac{||s_i||^2\rho_i^2(x_i(t))}{2}. \end{aligned} \tag{5.8}$$

Substituting (5.8) into (5.7), yields

$$\dot{V}_1 \leq -k_v\beta^T(e)\bar{R}_p\bar{R}_p^T\beta(e) + \sum_{i=1}^{N}\Bigg(s_i^T[f_i(x_i) - \dot{\nu}_i + (\sum_{j\in N_i}\frac{p_{ij}}{||p_{ij}||}e_{ij})] + \frac{||s_i||^2\rho_i^2(x_i(t))}{2} + \frac{||s_i||^2}{2}$$
$$+ \frac{\Upsilon_i^2(x_i(t-\tau_i))}{2} + s_i^T g_i(x_i)u_i\Bigg) + \frac{N}{2}. \tag{5.9}$$

To compensate for the unknown function $h_i(x_i(t-\tau_i))$, which is upper bounded by $\Upsilon_i(x_i)$, we add the following term to potential function V_1

$$M_3 = \tfrac{1}{2}\textstyle\sum_{i=1}^{N}\int_{t-\tau_i}^{t}\Upsilon_i^2(x_i(z))dz, \tag{5.10}$$

and its time-derivative is given by

$$\dot{M}_3 = \tfrac{1}{2}\textstyle\sum_{i=1}^{N}\left(\Upsilon_i^2(x_i(t)) - \Upsilon_i^2(x_i(t-\tau_i))\right). \tag{5.11}$$

Let us define potential function V_2 as $V_2 = V_1 + M_3$. Taking time-derivative of V_2, and from inequality (5.9) and equation (5.11) yields

$$\dot{V}_2 \leq -k_v\beta^T(e)\bar{R}_p\bar{R}_p^T\beta(e) + \sum_{i=1}^{N}\Bigg(s_i^T[T_i(s_i,x_i) - \dot{\nu}_i\sum_{j\in N_i}(\frac{p_{ij}}{||p_{ij}||}e_{ij})] + \frac{||s_i||^2}{2} + \frac{\Upsilon_i^2(x_i(t))}{2}$$
$$+ s_i^T g_i(x_i)u_i\Bigg) + \frac{N}{2}, \tag{5.12}$$

with $T_i(s_i,x_i) = f_i(x_i) + \frac{1}{2}s_i\rho_i^2(x_i(t))$.

Define $\check{\gamma} = \bar{R}_p^T\beta(e) \in \mathbb{R}^{2N}$, where $\check{\gamma} = [\check{\gamma}_1, ..., \check{\gamma}_N]^T$ with $\check{\gamma}_i = \sum_{j\in N_i}(\frac{p_{ij}}{||p_{ij}||}e_{ij})$. Motivated by [60], let $\{p_i, v_i\} \in \Omega_{x_i}$ be a compact set, then $\Omega_{\varphi_i} \subset \Omega_{x_i}$, where $\Omega_{\varphi_i} = \{s_i \mid ||s_i|| < o_i\}$ with o_i chosen as a small arbitrary constant. As Ω_{φ_i} is an open set, its complement set, $\Omega_{\varphi_i}^0 = \Omega_{x_i} - \Omega_{\varphi_i}$, is a compact set. The set Ω_{x_i} is the compact set in which the NN can approximate the unknown dynamics of an agent.

We propose the following control law for the multi-agent system (4.1)

$$u_i = \begin{cases} -c_i(t)s_i - \frac{1}{\underline{g}_i}\hat{\varpi}_i^T||\varphi_i(s_i,x_i)||^2 s_i - \gamma_i - (\frac{1}{2\underline{g}_i})s_i^{-1}\Upsilon_i^2(x_i(t)), & s_i \in \Omega_{\varphi_i}^0 \\ \mathbf{0}, & s_i \in \Omega_{\varphi_i} \end{cases} \tag{5.13}$$

where $\hat{\varpi}_i$ is the current estimation of ϖ_i, $s_i^{-1} = s_i/||s_i||^2$, control gain $c_i(t) > 0$, and γ_i is given by

$$\gamma_i = \frac{1}{\underline{g}_i}(||\check{\gamma}_i||^2 + ||k_r\dot{e}_r - k_v\dot{\check{\gamma}}_i||^2)s_i + \frac{b}{\underline{g}_i}\,sgn(s_i), \tag{5.14}$$

with $b \geq \sqrt{2}||\dot{v}_r||_\infty$. Agents' NN tuning law is given by

$$\dot{\hat{\varpi}}_i = \Pi_i||\varphi_i(x_i,s_i)||^2\,||s_i||^2 - \kappa_i\Pi_i\hat{\varpi}_i, \tag{5.15}$$

where $\kappa_i > 0$ is a constant and Π_i is a positive constant.

5.3.1 Stability Analysis

Theorem 5.1. *Let an undirected MIR graph model the required framework. Under Assumptions 2.1, 2.2, 4.1, 4.3-4.5, and 5.1-5.3, select the control input (5.13), $b \geq \sqrt{2}||\dot{v}_r||_\infty$, adaptive NN weights tuning law (5.15), and the control gain $c_i(t)$ as*

$$c_i(t) = \frac{\Gamma_i}{\underline{g}_i}\Big(\frac{1}{2||s_i||^2}\int_{t-\tau_M}^{t} \Upsilon_i^2(x(z))dz + \frac{k_c+3}{\Gamma_i}\Big), \tag{5.16}$$

where $-k_v\underline{\sigma}(\bar{R}_p) \leq -\frac{\underline{\Gamma}}{2}$, $\kappa_i \geq \underline{\Gamma}\Pi_i^{-1}$, and $k_c \geq \underline{\Gamma}$, $\underline{\Gamma} = min\{\Gamma_1, ..., \Gamma_N\}$. Then, the inter-agent distance errors and NN weights matrix estimation errors are UUB for initial conditions that belong to the compact set Ω_0:

$$\begin{aligned}\Omega_0 =& \{\mathbf{x}_1(0), \mathbf{x}_2(0), \hat{W}(0), p_r(0) | p_r(0) \in \Omega_r, \mathrm{d}(\mathbf{x}_1, \mathrm{Iso}(F^*)) < \mathrm{d}(\mathbf{x}_1, \mathrm{Amb}(F^*)),\\ & \sum_{(i,j)\in E^*} (||p_{ij}||^2 - d_{ij}^2)^2 \leq \delta \},\end{aligned} \tag{5.17}$$

where δ is a small positive constant.

Proof. The error dynamics with respect to e_{ij} and s_i in a closed loop system with (5.13)-(5.15) has right-hand side discontinuity because of $sgn(s_i)$ in (5.14). We choose the non-smooth Lyapunov function candidate $V = V_2 + M_4$, with $M_4 = \frac{1}{2}\tilde{\varpi}^T F^{-1}\tilde{\varpi}$, $F = \Pi = diag(\Pi_i)$ (see 4.18 and (4.21). Let $\dot{\varsigma}_i = \mathcal{F}_i(\varsigma_i, t)$ be the closed loop system where $\varsigma_i = [e_{ij}, s_i]$, then $\mathcal{F}_i(\varsigma_i, t)$ is continuous everywhere except in the set $\{(\varsigma_i, t) \mid ||s_i|| < o_i\}$. For this system Filippov solution exists by satisfying differential inclusion $\dot{\varsigma}_i \in K_i[\mathcal{F}_i](\varsigma_i, t)$ where $K_i[\mathcal{F}_i](\varsigma_i, t)$ is an upper semi-continuous, nonempty, set-valued map [8, p. 171]. Then, the time derivative of V is given by

$$\begin{aligned}\dot{V} &\overset{a.e.}{\in} \sum_{i=1}^{N} \frac{\partial V}{\partial \varsigma_i} K_i[\mathcal{F}_i](\varsigma_i, t)\\ &\subset -k_v\bar{R}_p\beta^T(e)\beta(e)\bar{R}_p^T + \sum_{i=1}^{N}\Bigg(s_i^T T_i(s_i, x_i) + \frac{\Upsilon_i^2(x_i(t))}{2} + \frac{||s_i||^2}{2} + s_i^T\Big(g_i(x_i)\big[-c_i(t)s_i\\ &- \frac{1}{\underline{g}_i}\hat{\varpi}_i^T||\varphi_i(s_i, x_i)||^2 s_i + (\frac{1}{\underline{g}_i})(-\sum_{j\in N_i}\frac{p_{ij}}{||p_{ij}||}e_{ij} + \gamma_i) - (\frac{1}{2\underline{g}_i})s^{-1}\Upsilon_i^2(x_i(t))\big] + \sum_{j\in N_i}\frac{p_{ij}}{||p_{ij}||}e_{ij} - \dot{\nu}_i\Big)\Bigg)\\ &+ \frac{N}{2} + \tilde{\varpi}^T F^{-1}\dot{\tilde{\varpi}}.\end{aligned} \tag{5.18}$$

Similar to (4.18), one can write

$$\sum_{i=1}^{N} s_i{}^T T_i(s_i, x_i) \leq \sum_{i=1}^{N} \Big(||W_i||_F^2 (||s_i||\ ||\varphi_i(x_i, s_i)||)^2 + \frac{1}{4\varrho_i^2} + ||s_i||^2 + \frac{1}{4\alpha_i^2}||\epsilon_i||^2 \Big), \tag{5.19}$$

From $\tilde{\varpi}_i = \|W_i\|_F^2$ and by applying Cauchy's inequality and substituting (5.14), one has

$$\begin{aligned} \dot{V} \leq & -k_v \underline{\sigma}(\bar{R}_p)\beta^T(e)\beta(e) + \sum_{i=1}^{N} \bigg(\frac{1}{4\varrho_i^2} + \frac{1}{4\alpha_i^2} + ||\epsilon_i||^2 + \frac{3||s_i||^2}{2} + s_i^T \Big(-g_i(x_i)c_i(t)s_i \\ & - (b\ sgn(s_i) + \dot{v}_r) \Big) \bigg) + \frac{N}{2} + \sum_{i=1}^{N} \tilde{\varpi}_i^T(\kappa_i \hat{\varpi}_i)]. \end{aligned} \tag{5.20}$$

Similar to (4.18), and by utilizing Young's inequality, substituting equations (5.15), (5.16) into (5.20), and using Young's inequality and assuming boundedness of ideal NN weights matrix by $||W||_F \leq W_M$, with a fixed bound W_M, one has

$$\begin{aligned} \dot{V} & \leq -\underline{\Gamma} M_1 - \underline{\Gamma} M_2 - \underline{\Gamma} M_3 - \underline{\Gamma} \sum_{i=1}^{N} \frac{\Pi_i^{-1}}{2} ||\tilde{\varpi}_i||_F^2 + \frac{N}{2} + \frac{1}{2}\sum_{i=1}^{N} \Big(\xi_i^2 + \kappa_i W_M^2 + \frac{1}{4\varrho_i^2} + \frac{1}{4\alpha_i^2} \Big) \\ & \leq -\underline{\Gamma} V + B_M, \end{aligned} \tag{5.21}$$

where $B_M = \frac{N}{2} + \frac{1}{2}\sum_{i=1}^{N} \Big(\xi_i^2 + \kappa_i W_M^2 + \frac{1}{4\varrho_i^2} + \frac{1}{4\alpha_i^2} \Big)$. From [77, Lemma 1.1], inequality (5.21) implies

$$V(t) \leq \frac{B_M}{\underline{\Gamma}} + (V(0) + \frac{B_M}{\underline{\Gamma}})e^{-\underline{\Gamma} t}. \tag{5.22}$$

It can be seen that using the control law (5.13), the distance errors are uniformly ultimately bounded (UBB). If $s_i \in \Omega_{\varphi_i}$, as o_i is chosen small enough, it follows that the formation control has been achieved and no more control effort is required. □

Remark 5.1. *If inequality (5.22) holds, as $t \to \infty$, the radius can be reduced by choosing $\underline{\Gamma}$ large enough. Thus, $\underline{\Gamma}$ directly impacts formation stability and tracking performance.*

Remark 5.2. *Through control law (5.13), the multi-agent system moves toward the equilibrium, which is located in Ω_0; as a result, the distance error remains in the invariant set Ω_0 [8]. Moreover,*

δ is chosen sufficiently small positive constant and consequently, $p_{ij} \neq 0$.

Lemma 5.1. *Consider the following function*

$$V = \frac{1}{2}\beta^T(e)\beta(e) + \frac{1}{2}\tilde{\varpi}^T F^{-1}\tilde{\varpi} + \frac{1}{2}\mathbf{s}^T\mathbf{s} + \frac{1}{2}\sum_{i=1}^{N}\int_{t-\tau_i}^{t} \Upsilon_i^2(x_i(z))dz, \tag{5.23}$$

If $\dot{V}$ satisfies $\dot{V} \leq -\alpha_1 V + \alpha_2$, then for a bounded initial conditions in a bounded set Ω_0 (5.17)
i) the states and NN weights remain within a bounded set

$$\Omega_{b_i} = \{p_i(t), v_i(t), \hat{W}_i(t) | \, ||p_i(t)|| \leq \bar{P}_i^*, ||v_i(t)|| \leq \bar{V}, ||\hat{\varpi}_i(t)|| \leq W_M^2 + \bar{W}_i, p_r(t) \in \Omega_r\}, \tag{5.24}$$

where constants $\bar{P}_i^*$ and $\bar{W}_i$ and $\bar{V}$ are defined as

$$\begin{aligned} \bar{P}_i^* &= (\alpha_i^* + 1)\bar{P} + \bar{P}_r + \bar{\zeta}, \\ \bar{W}_i &= \sqrt{\frac{2V(0) + \frac{2\alpha_2}{\alpha_1}}{\Pi_i}}, \\ \bar{V} &= \bar{S}(1 + k_v\bar{\sigma}(\bar{R}_p)) + \sqrt{2N}\big(||\dot{p}_r|| + \bar{\zeta}\,\big), \end{aligned} \tag{5.25}$$

and α_i^* denotes the number of vertices in the minimum path from the leader to the i-th agent and

$$\begin{aligned} \bar{S} &= \sqrt{2V(0) + \frac{2\alpha_1}{\alpha_2}}, \\ \bar{P} &= \sqrt{2V(0) + \frac{2\alpha_2}{\alpha_1}} + D, \\ \bar{\zeta} &= ||e_r(0)|| + \frac{\sqrt{2}\bar{S}}{k_r}(1 + k_v\bar{\sigma}(R_p)). \end{aligned} \tag{5.26}$$

ii) The states and weights converge to a compact set

$$\Omega_{c_i} = \{p_i(t), \hat{W}_i(t) | \lim_{t\to\infty} ||e_{ij}|| = \Xi_{e_i}, \lim_{t\to\infty} ||\tilde{W}_i|| = \Xi_{W_i}\}, \tag{5.27}$$

with $\Xi_{e_i} = \sqrt{\frac{2\alpha_2}{\alpha_1}}$ and $\Xi_{W_i} = \sqrt{\frac{2\alpha_2}{\alpha_1\Pi_i}}$.

Proof. Similar proof is provided in [77], hence we skip the proof here. $\square$

It can be shown, using Gershgorin circle theorem, that $\bar{\sigma}(\bar{R}_p) \leq \sqrt{2N-2}$ (see Lemma 3.2). Thus, the compact set of $\Omega^0_{\varphi_i}$ defined in (5.13) can be specified as

$$\Omega^0_{\varphi_i} = \{p_i, v_i, s_i \mid ||p_i|| \leq \bar{P}^*_i, ||v_i|| \leq \bar{V}, ||s_i|| \leq \bar{S}\}. \tag{5.28}$$

Remark 5.3. *The variables s_i and γ_i are bounded as all of their components are bounded as well as the control gain $c_i(t)$ and the control input (5.13).*

5.4 Simulation Results

Example 5.1. *Consider a nonlinear multi-agent system with four agents in a plane, where the dynamics of each agent is given by*

$$\begin{aligned}
\dot{p}_i(t) =& v_i(t), \\
\dot{v}_i(t) =& \begin{pmatrix} a_{i1}v_{i2}(t)v_{i1}(t) + sin(a_{i1}p_{i1}(t)) \\ b_{i1}p_{i2}(t)v_{i2}(t) + cos(b_{i1}p_{i2}(t)) \end{pmatrix} + \begin{pmatrix} 1 + cos(v_{i4})sin(v_{i3}^2) & 0 \\ 0 & 1 + cos(v_{i3})sin(v_{i4}^2) \end{pmatrix} u_i(t) \\
&+ \begin{pmatrix} c_{i1}p_{i1}(t-\tau_i)cos(v_{i1}(t-\tau_i)) \\ c_{i2}p_{i2}(t-\tau_i)sin(v_{i2}(t-\tau_i)) \end{pmatrix} + \begin{pmatrix} d_{i1}v_{i2}p_{i1}^2 cos(1.5t) \\ d_{i2}(v_{i1}+p_{i2})sin(t) \end{pmatrix}, \quad i = 1, ..., 4.
\end{aligned} \tag{5.29}$$

Parameters a_{i1}, b_{i1}, c_{i1}, c_{i2}, d_{i1}, d_{i2} of each agent are given in Table 5.1. The initial conditions for the four agents are: $p_1(0) = (0, 1)^T$, $v_1(0) = (1, 1.5)^T$, $p_2(0) = (-0.2, 0)^T$,$v_2(0) = (-1, 1)^T$, $p_3(0) = (0.2, -1)^T$, $v_3(0) = (1, -1)^T$, and $p_4(0) = (0.3, 0.5)^T$, $v_4(0) = (0.5, 0.5)^T$. The time delays are $\tau_1 = 0.10$, $\tau_2 = 0.18$, $\tau_3 = 0.13$, $\tau_4 = 0.12$, and $\tau_M = 0.2$. The target velocity and initial position are $v_r = [0.2, 0.5cos(2t)]^T$ and $p_r(0) = [0, 0]^T$, respectively. Considering $||\dot{v}_r||_\infty = 1$, we choose $b = 3$ and $k_r = 2$. RBFNN is selected with 9 neurons and $\kappa_i = 2.3, F_i = 10I_9, k_v = 15$. To satisfy Assumptions 5.1-5.2, we choose $\Upsilon_i(x_i(t)) = \sqrt{(c_{i1}p_{i1})^2 + (c_{i2}p_{i2})^2}$ and $\Gamma_i = 2$, $k_c = 22$ in (5.16).

The desired distances and communication topology are given in Figure 3.4, with $d = 1$. Figures 5.1-5.3 show results of the proposed control law (5.13) for a nonlinear multi-agent system. Figure 5.1(a) shows the performance of the multi-agent system, which achieves the desired formation ($d =$

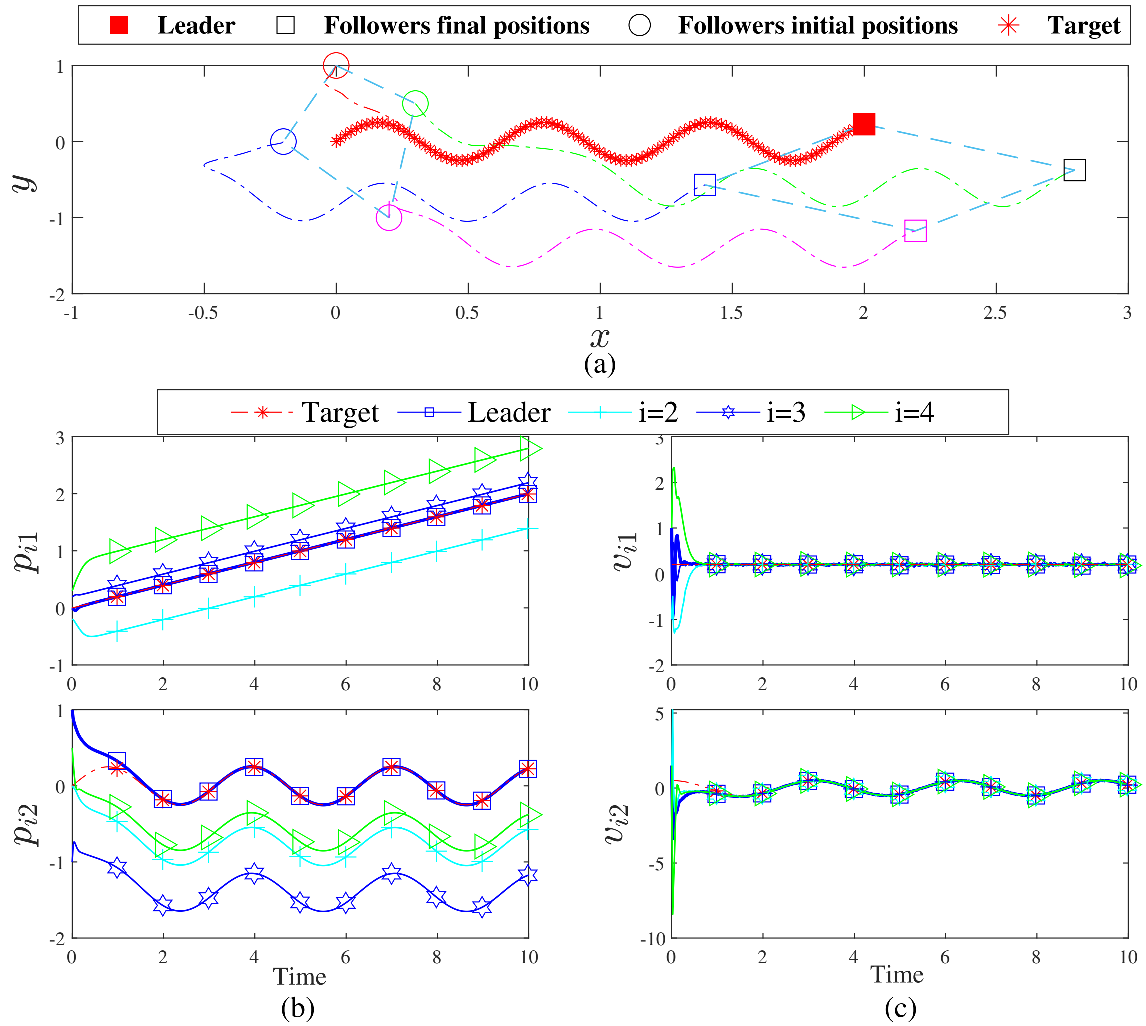

Figure 5.1: (a) The desired formation is a square with side $d = 1$; (b) Trajectories of the agents and the target along x and y directions; (c) Velocities of agents and the target along x and y directions.

1). *Figure 5.1(b) represents the trajectories of the agents and the target in x and y directions. The velocity of agents and the target in x and y directions are shown in Figure 5.1(c). Figure 5.2(a) illustrates the distance errors e_{ij}, $(i, j) \in E$ of the proposed method, and Figure 5.2(b) demonstrates the target tracking error of the leader and its time derivative of the proposed method.*

To compare the results with a displacement-based method, the modified version of [76] is simulated. We selected the control parameters of [76] as follows: number of neurons is 9, $\kappa_{i,q} = 10$, and $C_{i,m,m} = 0.2$.

We use AFDE (4.70) to compare our results with [76]. As shown in Figure 5.3(a), the proposed

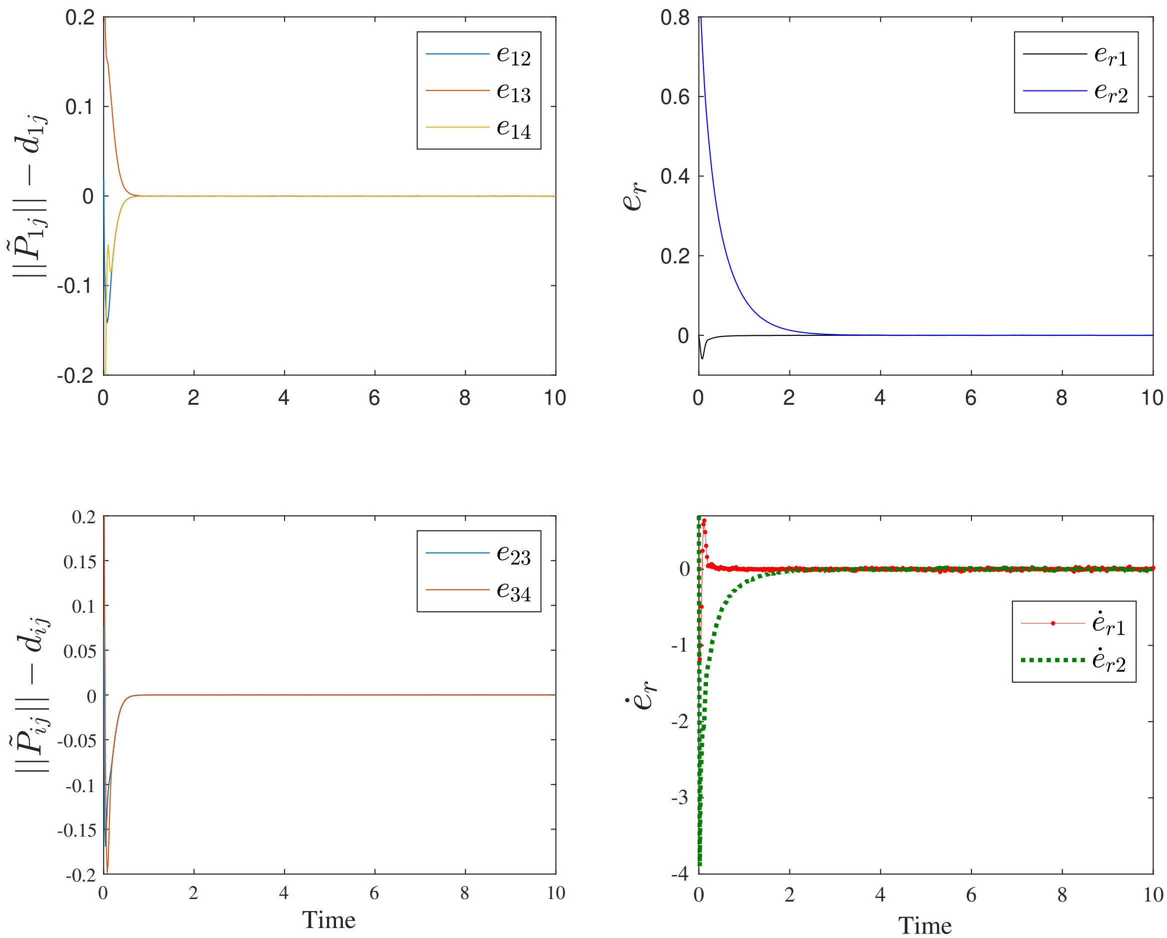

Figure 5.2: (a) The distance errors $e_{ij},\ (i,j) \in E$ of the proposed method. (b) The target tracking error of the leader and its time derivative of the proposed method.

method improves the AFDE when applied to second-order nonlinear multi-agent systems. Moreover, in order to provide a better comparison, using Example 3.2, the smallest singular values of normalized rigidity matrix for our proposed method (dashed line) and method in [76] (dash-dotted line) are depicted in Figure 5.3. (b). From Example 3.2 and Figure 5.3, one can see the performance improvement in comparison with the presented method in [76]. Moreover, it can be noted that the smallest singular value of the normalized rigidity matrix is always less than the introduced upper bound in Theorem 3.1.

Table 5.1: Parameters $a_{i1}, b_{i1}, c_{i1}, c_{i2}, d_{i1}, d_{i2}$ for the i-th agent.

i	a_{i1}	b_{i1}	c_{i1}	c_{i2}	d_{i1}	d_{i2}
1	0.3	1	1	-1	-2.4	2.1
2	0.7	-0.2	-1.2	-2.2	1.8	-1.5
3	-0.7	-0.8	2.1	1.2	-0.4	1.3
4	-0.6	0.4	-0.5	-0.7	0.6	0.8

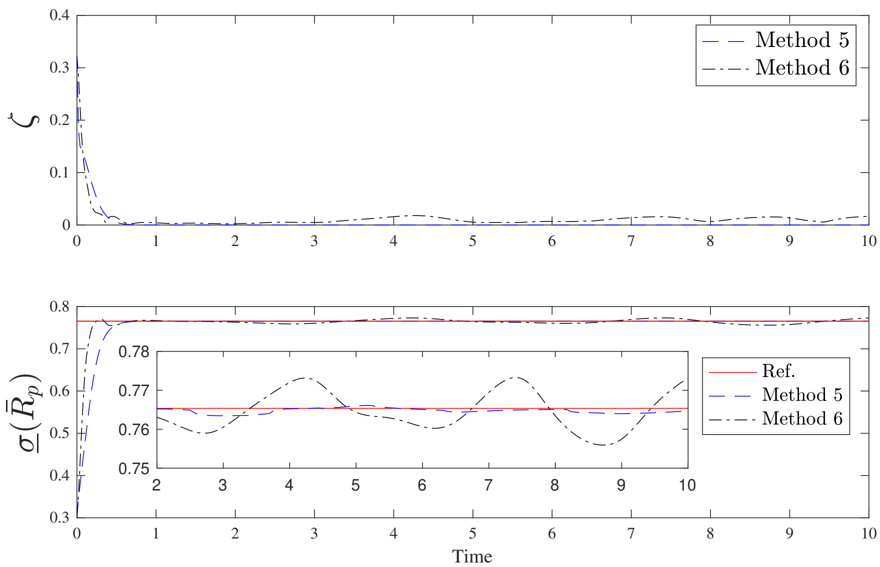

Figure 5.3: (a) Performance comparison (AFDE) between proposed distance-based method (Method 5) and displacement method (Method 6) [76]; (b) Smallest singular value of normalized rigidity matrix comparison between proposed distance-based method (Method 5) and displacement method (Method 6) [76] (solid line is the desired value for the smallest singular value of normalized rigidity matrix in Example 3.2).

5.5 Conclusion

A neuro-adaptive backstepping and rigid graph theory-based control have been proposed for a distance-based formation control and target tracking of second-order nonlinear multi-agent systems modeled by an undirected graph in the presence of bounded disturbance and unknown state time delay. The RBFNN has been used to compensate for the unknown nonlinearity of the dynamical system and disturbance. The rigorous stability analysis based on the Lyapunov stability theory showed UUB of distance error. The normalized rigidity matrix has been used for designing the control law. The simulation results have verified the performance of the proposed method. Two comparisons have been provided to demonstrate the efficiency and improvements of the proposed method compared with the recent results in the literature.

Chapter 6

Directed Formation Control of Nonlinear Multi-Agent Systems Using Three-Layer Neural Networks

This chapter focuses on leader-following formation control problem for heterogeneous, second-order, uncertain, input-affine, nonlinear multi-agent systems modeled by a directed graph. A tunable, three-layer NN is proposed with an input layer, two hidden layers, and an output layer to approximate an unknown nonlinearity. Rather than relying on trial and error to select the number of neurons or hyperparameters in a conventional neural network, this approach leverages prior knowledge of the number of states to set up the appropriate number of neurons for each layer. The NN weights tuning laws are derived using the Lyapunov theory. The leader-following and formation control problems are addressed by RISE feedback and an NN-based control. The RISE feedback term compensates for unknown leader dynamics and the bounded disturbance in the agent error dynamics. The NN-based term compensates for the unknown nonlinearity in the dynamics of multi-agent systems. The semi-global asymptotic tracking results are rigorously proven using the Lyapunov stability theory.

6.1 Introduction

6.1.1 Related Works on Formation Control of Nonlinear Multi-Agent Systems Using Multi-layer Neural Networks

In the formation control problem of multi-agent systems, it is common to consider single- and double-integrator dynamics [59,78,79], or nonlinear dynamics [14,28,54,80] to model multi-agent systems. Some literature that considered unknown nonlinear dynamics, utilized NNs or fuzzy logic controllers to approximate the uncertain nonlinearity in the system dynamics. There are two main reasons for this: (i) the multi-layer NNs and fuzzy logic controllers are universal approximators that can approximate any continuous and smooth function over a compact set with a desired accuracy [14, 81]; (ii) a precise model for the dynamics of a multi-agent system is not required, which eliminates an extra effort to acquire an accurate system model [82].

Intelligent control results in formation control mainly used one-layer NNs, e.g., radial basis function neural networks (RBFNNs) [28, 83, 84] or two-layer NNs [54], to compensate for the unknown nonlinearities in the system dynamics. These studies commonly used the universal approximation property, where the RBFNNs and the Gaussian activation functions were utilized. In RBFNN, hidden layer neurons are usually uniformly distributed on a regular lattice, or they are randomly initialized. In [85], authors constructed an RBFNN, where the distance of any two adjacent centers of the bell-shaped activation functions was the same as the width of the activation function.

An RBFNN can approximate a nonlinearity if the input variables of the activation function are located in certain neighborhoods of the RBF centers [85]. Thus, one can select a large number of neurons (not a priori known) and distribute activation functions over a regular lattice uniformly to cover the compact set. A one-layer NN with a tunable, hidden layer in the form of linear-in-the-parameters can approximate a nonlinearity in the dynamics of a nonlinear system at the desired accuracy. The exact number of neurons for control systems design is not clearly established. Although the self-organizing receptive field method was introduced in [86] to optimize the locations in RBFNN, these results have not been used in the formation control problem to approximate the unknown nonlinearity.

These limitations and restrictions motivated us to propose a three-layer NN with two hidden layers, where the numbers of neurons in hidden layers are set based on the order of the agents' model (see Remark 6.6). Increasing the number of layers and neurons inevitably increases computational complexity. However, setting the number of neurons a priori reduces the controller design time.

To address the issue of the number of neurons in a NN, a self-structuring NN was proposed in [82], where a neuron is divided into two by satisfying a specific condition, but the output of these two neurons remains identical to the output of a neuron without division. This work was extended to a nonlinear multi-agent system [54], where authors designed an observer to estimate the states of the leader for each agent and addressed the cooperative tracking control problem of a leader. Compared with existing results, we used two hidden layers instead of one [31, 32, 54, 82, 87], and we developed tuning laws for all three layers. The other novelty is that the number of neurons is fixed.

The RISE feedback controller is utilized to eliminate the chattering effect that occurs in sliding mode controllers [31, 32, 88–91]. Although a RISE feedback control can potentially exceed the actuator's limit due to the large integral gain, it has been shown that it can be implemented in real-time applications, e.g., [91]. Authors in [88] used the RISE feedback to compensate for nonlinearity in a class of higher-order, multi-input multi-output systems. These results were extended in [32], where a tracking problem of an uncertain system was addressed by an NN-based controller. In [32], the authors used the discontinuous projection algorithm, which requires an a priori knowledge of the convex set, as well as maximum and minimum of NN's weights [92]. In a similar study, in [89], authors used two-layer NN (input, hidden, and output layers), where only the weights between two outer layers can be tuned. The tuning laws in [89] were derived using the Lyapunov stability theory. These results were further extended in [31, 91], where a discontinuous projection algorithm has tuned the NN weights matrices between any two consecutive layers for a two-layer NN.

The novelty of our work in comparison with [31, 32, 88, 89, 91, 92], is that we employ a three-layer NN comprised of an input layer, two hidden layers, and an output layer. Moreover, all NN weights matrices are tunable, and the tuning laws are derived through the Lyapunov theory.

The NN-based formation control results addressing the displacement-based, leader-following problem have demonstrated only uniform ultimate bounded stability due to NN approximation error and lack of communication between the leader and all followers [14–16, 53, 54, 60]. A RISE feedback controller with two hidden layers NN is proposed to achieve semi-global, asymptotic stability for the leader-following formation control for heterogeneous, second-order, uncertain, input-affine, nonlinear multi-agent systems.

The main contributions of the chapter are given as follows:

(1) We consider the leader to be connected to at least one of the other agents. Unlike [31, 32, 87, 89, 91], where the desired trajectory signals (information from the leader) are fed into the first layer of the NN, the novelty here is that the NN is designed without these signals. The leader-following is achieved by a RISE feedback controller, where the effects of the leader dynamics and unknown disturbances in the tracking error of each agent are ameliorated by a robustifying term.

(2) We determined the number of neurons in each layer and derived the tuning laws for the NN weights matrices. Although the controls literature mostly considered one- or two-layer NNs [15, 28, 31, 35, 60, 87, 91], we developed the results for a three-layer NN. This work differs in that it sets the number of neurons in NN layers using *a priori* knowledge, such as the number of system states.

(3) The semi-global, asymptotic, leader-following performance is achieved, which distinguishes our work from [14, 15, 28, 53].

6.2 Problem Formulation

A multi-agent system with N agents is considered, with the dynamics of each agent given by

$$\begin{aligned} \dot{p}_i &= v_i, \\ \dot{v}_i &= f_i(p_i, v_i) + g_i(p_i, v_i)u_i(t) + w_i(t), \qquad i = 1, ..., N, \end{aligned} \tag{6.1}$$

where the variables $p_i \in \mathbb{R}^n$ and $v_i \in \mathbb{R}^n$ denote the position and velocity states of each agent, respectively. The functions $f_i(p_i, v_i) \in \mathbb{R}^n$ and $g_i(p_i, v_i) \in \mathbb{R}^{n\times n}$ are unknown nonlinear $\mathcal{C}^2$ functions. The control input is $u_i \in \mathbb{R}^n$, while a disturbance affecting the agent is denoted by

$w_i \in \mathbb{R}^n$.

The dynamics of the multi-agent system can be written in a compact form as follows:

$$\begin{aligned}
\dot{\mathbf{x}}_1 &= \mathbf{x}_2, \\
\dot{\mathbf{x}}_2 &= f(\mathbf{x_1}, \mathbf{x_2}) + g(\mathbf{x_1}, \mathbf{x_2})u + w,
\end{aligned} \tag{6.2}$$

where $\mathbf{x}_1$ and $\mathbf{x}_2$ are stacked vectors of positions and velocities of all agents, respectively. The stacked vector $\mathbf{x}_1 = [p_1^T, p_2^T, ..., p_N^T]^T \in \mathbb{R}^{nN}$ and $\mathbf{x}_2 = [v_1^T, v_2^T, ..., v_N^T]^T \in \mathbb{R}^{nN}$. The overall states of the multi-agent system are represented by $\mathbf{x} = [\mathbf{x}_1^T, \mathbf{x}_2^T]^T$. The function $f(\mathbf{x}) = [f_1^T(p_1, v_1), f_2^T(p_2, v_2), ..., f_N^T(p_N, v_N)]^T \in \mathbb{R}^{nN}$ is the stacked nonlinearities of all agents. The control input gain matrix is $g(\mathbf{x}) = diag(g_1(p_1, v_1), g_2(p_2, v_2), ..., g_N(p_N, v_N)) \in \mathbb{R}^{nN \times nN}$, the stacked control input vector is $u = [u_1^T, u_2^T, ..., u_N^T]^T \in \mathbb{R}^{nN}$, and the stacked disturbance vector is $w = [w_1^T, w_2^T, ..., w_N^T]^T \in \mathbb{R}^{nN}$.

The leader's dynamics is given by

$$\begin{aligned}
\dot{p}_l &= v_l, \\
\dot{v}_l &= f_l(p_l, v_l),
\end{aligned} \tag{6.3}$$

where $p_l, v_l \in \mathbb{R}^n$ denote the position and velocity states of the leader, respectively. Here we use some standard assumptions [31, 32, 35, 90, 93–95].

Assumption 6.1. *The trajectory of the leader and its first three time derivatives are bounded, i.e.,* $p_l, v_l, f_l, \dot{f}_l \in \mathcal{L}_\infty$. *The bounds of* $p_l, v_l, f_l, \dot{f}_l$ *are considered to be unknown.*

Assumption 6.2. *The gain matrix* $g_i(p_i, v_i)$ *is a symmetric, positive definite matrix, and its inverse satisfies the following inequality*

$$\underline{g}||x||^2 \leq x^T g_i^{-1} x \leq \bar{g}||x||^2, \tag{6.4}$$

where $x \in \mathbb{R}^n$ *and unknown constants* $\underline{g}$, $\bar{g}$ *are positive.*

Remark 6.1. *Assumption 6.2 states the condition for the controllability of the system (6.1). These bounds are considered for analytical purposes, and their exact values are considered to be unknown* *for control design. We removed an a priori knowledge about $\underline{g}$ in our control design. Its exact value is not required, and this consideration distinguishes our work from [28, 35, 60, 96]. There are many nonlinear systems that meet this assumption, including those described by Euler-Lagrange formulations [27, 32].*

Assumption 6.3. *The disturbance w_i and its first two time derivatives $\dot{w}_w, \ddot{w}_i$ are considered to be bounded with unknown bounds.*

Let us define the error vector for i-th agent as [80]

$$e_i = \sum_{j \in N_i} a_{ij}(p_i - p_j - d_i + d_j) + b_i(p_i - p_l - d_i), \tag{6.5}$$

where the constant vectors $d_i \in \mathbb{R}^n, i = 1, ..., N$ represent the desired relative position between agent i and the leader. Note that we define the desired relative position between agents i and j as $d_{ij} = d_i - d_j$. For the agent i, define δ_i as $\delta_i \triangleq \dot{e}_i$

$$\delta_i = \sum_{j \in N_i} a_{ij}(v_i - v_j) + b_i(v_i - v_l). \tag{6.6}$$

The control objective is to design a robust, distributed controller for each agent using local information that ensures all agents achieve the desired formation and maintain the leader's velocity:

$$\begin{aligned} &\lim_{t \to \infty} ||p_i - p_l - d_i|| = 0 \\ &\lim_{t \to \infty} ||v_i - v_l|| = 0. \end{aligned} \tag{6.7}$$

Recall the three-layer NN covered in Section 2.4.2. Then the following results can be derived using the problem formulation stated above.

Considering 2.20, let us define $\tilde{y} = y - \hat{y}$, $\tilde{\sigma}_k = \sigma_k - \hat{\sigma}_k$, $\tilde{V} = V - \hat{V}$, $\tilde{Z} = Z - \hat{Z}$, and $\tilde{W} = W - \hat{W}$. Let us define $\sigma_1 \triangleq \sigma_1(Z^T \sigma_2)$, with $\sigma_2 \triangleq \sigma_2(V^T \mathcal{X})$ and $\hat{\sigma}_1 \triangleq \sigma_1(\hat{Z}^T \hat{\sigma}_2)$ with $\hat{\sigma}_2 \triangleq \sigma_2(\hat{V}^T \mathcal{X})$. Moreover, we express $\hat{\sigma}_1' \triangleq \frac{d\sigma_1(s)}{ds}|_{s=\hat{Z}^T \hat{\sigma}_2}$ and $\hat{\sigma}_2' \triangleq \frac{d\sigma_2(s)}{ds}|_{s=\hat{V}^T \mathcal{X}}$.

Lemma 6.1. *The estimation error satisfies the following*

$$y - \hat{y} =\tilde{W}^T\big(\hat{\sigma}_1 - \hat{\sigma}_1'\hat{Z}^T\hat{\sigma}_2 - \hat{\sigma}_1'\hat{Z}^T\hat{\sigma}_2'\hat{V}^T\mathcal{X}\big) + \hat{W}^T\hat{\sigma}_1'\tilde{Z}^T\big(\hat{\sigma}_2 - \hat{\sigma}_2'\hat{V}^T\mathcal{X}\big) + \hat{W}^T\big(\hat{\sigma}_1'\hat{Z}^T\hat{\sigma}_2'\tilde{V}^T\mathcal{X}\big)$$
$$+ \bar{\epsilon}, \tag{6.8}$$

with

$$\bar{\epsilon} =\hat{W}^T\hat{\sigma}_1'Z^TO_2(.) + \hat{W}^T\hat{\sigma}_1'\tilde{Z}^T\hat{\sigma}_2'V^T\mathcal{X}[\tilde{W}^T(\hat{\sigma}_1'Z^T\sigma_2) + \tilde{W}\hat{\sigma}_i'\hat{Z}^T\hat{\sigma}_2'\hat{V}^T\mathcal{X} + W^TO_1(.) + \epsilon], \tag{6.9}$$

where $O_1(.)$ and $O_2(.)$ are higher-order terms of Taylor series expansion of $\sigma_1(Z^T\sigma_2(V^T\mathcal{X}))$ at $\hat{Z}^T\sigma_2(\hat{V}^T\mathcal{X})$ and $\sigma_2(V^T\mathcal{X})$ at $\hat{V}^T\mathcal{X}$, respectively.

Proof. Following the procedure in [27, 82], from (2.17) and (2.19), one can write

$$y - \hat{y} = W^T\sigma_1(Z^T\sigma_2(V^T\mathcal{X})) - \hat{W}^T\sigma_1(\hat{Z}^T\sigma_2(\hat{V}^T\mathcal{X})) + \epsilon. \tag{6.10}$$

By adding and subtracting $W^T\hat{\sigma}_1 + \hat{W}^T\tilde{\sigma}_1$, and rearranging (6.10), one has

$$y - \hat{y} = \tilde{W}^T\hat{\sigma}_1 + \tilde{W}^T\tilde{\sigma}_1 + \hat{W}^T\tilde{\sigma}_1 + \epsilon. \tag{6.11}$$

Taylor series expansions of $\sigma_1(Z^T\sigma_2(V^T\mathcal{X}))$ at $\hat{Z}^T\sigma_2(\hat{V}^T\mathcal{X})$ and $\sigma_2(V^T\mathcal{X})$ at $\hat{V}^T\mathcal{X}$ is

$$\begin{aligned}\sigma_1(Z^T\sigma_2(V^T\mathcal{X})) =&\sigma_1(\hat{Z}^T\sigma_2(\hat{V}^T\mathcal{X})) + \hat{\sigma}_1'[Z^T\sigma_2(V^T\mathcal{X}) - \hat{Z}^T\sigma_2(\hat{V}^T\mathcal{X})] + O_1(.)\\ =&\hat{\sigma}_1 + \hat{\sigma}_1'[Z^T\sigma_2 - \hat{Z}^T\hat{\sigma}_2] + O_1(.),\end{aligned} \tag{6.12}$$

$$\sigma_2(V^T\mathcal{X}) = \hat{\sigma}_2 + \hat{\sigma}_2'\tilde{V}^T\mathcal{X} + O_2(.). \tag{6.13}$$

Note that $O_1(.)$ and $O_2(.)$ are shortened notations for $O_1(Z^T\sigma_2(V^T\mathcal{X}) - \hat{Z}^T\sigma_2(\hat{V}^T\mathcal{X}))$ and $O_2(\tilde{V}^T\mathcal{X})$, respectively. From (6.12) and (6.13), it is evident that

$$\begin{aligned} \tilde{\sigma}_1 &= \hat{\sigma}_1'[Z^T\sigma_2 - \hat{Z}^T\hat{\sigma}_2] + O_1(.), \\ \tilde{\sigma}_2 &= \hat{\sigma}_2'\tilde{V}^T\mathcal{X} + O_2(.). \end{aligned} \tag{6.14}$$

Substituting (6.14) in (6.11), one has

$$y - \hat{y} = \tilde{W}^T\big(\hat{\sigma}_1 + \hat{\sigma}_1'[Z^T\sigma_2 - \hat{Z}^T\hat{\sigma}_2] + O_1(.)\big) + \hat{W}^T\tilde{\sigma}_1 + \epsilon. \tag{6.15}$$

Rearranging (6.15), yields

$$y - \hat{y} = \tilde{W}^T\big(\hat{\sigma}_1 - \hat{\sigma}_1'\hat{Z}^T\hat{\sigma}_2 + \hat{\sigma}_1'\hat{Z}^T\tilde{\sigma}_2\big) + \hat{W}^T\tilde{\sigma}_1 + [\tilde{W}^T(\hat{\sigma}_1'[\tilde{Z}^T\sigma_2 + \hat{Z}^T\hat{\sigma}_2] + O_1(.)) + \epsilon]. \tag{6.16}$$

From (6.14), (6.16) can be written as

$$\begin{aligned} y - \hat{y} =& \tilde{W}^T\big(\hat{\sigma}_1 - \hat{\sigma}_1'\hat{Z}^T\hat{\sigma}_2 - \hat{\sigma}_1'\hat{Z}^T\hat{\sigma}_2'\hat{V}^T\mathcal{X}\big) + \hat{W}^T\tilde{\sigma}_1 + [\tilde{W}^T(\hat{\sigma}_1'[\tilde{Z}^T\sigma_2 + \hat{Z}^T\hat{\sigma}_2 + \hat{Z}^T\hat{\sigma}_2'V^T\mathcal{X} \\ &+ \hat{Z}^T O_2(.)] + O_1(.)) + \epsilon]. \end{aligned} \tag{6.17}$$

Following the same procedure for $\hat{W}^T\tilde{\sigma}_1$ and from (6.14), one has

$$\begin{aligned} y - \hat{y} =& \tilde{W}^T\big(\hat{\sigma}_1 - \hat{\sigma}_1'\hat{Z}^T\hat{\sigma}_2 - \hat{\sigma}_1'\hat{Z}^T\hat{\sigma}_2'\hat{V}^T\mathcal{X}\big) + \hat{W}^T\hat{\sigma}_1'[\tilde{Z}^T\tilde{\sigma}_2 + \tilde{Z}^T\hat{\sigma}_2] + \hat{W}^T\hat{\sigma}_1'[\hat{Z}^T\tilde{\sigma}_2] \\ &+ \hat{W}^T O_1(.) + [\tilde{W}^T(\hat{\sigma}_1'[\tilde{Z}^T\sigma_2 + \hat{Z}^T\hat{\sigma}_2 + \hat{Z}^T\hat{\sigma}_2'V^T\mathcal{X} + \hat{Z}^T O_2(.)] + O_1(.)) + \epsilon]. \end{aligned} \tag{6.18}$$

Substituting (6.14) in (6.18) leads to

$$\begin{aligned} y - \hat{y} =& \tilde{W}^T\big(\hat{\sigma}_1 - \hat{\sigma}_1'\hat{Z}^T\hat{\sigma}_2 - \hat{\sigma}_1'\hat{Z}^T\hat{\sigma}_2'\hat{V}^T\mathcal{X}\big) + \hat{W}^T\hat{\sigma}_1'\tilde{Z}^T(\hat{\sigma}_2 - \hat{\sigma}_2'\hat{V}^T\mathcal{X}) + \hat{W}^T\hat{\sigma}_1'\tilde{Z}^T O_2(.) \\ &+ \hat{W}^T\hat{\sigma}_1'\tilde{Z}^T\hat{\sigma}_2'V^T\mathcal{X} + \hat{W}^T\hat{\sigma}_1'\hat{Z}^T\hat{\sigma}_2'\tilde{V}^T\mathcal{X} + \hat{W}^T\hat{\sigma}_1'\hat{Z}^T O_2(.) + W^T O_1(.) \\ &+ \tilde{W}^T(\hat{\sigma}_1'[\tilde{Z}^T\sigma_2 + \hat{Z}^T\hat{\sigma}_2 + \hat{Z}^T\hat{\sigma}_2'V^T\mathcal{X} + \hat{Z}^T O_2(.)]) + \epsilon. \end{aligned} \tag{6.19}$$

From (6.13) and (6.19), one can derive $\bar{\epsilon}$ as (6.9). □

The following Lemma provides a bound for $\bar{\epsilon}$.

Lemma 6.2. *The term $\bar{\epsilon}$ (6.9) satisfies the following inequality*

$$||\bar{\epsilon}|| \leq \Gamma\mu, \tag{6.20}$$

where Γ is an unknown positive constant, and μ is defined as follows:

$$\begin{aligned}\mu =&||\hat{W}||_F + ||\hat{W}||_F||\mathcal{X}|| + ||\hat{W}||_F||\hat{V}||_F||\mathcal{X}|| + ||\hat{W}||_F||\hat{Z}||_F||\mathcal{X}|| + ||\hat{Z}||_F||\hat{V}||_F||\mathcal{X}|| \\ &+ ||\hat{W}||_F||\hat{Z}||_F||\hat{V}||_F||\mathcal{X}|| + ||\hat{Z}||_F + 1.\end{aligned} \tag{6.21}$$

Proof. Following the procedure in [27, Lemma 4.3.1], [82], as well as using the fact that $\sigma_k(.)$ and its derivative are bounded, and from (6.14), one can show that

$$\begin{aligned}&||O_2(.)|| \leq c_0 + c_1||\mathcal{X}|| + c_2||\hat{V}||_F||\mathcal{X}||, \\ &||O_1(.)|| \leq c_3 + c_4||\hat{Z}||_F,\end{aligned} \tag{6.22}$$

where c_i, $i \in \{0, .., 4\}$ are positive constants. Using Assumption 2.3, and by substituting (6.22) in (6.9), one has

$$\begin{aligned}||\bar{\epsilon}|| \leq&||\hat{W}^T\hat{\sigma}_1'Z^T||\ ||O_2(.)|| + ||\hat{W}^T\hat{\sigma}_1'\tilde{Z}^T\hat{\sigma}_2'V^T\mathcal{X}|| + ||\tilde{W}^T\hat{\sigma}_1'Z^T\sigma_2|| + ||\tilde{W}\hat{\sigma}_i'\hat{Z}^T\hat{\sigma}_2'\hat{V}^T\mathcal{X}|| \\ &+ ||W^TO_1(.) + \epsilon|| \\ \leq& d_0||\hat{W}||_F(c_0 + c_1||\mathcal{X}|| + c_2||\hat{V}||_F||\mathcal{X}||) + d_1||\hat{W}||_F\ ||\mathcal{X}|| + d_2||\hat{W}||_F||\hat{Z}||_F||\mathcal{X}|| \\ &+ d_3||\hat{W}||_F + d_4||\hat{Z}||_F||\hat{V}||_F||\mathcal{X}|| + d_5||\hat{W}||_F||\hat{Z}||_F||\hat{V}||_F||\mathcal{X}|| + d_6(c_3 + c_4||\hat{Z}||_F) + d_7,\end{aligned} \tag{6.23}$$

where d_i, $i = 1, .., 7$ are positive constants. Rearranging (6.23) yields

$$\begin{aligned}||\bar{\epsilon}|| \leq&(d_0c_0 + d_3)||\hat{W}||_F + (c_1 + d_1)||\hat{W}||_F||\mathcal{X}|| + c_2||\hat{W}||_F||\hat{V}||_F||\mathcal{X}|| + d_2||\hat{W}||_F||\hat{Z}||_F||\mathcal{X}|| \\ &+ d_4||\hat{Z}||_F||\hat{V}||_F||\mathcal{X}|| + d_5||\hat{W}||_F||\hat{Z}||_F||\hat{V}||_F||\mathcal{X}|| + d_6c_3 + d_7 + c_4||\hat{Z}||_F).\end{aligned} \tag{6.24}$$

From (6.24), one has

$$||\bar{\epsilon}|| \leq \Gamma(||\hat{W}||_F + ||\hat{W}||_F||\mathcal{X}|| + ||\hat{W}||_F||\hat{V}||_F||\mathcal{X}|| + ||\hat{W}||_F||\hat{Z}||_F||\mathcal{X}|| + ||\hat{Z}||_F||\hat{V}||_F||\mathcal{X}|| + ||\hat{W}||_F||\hat{Z}||_F||\hat{V}||_F||\mathcal{X}|| + ||\hat{Z}||_F + 1), \tag{6.25}$$

with

$$\Gamma \triangleq max\{d_0c_0 + d_3, c_1 + d_1, c_2, d_2, d_4, d_5, d_6c_3 + d_7 + c_4\}. \tag{6.26}$$

From (6.26), it is straightforward to verify that selecting μ as (6.21) implies (6.20). □

Remark 6.2. *Lemma 6.2 provides an upper bound for $\bar{\epsilon}$ using a three-layer NN. Note that this error is bounded by $||\bar{\epsilon}|| \leq \Gamma\mu$, where Γ is considered to be an unknown constant. Therefore, one can write it as $||\bar{\epsilon}|| \leq \bar{\epsilon}_M$, where $\bar{\epsilon}_M$ is considered unknown and is not necessarily a constant. Note that we consider this bound for analytical purposes, and its exact value is not necessary for the control design.*

6.3 Controller Design

This section details the control design of RISE feedback and adaptive NN weights matrices tuning laws.

Let us define $\delta = [\delta_1^T, ..., \delta_N^T]^T \in \mathbb{R}^{nN}$ and $\mathbf{e} = [e_1^T, ..., e_N^T]^T \in \mathbb{R}^{nN}$. Then, one can write (6.5) and (6.5) as

$$\begin{aligned} \mathbf{e} &= [(L + B) \otimes I_n](\mathbf{x}_1 - \mathbf{p}_l - d), \\ \delta &= [(L + B) \otimes I_n](\mathbf{x}_2 - \mathbf{v}_l), \end{aligned} \tag{6.27}$$

where $\mathbf{p}_l = \mathbf{1}_N \otimes p_l$, $d = [d_1^T, ..., d_N^T]^T$ and $\mathbf{v}_l = \mathbf{1}_N \otimes v_l$. Let us define an auxiliary variable of $\zeta_i = \delta_i + k_1 e_i$ as in [14], where k_1 is a positive constant gain. Then the stacked vector $\zeta = [\zeta_1^T, ..., \zeta_N^T]^T \in \mathbb{R}^{nN}$ is defined as

$$\zeta = \delta + k_1\mathbf{e}. \tag{6.28}$$

One can derive the time derivative of (6.28) as

$$\dot{\zeta} = [(L+B)\otimes I_n]\big(f(\mathbf{x}) + g(\mathbf{x})u + w - \mathbf{f}_l\big) + k_1\delta, \tag{6.29}$$

where $\mathbf{f}_l = \mathbf{1}_N \otimes f_l$.

6.3.1 Robust Integral of the Sign of the Error (RISE) Feedback

The filtered error is given by

$$r = \dot{\zeta} + k_2\zeta, \tag{6.30}$$

where k_2 is a positive constant. The time derivative of (6.30) is given by

$$\dot{r} = \ddot{\zeta} + k_2\dot{\zeta}. \tag{6.31}$$

From Assumption 6.2, Remark 6.1, Lemma 2.2, and (6.31), one can express the following equation similar to [87] as

$$\mathcal{G}(\mathbf{x})Q\dot{r} = \mathcal{G}(\mathbf{x})Q(\ddot{\zeta} + k_2\dot{\zeta}), \tag{6.32}$$

where $\mathcal{G}(\mathbf{x}) \triangleq g^{-1}(\mathbf{x})$ and $Q \triangleq [(L+B)\otimes I_n]^{-1}$. By adding and subtracting $\frac{1}{2}\dot{\mathcal{G}}(\mathbf{x})Qr + k_2\zeta$, and from (6.27)-(6.29), (6.32) can be rewritten as

$$\begin{aligned}
\mathcal{G}(\mathbf{x})Q\dot{r} =& \mathcal{G}(\mathbf{x})\Big((k_2+k_1)f(\mathbf{x}) + (k_2+k_1)g(\mathbf{x})u + (k_2+k_1)w - (k_2+k_1)\mathbf{f}_l + k_1k_2(\mathbf{x}_2 - \mathbf{v}_\mathbf{l})\\
&+ \dot{f}(\mathbf{x}) + \dot{g}(\mathbf{x})u + g(\mathbf{x})\dot{u} + \dot{w} - \dot{\mathbf{f}}_l\Big) + \frac{1}{2}\dot{\mathcal{G}}(\mathbf{x})Qr + k_2\zeta - \frac{1}{2}\dot{\mathcal{G}}(\mathbf{x})Qr - k_2\zeta\\
=& -\frac{1}{2}\dot{\mathcal{G}}(\mathbf{x})Qr - k_2\zeta + \dot{u} + \mathcal{N}_1 + \mathcal{N}_2,
\end{aligned} \tag{6.33}$$

where

$$\begin{aligned}
\dot{\mathcal{G}}(\mathbf{x}) &= \frac{\partial \mathcal{G}}{\partial \mathbf{x}_1}\mathbf{x}_2 + \frac{\partial \mathcal{G}}{\partial \mathbf{x}_2}\big(f(\mathbf{x}) + g(\mathbf{x})u + w\big),\\
\dot{f}(\mathbf{x}) &= \frac{\partial f}{\partial \mathbf{x}_1}\mathbf{x}_2 + \frac{\partial f}{\partial \mathbf{x}_2}\big(f(\mathbf{x}) + g(\mathbf{x})u + w\big),\\
\dot{\mathbf{f}}_l &= \mathbf{1}_N \otimes \big(\frac{\partial f_l}{\partial p_l}v_l + \frac{\partial f_l}{\partial v_l}f_l\big).
\end{aligned} \tag{6.34}$$

Using the fact that $\mathcal{G}(\mathbf{x})g(\mathbf{x}) = I_{nN}$, and from Assumption 6.2, $\mathcal{N}_1$ and $\mathcal{N}_2$ are given as follows:

$$\begin{aligned}\mathcal{N}_1 =&(k_1+k_2)(\mathcal{G}(\mathbf{x})f(\mathbf{x})+u)+\mathcal{G}(\mathbf{x})\frac{\partial f}{\partial \mathbf{x}_1}\mathbf{x}_2+\mathcal{G}(\mathbf{x})\frac{\partial f}{\partial \mathbf{x}_2}\big(f(\mathbf{x})\\&+g(\mathbf{x})u\big)+k_2\mathbf{x}_2+k_2k_1(\mathbf{x}_1-d)+\frac{1}{2}\Big(\frac{\partial \mathcal{G}}{\partial \mathbf{x}_1}\mathbf{x}_2+\frac{\partial \mathcal{G}}{\partial \mathbf{x}_2}\big(f(\mathbf{x})\\&+g(\mathbf{x})u\big)\Big)\big(f(\mathbf{x})-g(\mathbf{x})u+(k_1+k_2)\mathbf{x}_2+k_1k_2(\mathbf{x}_1-d)\big)+k_1k_2\mathcal{G}(\mathbf{x})\mathbf{x}_2,\end{aligned} \tag{6.35}$$

and

$$\begin{aligned}\mathcal{N}_2 =&(k_1+k_2)(\mathcal{G}(\mathbf{x})w-\mathcal{G}(\mathbf{x})\mathbf{f}_l)+\mathcal{G}(\mathbf{x})(\dot{w}-\dot{\mathbf{f}}_l)-k_1k_2\mathbf{p}_l+\mathcal{G}(\mathbf{x})\frac{\partial f}{\partial \mathbf{x}_2}w-k_1k_2\mathcal{G}(\mathbf{x})\mathbf{v}_l-\\&\frac{\partial \mathcal{G}}{\partial \mathbf{x}_2}wg(\mathbf{x})u-k_2\mathbf{v}_l+\frac{1}{2}\Big(\frac{\partial \mathcal{G}}{\partial \mathbf{x}_1}\mathbf{x}_2+\frac{\partial \mathcal{G}}{\partial \mathbf{x}_2}\big(f(\mathbf{x})+g(\mathbf{x})u\big)\Big)(w-\dot{\mathbf{v}}_l).\end{aligned} \tag{6.36}$$

Note that functions $\mathcal{N}_1 = [\mathcal{N}_{1_1}^T, ..., \mathcal{N}_{1_N}^T]^T \in \mathbb{R}^{nN}$ and $\mathcal{N}_2 = [\mathcal{N}_{2_1}^T, ..., \mathcal{N}_{2_N}^T]^T \in \mathbb{R}^{nN}$ consist of unknown terms. The difference between $\mathcal{N}_{1_i}$ and $\mathcal{N}_{2_i}$ is that, for each agent, we use NN to approximate the variable $\mathcal{N}_{1_i}$, while we use a time-varying robustifying term to compensate for $\mathcal{N}_{2_i}$. The variable $\mathcal{N}_{1_i}$ is a function of available states and the agent's control input. Note that feeding the agent's control input into the input layer of the NN causes the circular design problem. To avoid this problem, similar to [31, 82], we created the NN input from the NN weights matrices, states of the system dynamics, the robustifying term, and ζ_i. This distinguishes our results from [87].

Remark 6.3. *It is common to consider that the leader's information (6.3) is known and use it in the NN input layer [31, 32, 87, 89, 91]. To relax this requirement, we consider that the leader dynamics is unknown, and the NN is not designed using the leader's information, thus offering more flexibility in the controller design.*

Considering (6.33), the NN-based control law is derived as

$$\dot{u} = -(k_3+k_4)\dot{\zeta} - k_2(k_3+k_4)\zeta - \hat{\mathcal{N}}_1 - \kappa(t)\mathrm{sgn}(\zeta(t)), \tag{6.37}$$

where k_3, k_4 are positive constants, $\hat{\mathcal{N}}_1$ is the output of NN, and $\kappa(t) = [diag(\kappa_1, ..., \kappa_N)] \otimes I_n \in \mathbb{R}^{nN\times nN}$ is the time-varying gain. The last term in (6.37) is responsible for compensating the unknown term of $\mathcal{N}_2$ in (6.33) and the NN approximation error. For the agent i, let us define $\hat{\mathcal{N}}_{2_i} \triangleq \kappa_i \text{sgn}(\zeta_i)$. The block diagram of proposed control law is illustrated in Figure 6.1.

We choose the following NN input vector for each agent:

$$\bar{\mathcal{X}}_i = [p_i^T, v_i^T, \zeta_i^T, ||\hat{V}_i||_F, ||\hat{Z}_i||_F, ||\hat{W}_i||_F, \kappa_i(t)]^T \in \mathbb{R}^{3n+4}, \tag{6.38}$$

and $\mathcal{X}_i = [1, \bar{\mathcal{X}}_i^T]^T \in \mathbb{R}^{3n+5}$. Let $\mathcal{N}_{1_i} \triangleq y(\mathcal{X}_i)$, then the NN output for i-th agent is described as (2.19), i.e., $\hat{\mathcal{N}}_{1_i} \triangleq \hat{y}(\mathcal{X}_i)$. Let $\tilde{V} = diag(\tilde{V}_i) \in \mathbb{R}^{(3n+5)N \times m_1 N}$, $\tilde{Z} = diag(\tilde{Z}_i) \in \mathbb{R}^{(m_1+1)N \times m_2 N}$, $\tilde{W} = diag(\tilde{W}_i) \in \mathbb{R}^{(m_2+1)N \times nN}$, $\hat{V} = diag(\hat{V}_i)$, $\hat{Z} = diag(\hat{Z}_i)$, $\hat{W} = diag(\hat{W}_i)$, $\hat{\sigma}_s = [\hat{\sigma}_1^T, ..., \hat{\sigma}_N^T]^T$, and $\hat{\sigma}'_s = [\hat{\sigma}_1'^T, ..., \hat{\sigma}_N'^T]^T$, $s \in \{1, 2\}$. Let us define $\mathcal{X} = [\mathcal{X}_1^T, ..., \mathcal{X}_N^T]^T$.

Define $\hat{\mathcal{N}}_1 = \hat{W}^T \sigma_1(\hat{Z}^T \sigma_2(\hat{V}^T \mathcal{X}))$ and $\tilde{\mathcal{N}}_1 = [\tilde{\mathcal{N}}_{1_1}^T, ..., \tilde{\mathcal{N}}_{1_N}^T]^T$, with $\tilde{\mathcal{N}}_{1_i} = \mathcal{N}_{1_i} - \hat{\mathcal{N}}_{1_i}$ as

$$\begin{aligned} \tilde{\mathcal{N}}_{1_i} &= \tilde{W}_i^T \left(\hat{\sigma}_1 - \hat{\sigma}'_1 \hat{Z}_i^T \hat{\sigma}_2 - \hat{\sigma}'_1 \hat{Z}_i^T \hat{\sigma}'_2 \hat{V}_i^T \mathcal{X}_i\right) + \hat{W}_i^T \hat{\sigma}'_1 \tilde{Z}_i^T \left(\hat{\sigma}_2 - \hat{\sigma}'_2 \hat{V}_i^T \mathcal{X}_i\right) \\ &\quad + \hat{W}_i^T \left(\hat{\sigma}'_1 \hat{Z}_i^T \hat{\sigma}'_2 \tilde{V}_i^T \mathcal{X}_i\right). \end{aligned} \tag{6.39}$$

For the sake of the notation simplicity, the indices of i and arguments of σ_1 and σ_2 are dropped. From (6.30), (6.33), (6.37), Lemma 6.1, and Remark 6.2, one has

$$\mathcal{G}(\mathbf{x}) Q \dot{r} = -\frac{1}{2} \dot{\mathcal{G}}(\mathbf{x}) Q r - k_2 \zeta - (k_3 + k_4) r - \kappa(t) \text{sgn}(\zeta) + \tilde{\mathcal{N}}_1 + \mathcal{N}_2 + \epsilon, \tag{6.40}$$

where $\epsilon = [\epsilon_1^T, ..., \epsilon_N^T]^T \in \mathbb{R}^{nN}$.

Remark 6.4. *Let $\mathbf{x} \in \Omega_{\mathbf{x}}$, where set $\Omega_{\mathbf{x}}$ is a compact set. Following the same procedure as in [87] and considering the Assumptions 6.2 and 6.3, if the control input signal is bounded, i.e., $u \in L_\infty$, the variable $\dot{\mathbf{x}}$ is bounded. As the $\mathbf{p}_l$, $\mathbf{v}_l$ and $\mathbf{f}_l$ are bounded (Assumption 6.1), signals $\mathbf{e}, \delta$, and ζ remain bounded, as well as $\dot{\zeta}$, i.e., $\dot{\zeta} \in \Omega_{\dot{\zeta}}$ (see (6.29)). Moreover, considering $\kappa \in \Omega_\kappa$, $\zeta \in \Omega_\zeta$, $Y \in \Omega_Y$ with $Y = [||\hat{W}||_F, ||\hat{Z}||_F, ||\hat{V}||_F]^T$, and with the help of (6.37), variable $\dot{u}$ is bounded, i.e., $\dot{u} \in L_\infty$. Then, take the time derivative of (6.38), consider Assumptions 6.1, 6.3, (6.29) and (6.30). Then it follows that $\dot{\mathcal{X}}$ remains bounded in the compact set of $\Omega_{\mathcal{X}}$ with $\Omega_{\mathcal{X}} \triangleq \Omega_{\mathbf{x}} \times \Omega_{\mathbf{u}} \times \Omega_\kappa \times \Omega_Y$, where $\Omega_{\mathbf{u}}$ is the compact set in which u is bounded.*

Let us define an agent's NN weights matrices tuning laws as

$$
\begin{aligned}
\hat{W}_i(t) =&\alpha_i\Big(k_2\int_0^t \big(\hat{\sigma}_1-\hat{\sigma}_1'\hat{Z}_i^T(s)\hat{\sigma}_2-\hat{\sigma}_1'\hat{Z}_i^T(s)\hat{\sigma}_2'\hat{V}_i^T(s)\mathcal{X}_i(s)\big)\zeta_i^T(s)ds,-\|\zeta_i\|_1\hat{W}_i\Big),\\
\hat{Z}_i(t) =&\beta_i\Big(k_2\int_0^t \big(\hat{\sigma}_2-\hat{\sigma}_2'\hat{V}_i^T(s)\mathcal{X}_i\big)\zeta_i^T(s)\hat{W}_i^T(s)\hat{\sigma}_1'ds-\|\zeta_i\|_1\hat{Z}_i\Big),\\
\hat{V}_i(t) =&\gamma_i\big(k_2\int_0^t \mathcal{X}_i(s)\zeta_i^T(s)\hat{W}_i^T(s)\hat{\sigma}_1'\hat{Z}_i^T(s)\hat{\sigma}_2'ds-\|\zeta_i\|_1\hat{V}_i\big),
\end{aligned}
\tag{6.41}
$$

with $\alpha_i,\beta_i,\gamma_i$ being positive constants. Let us define α, β, and γ as follows:

$$
\begin{aligned}
\alpha &= diag(\mathbf{1}_{m_2+1}^T\alpha_1,...,\mathbf{1}_{m_2+1}^T\alpha_N)\in\mathbb{R}^{(m_2+1)N\times(m_2+1)N},\\
\beta &= diag(\mathbf{1}_{m_1+1}^T\beta_1,...,\mathbf{1}_{m_1+1}^T\beta_N)\in\mathbb{R}^{(m_1+1)N\times(m_1+1)N},\\
\gamma &= diag(\mathbf{1}_{3n+5}^T\gamma_1,...,\mathbf{1}_{3n+5}^T\gamma_N)\in\mathbb{R}^{(3n+5)N\times(3n+5)N}.
\end{aligned}
\tag{6.42}
$$

Let the time-varying gain $\kappa_i(t)$ be defined as [87, 97]

$$
\dot{\kappa}_i(t) = r_i^T\text{sgn}(\zeta_i).
\tag{6.43}
$$

From (6.30) and by taking the integral from (6.43), one has

$$
\begin{aligned}
\kappa_i(t) &= \int_0^t \big(\dot{\zeta}_i^T(s)\text{sgn}(\zeta_i(s))+k_2\zeta_i^T(s)\text{sgn}(\zeta_i(s))\big)ds\\
&=\sum_{j=1}^n\int_0^t\frac{d\zeta_{i_j}(s)}{ds}\text{sgn}(\zeta_{i_j}(s))ds+\int_0^t k_2\|\zeta_i(s)\|_1 ds\\
&=\|\zeta_i(t)\|_1-\|\zeta_i(0)\|_1+k_2\int_0^t\|\zeta_i(s)\|_1 ds.
\end{aligned}
\tag{6.44}
$$

Remark 6.5. *The unknown term $\mathcal{N}_2$ includes disturbance, its time derivative, the leader's velocity, and its time derivative. Following the similar procedure as in [87, 88], considering the smooth functions for f and g in system dynamics as well as Assumptions 6.1 and 6.3, one has $||\mathcal{N}_2||\leq d_M$ and $||\dot{\mathcal{N}}_2||\leq d_{dM}$, where d_M and d_{dM} are considered to be unknown.*

Take the time derivative of (6.9), recall Remark 6.4, and consider Assumption 2.4, the boundedness of the activation function and its derivative, $\mathbf{x}$, $\dot{\mathbf{x}}$, Y, and $\dot{\mathcal{X}}$ over the compact set of $\Omega_{\mathcal{X}}$, then the boundedness of $||\dot{\bar{\epsilon}}(\mathcal{X},\dot{\mathcal{X}})||$ follows – namely, $||\dot{\bar{\epsilon}}(\mathcal{X},\dot{\mathcal{X}})||\leq\bar{\epsilon}_{dM}$. We consider $\bar{\epsilon}_M$ and $\bar{\epsilon}_{dM}$ to

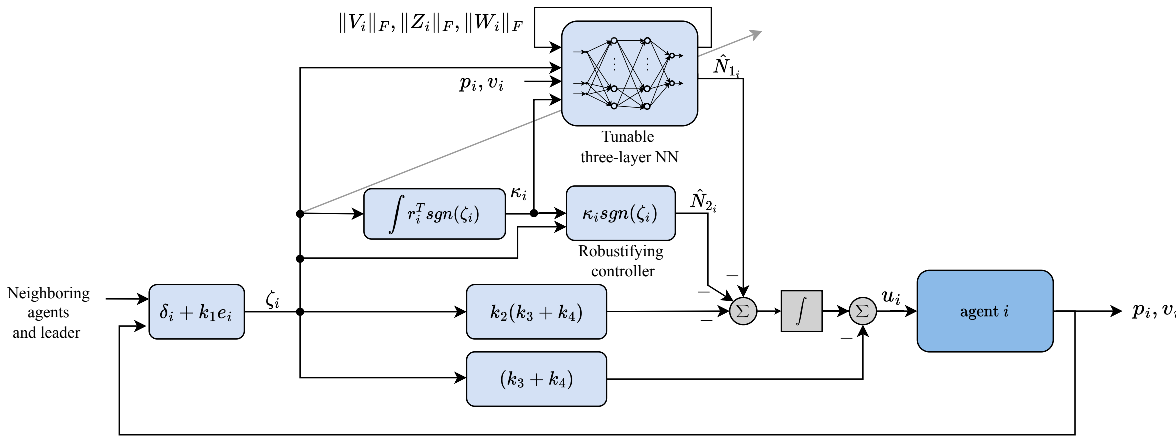

Figure 6.1: The block diagram of proposed control law (6.37) for agent i. Note that if $b_i \neq 0$, then the agent i has the information of the leader.

be unknown while authors in [32, 89, 90] considered these bounds to be known.

For the agent i, one has $||\bar{\epsilon}_i|| \leq \bar{\epsilon}_{M_i}$, $||\dot{\bar{\epsilon}}_i(\mathcal{X}_i, \dot{\mathcal{X}}_i)|| \leq \bar{\epsilon}_{dM_i}$, $||\mathcal{N}_{2_i}|| \leq d_{M_i}$, and $||\dot{\mathcal{N}}_{2_i}|| \leq d_{dM_i}$. Let us define $\bar{\mathcal{N}}_{2_i} \triangleq \mathcal{N}_{2_i} + \bar{\epsilon}_i$. Note that values of $\bar{\epsilon}_{M_i}$, $\bar{\epsilon}_{dM_i}$, d_{M_i}, and d_{dM_i} are considered to be unknown, and they only are used for analytical purposes.

For the agent i, consider (6.39) and recall the fact that the activation function and its derivative are bounded. Using the Assumption 2.3, for an arbitrary set of $\Omega_{\mathbf{x}}$, the inputs of the NN ($\mathcal{X}_i$) are bounded and their derivatives ($\dot{\mathcal{X}}_i$) are bounded. Therefore, we can conclude that there exists upper bounds for $\tilde{\mathcal{N}}_{1i}$ and $\dot{\tilde{\mathcal{N}}}_{1i}$, namely $\|\tilde{\mathcal{N}}_{1i}\| \leq N_{Mi}$ and $\|\dot{\tilde{\mathcal{N}}}_{1i}\| \leq N_{dMi}$, which are considered to be unknown. This fact also can be found in [32, 87, 88, 97].

As continuous differentiability is a sufficient condition for being locally Lipschitz [98, Corollary 4.1.1], [71, Theorem 8.4] can be written as follows:

Lemma 6.3 ([88])**.** *Consider the closed-loop system $\dot{\chi} = f(\chi, t)$, where $f : D \times [0, \infty)$, with $D \in \mathbb{R}^n$ being a set containing $\chi = 0$. Let a continuously differentiable scalar function $V : D \times [0, \infty)$ satisfy the following inequalities*

$$\begin{aligned} W_1(\chi) \leq & V(\chi, t) \leq W_2(\chi) \\ \dot{V}(\chi, t) \leq & -W_3(\chi), \quad \forall t \geq 0,\ \forall \chi \in D, \end{aligned} \tag{6.45}$$

where W_1, W_2 are continuous positive definite functions and W_3 is a uniformly continuous positive semi-definite function. Select a closed ball $B(0,R)$ with the radius of $R > 0$, and let $\rho < min_{||\chi||=R} W_1(\chi)$. Then, solutions of $\dot{\chi} = f(\chi,t)$ with $\chi(t_0) \in \{\chi \in D| \; W_2(\chi) \leq \rho\}$ are bounded and

$$W_3(\chi) \rightarrow 0\,, \quad as\; t \rightarrow \infty. \tag{6.46}$$

6.3.2 Stability Analysis

We prove in this section that the proposed control law (6.37) ensures stability in the leader-following formation control for a group of heterogeneous, second-order, uncertain, nonlinear multi-agents (6.1). Before presenting the main result of the chapter, a Lemma is presented that is utilized in the proof.

Lemma 6.4. *Let an auxiliary function $L_i(t) \in R$ be defined as follows:*

$$L_i(t) \triangleq r_i^T\big(\bar{\mathcal{N}}_{2_i} - \kappa_{d_i} sgn(\zeta_i)\big) + \dot{\zeta}_i^T \tilde{\mathcal{N}}_{1_i} + (W_m^2 + V_m^2 + Z_m^2)\zeta_i^T sgn(\zeta_i). \tag{6.47}$$

Set $\kappa_{d_i} = d_{M_i} + \bar{\epsilon}_{M_i} + \frac{1}{k_2}\max\{d_{dM_i} + \bar{\epsilon}_{dM_i} + N_{dM_i} + (W_m^2 + V_m^2 + Z_m^2), k_2 N_{M_i}\}$. Then, the following inequality holds

$$M_i \triangleq \kappa_{d_i}||\zeta_i(0)||_1 - \zeta_i^T(0)(\bar{\mathcal{N}}_{2_i}(0) + \tilde{\mathcal{N}}_{1_i}(0)) - \int_0^t L_i(s)ds \geq 0. \tag{6.48}$$

Proof. For a discontinuous function $L(t)$, using differential inclusion [72,73], there exists an absolutely continuous Filipov's solution with an upper semi-continuous, compact, and convex set-valued map $K[\mathcal{L}]$. From (6.30) and by integrating (6.47) [97], one has

$$
\begin{aligned}
\int_0^t L_i(s)ds &\overset{a.e.}{\in} \int_0^t \dot{\zeta}_i^T(s)\big(\bar{\mathcal{N}}_{2_i}(s) + \tilde{\mathcal{N}}_{1_i}(s)\big)ds - \kappa_{d_i}\int_0^t \dot{\zeta}_i^T(s)\mathrm{Sgn}(\zeta_i(s))ds \\
&\quad + k_2\int_0^t \zeta_i^T(s)\Big(\bar{\mathcal{N}}_{2_i}(s) - \kappa_{d_i}\mathrm{Sgn}(\zeta_i(s)) + \frac{(W_m^2 + V_m^2 + Z_m^2)}{k_2}\mathrm{Sgn}(\zeta_i(s))\Big)ds \\
&\le \zeta_i^T(s)(\bar{\mathcal{N}}_{2_i}(s) + \tilde{\mathcal{N}}_{1_i}(s))\Big|_0^t + k_2\int_0^t \zeta_i^T(s)\Big(- \bar{\mathcal{N}}_{2_i}(s) - \tilde{\mathcal{N}}_{1_i}(s) - \kappa_{d_i}\mathrm{Sgn}(\zeta_i(s)) + \\
&\quad \frac{(W_m^2 + V_m^2 + Z_m^2)}{k_2}\mathrm{Sgn}(\zeta_i(s)) - \frac{1}{k_2}\dot{\bar{\mathcal{N}}}_{2_i}(s) - \frac{1}{k_2}\dot{\tilde{\mathcal{N}}}_{1_i}(s)ds\Big) - \kappa_{d_i}\|\zeta_i(s)\|_1\Big|_0^t,
\end{aligned} \tag{6.49}
$$

where we used the notation $\mathrm{Sgn}(\zeta_i) = [\mathrm{Sgn}(\zeta_{i1}), ..., \mathrm{Sgn}(\zeta_{in})]^T$. The definition of the set-valued map $\mathrm{Sgn}(x_i)$, for $x_i \in R$ is given as [73, 99]:

$$
\mathrm{Sgn}(x_i) = \begin{cases} -1 & \text{if } x_i < 0, \\ [-1, 1] & \text{if } x_i = 0, \\ 1 & \text{if } x_i > 0. \end{cases} \tag{6.50}
$$

Using Cauchy–Schwarz inequality and the definition of κ_{d_i}, one has

$$
\begin{aligned}
\int_0^t L_i(s) &\le \zeta_i^T(t)(\bar{\mathcal{N}}_{2_i}(t) + \tilde{\mathcal{N}}_{1_i}(t)) - \zeta_i^T(0)(\bar{\mathcal{N}}_{2_i}(0) + \tilde{\mathcal{N}}_{1_i}(0)) - k_{d_i}\|\zeta_i(t)\|_1 + k_{d_i}\|\zeta_i(0)\|_1 \\
&\le \kappa_{d_i}||\zeta_i(0)||_1 - \zeta_i^T(0)(\bar{\mathcal{N}}_{2_i}(0) + \tilde{\mathcal{N}}_{1_i}(0)).
\end{aligned} \tag{6.51}
$$

Therefore, (6.48) is valid and this completes the proof. □

Remark 6.6. *We propose to set the number of neurons for the first and second hidden-layers to $m_1 = 3n + 4$ and $m_2 = 2(3n + 4) + 2$, for each agent. From [100, Theorem 2.4], one can see that a three-layer NN with $3n + 4$ inputs, $3n + 4$ neurons in the first hidden-layer, $2(3n + 4) + 2$ neurons in the second hidden-layer, and the sigmoid activation function, can approximate function $\mathcal{N}_{1_i}$ with arbitrary accuracy.*

Remark 6.7. *Although a high number of neurons and three layers implies a higher computational burden, we should note that the proposed method reduces the time allotted to tune one-layer NN,* *e.g., RBFNN centroids, the width of activation functions, and the number of neurons. In the NN control literature, it is commonly assumed the existence of a large enough positive integer for ideal neuron numbers for a one-layer NN [15, 16]. There is a trade-off between the setting of neuron and layer numbers and the computation complexity. In this chapter, we specify the number of neurons in each layer. The NN approximation error is then compensated with the robustifying term.*

Note that an *a priori* information required to determine the number of neurons in each layer is the number of position/velocity states n.

Theorem 6.1. *Let a strongly connected directed graph model the multi-agent system (6.1). For each agent, select the number of the hidden-layer neurons in (2.19) as $m_1 = 3n+4$, $m_2 = 2(3n+4)+2$, and the NN input as (6.38). Under Assumptions 2.3, 2.4, and 6.1-6.3, choose $k_1 > \frac{1}{2}$ and*

$$k_2 > \frac{1 + \bar{\sigma}(P(L+B))}{\underline{\sigma}(P(L+B))}. \tag{6.52}$$

Set the control input as

$$\begin{aligned} u_i(t) = &-(k_3+k_4)\zeta_i(t) + (k_3+k_4)\zeta(0) - \int_0^t \Big(\hat{W}_i^T(s)\sigma_1\big(\hat{Z}_i^T(s)\sigma_2(\hat{V}_i^T(s)\mathcal{X}_i(s))\big) \\ &+ k_2(k_3+k_4)\zeta_i(s) + \kappa_i(s)sgn(\zeta_i(s))\Big)ds, \end{aligned} \tag{6.53}$$

where k_3 and k_4 satisfy the following conditions

$$k_3 > \frac{k_2}{2\underline{\sigma}(P(L+B))},\ k_4 > \frac{\bar{\sigma}(P(L+B))}{2}. \tag{6.54}$$

Set the time-varying gain $\kappa_i(t)$ as (6.44), and the neural networks weights matrices tuning laws as

$$\begin{aligned} \dot{\hat{W}}_i &= \alpha_i\Big(k_2\big(\hat{\sigma}_1 - \hat{\sigma}_1'\hat{Z}_i^T\hat{\sigma}_2 - \hat{\sigma}_1'\hat{Z}_i^T\hat{\sigma}_2'\hat{V}_i^T\mathcal{X}_i\big)\zeta_i^T - \|\zeta_i\|_1\hat{W}_i\Big), \\ \dot{\hat{Z}}_i &= \beta_i\Big(k_2\big(\hat{\sigma}_2 - \hat{\sigma}_2'\hat{V}_i^T\mathcal{X}_i\big)\zeta_i^T\hat{W}_i^T\hat{\sigma}_1' - \|\zeta_i\|_1\hat{Z}_i\Big), \\ \dot{\hat{V}}_i &= \gamma_i\big(k_2\mathcal{X}_i\zeta_i^T\hat{W}_i^T\hat{\sigma}_1'\hat{Z}_i^T\hat{\sigma}_2' - \|\zeta_i\|_1\hat{V}_i\big). \end{aligned} \tag{6.55}$$

Then, all the closed-loop signals are bounded, $\zeta_i \to 0$ as $t \to \infty$, and agents achieve the desired formation and maintain the leader's velocity.

Proof. Let us define the Lyapunov function candidate

$$V = \frac{1}{2}\mathbf{e}^T\mathbf{e} + \frac{1}{4}\zeta^T\Pi\zeta + \frac{1}{2}r^T\mathcal{G}Qr + M + \frac{1}{2}\tilde{\kappa}^T\tilde{\kappa} + \bar{y}, \tag{6.56}$$

with the semi-positive term $M \triangleq \sum_{i=1}^{N} M_i$. The variable M_i is defined using Lemma 6.4, and $\bar{y}$ is given by

$$\begin{aligned}\bar{y} \triangleq &\frac{1}{2}tr(\tilde{W}^T\alpha^{-1}\tilde{W}) + \frac{1}{2}tr(\tilde{Z}^T\beta^{-1}\tilde{Z}) + \frac{1}{2}tr(\tilde{V}^T\gamma^{-1}\tilde{V})\\ =&\frac{1}{2}\text{vec}(\alpha^{\frac{-1}{2}}\tilde{W})^T\text{vec}(\alpha^{\frac{-1}{2}}\tilde{W}) + \frac{1}{2}\text{vec}(\beta^{\frac{-1}{2}}\tilde{Z})^T\text{vec}(\beta^{\frac{-1}{2}}\tilde{Z}) + \frac{1}{2}\text{vec}(\gamma^{\frac{-1}{2}}\tilde{V})^T\text{vec}(\gamma^{\frac{-1}{2}}\tilde{V}).\end{aligned} \tag{6.57}$$

Let us define $\bar{\kappa} = [\kappa_1, ..., \kappa_N]^T \in \mathbb{R}^N$, $\kappa_d = [\kappa_{d_1}, ..., \hat{\kappa}_{d_N}]^T \in \mathbb{R}^N$ and $\tilde{\kappa} = [\tilde{\kappa}_1, ..., \tilde{\kappa}_N] \in \mathbb{R}^N$, where $\tilde{\kappa}_i \triangleq \kappa_i - \kappa_{d_i}$. Moreover, let $\chi = [\mathbf{e}^T, \zeta^T, r^T, \sqrt{M}, \text{vec}(\alpha^{\frac{-1}{2}}\hat{W})^T, \text{vec}(\beta^{\frac{-1}{2}}\hat{Z})^T,$ $\text{vec}(\gamma^{\frac{-1}{2}}\hat{V})^T, \kappa^T]^T$. It can be shown that the following inequalities are valid for (6.56)

$$L_b(\chi) \leq V \leq U_b(\chi), \tag{6.58}$$

with

$$L_b(\chi) = \underline{\eta}||\chi||^2,\ U_b(\chi) = \bar{\eta}||\chi||^2, \tag{6.59}$$

where $\underline{\eta} \triangleq \min\{\frac{1}{2}\underline{g}\underline{\sigma}(Q), \frac{1}{2}, \frac{1}{4}\underline{\sigma}(\Pi)\}$, $\bar{\eta} \triangleq \max\{\frac{1}{2}\bar{g}\bar{\sigma}(Q), 1, \frac{1}{4}\bar{\sigma}(\Pi)\}$. To use Lemma 6.3, we should study the existence of Filippov's solution for $\dot{\chi} = f(\chi, t)$, as $\dot{M}$ and $\dot{\kappa}$ are differential equations with discontinuous right-hand side [8]. Using differential inclusion [72, 73], an absolutely continuous Filipov's solution exists for $\dot{\chi} \in K[\mathcal{F}](\chi, t)$ where an upper semi-continuous, compact and convex set-valued map $K[\mathcal{F}](\chi, t)$ is defined as follows:

$$K[\mathcal{F}](\chi, t) \triangleq \bigcap_{R>0} \bigcap_{\mu(H)=0} \overline{co} f(B(\chi, R)\backslash H, t), \tag{6.60}$$

where $B(\chi, R)$ is the closed ball with center χ and the radius R. Using (6.60) and from [101, Theorem 2.2], the time derivative of the Lyapunov function candidate exists almost everywhere:

$$\dot{V}(\chi) \overset{a.e.}{\in} \bigcap_{\Lambda \in \partial V(\chi)} \Lambda^T [K^T[\mathcal{F}](\chi)]^T. \tag{6.61}$$

As the Lyapunov function candidate (6.56) is continuously smooth, (6.61) can be written as follows:

$$\dot{V}(\chi) \overset{a.e.}{\in} \nabla V \; K[\dot{\mathbf{e}}^T, \dot{\zeta}^T, \dot{r}^T, \dot{\mathcal{G}}^T, \dot{M}, \text{vec}(\alpha^{-\frac{1}{2}}\dot{\hat{W}})^T, \text{vec}(\beta^{-\frac{1}{2}}\dot{\hat{Z}})^T, \text{vec}(\gamma^{-\frac{1}{2}}\dot{\hat{V}})^T, \dot{\tilde{\kappa}}^T]^T, \tag{6.62}$$

where $\nabla V \triangleq [\mathbf{e}^T, \frac{1}{2}\zeta^T \Pi, r^T \mathcal{G} Q, \frac{1}{2}\frac{\partial(r^T \mathcal{G} Q r)}{\partial \mathcal{G}}, 1, \text{vec}(\alpha^{-\frac{1}{2}}\hat{W})^T, \text{vec}(\beta^{-\frac{1}{2}}\hat{Z})^T, \text{vec}(\gamma^{-\frac{1}{2}}\hat{V})^T, \tilde{\kappa}^T]$. Using (6.57) and (6.62), the time derivative of (6.56) is given by

$$\begin{aligned}\dot{V} \overset{a.e.}{\in} & \mathbf{e}^T \dot{\mathbf{e}} + \frac{1}{2}\zeta^T \Pi \dot{\zeta} + \frac{1}{2} r^T \dot{\mathcal{G}} Q r + r^T \mathcal{G} Q \dot{r} + \dot{M} + \tilde{\kappa}^T \dot{\tilde{\kappa}} \\ & + tr(\tilde{W}^T \alpha^{-1} \dot{\hat{W}}) + tr(\tilde{Z}^T \beta^{-1} \dot{\hat{Z}}) + tr(\tilde{V}^T \gamma^{-1} \dot{\hat{V}}).\end{aligned} \tag{6.63}$$

Substituting (6.28), (6.30), (6.40), and (6.48) in (6.63) yields

$$\begin{aligned}\dot{V} =& \mathbf{e}^T(\zeta - k_1 \mathbf{e}) + \frac{1}{2}\zeta^T \Pi (r - k_2 \zeta) + r^T \Big(- k_2 \zeta - (k_3 + k_4) r - \kappa(t) \text{Sgn}(\zeta) \\ & + \tilde{W}^T \big(\hat{\sigma}_1 - \hat{\sigma}_1' \hat{Z}^T \hat{\sigma}_2 - \hat{\sigma}_1' \hat{Z}^T \hat{\sigma}_2' \hat{V}^T \mathcal{X}\big) + \hat{W}^T \hat{\sigma}_1' \tilde{Z}^T \big(\hat{\sigma}_2 - \hat{\sigma}_2' \hat{V}^T \mathcal{X}\big) \\ & + \hat{W}^T \big(\hat{\sigma}_1' \hat{Z}^T \hat{\sigma}_2' \tilde{V}^T \mathcal{X}\big) + \mathcal{N}_2 + \bar{\epsilon}_M \Big) + \tilde{\kappa}^T \dot{\tilde{\kappa}} - \sum_{i=1}^{N} \Big(r_i^T \big(\bar{\mathcal{N}}_{2_i} - \kappa_{d_i} \text{Sgn}(\zeta_i)\big) \\ & + \dot{\zeta}_i^T \tilde{\mathcal{N}}_{1_i} + (W_m^2 + V_m^2 + Z_m^2) \zeta_i^T \text{Sgn}(\zeta_i) \Big) + tr(\tilde{W}^T \alpha^{-1} \dot{\hat{W}}) + tr(\tilde{Z}^T \beta^{-1} \dot{\hat{Z}}) \\ & + tr(\tilde{V}^T \gamma^{-1} \dot{\hat{V}}).\end{aligned} \tag{6.64}$$

Reorganizing (6.64), from (6.30) and (6.39), one has

$$\begin{aligned}\dot{V} \leq & \mathbf{e}^T(\zeta - k_1\mathbf{e}) + \frac{1}{2}\zeta^T\Pi(r - k_2\zeta) + r^T\big(- k_2\zeta - (k_3 + k_4)r\big) + \tilde{\kappa}^T\dot{\tilde{\kappa}} \\ & + \sum_{i=1}^{N}(\kappa_{d_i} - \kappa_i(t))r_i^T\text{Sgn}(\zeta_i) - (W_m^2 + V_m^2 + Z_m^2)\zeta_i^T\text{Sgn}(\zeta_i) \\ & + \sum_{i=1}^{N}\Big(tr(\tilde{W}_i^T(\alpha_i^{-1}\dot{\tilde{W}}_i + k_2(\hat{\sigma}_1 - \hat{\sigma}_1'\hat{Z}_i^T\hat{\sigma}_2 - \hat{\sigma}_1'\hat{Z}_i^T\hat{\sigma}_2'\hat{V}_i^T\mathcal{X}_i)\zeta_i^T)) \\ & + tr\big(\tilde{Z}_i^T(\beta^{-1}\dot{\tilde{Z}}_i + k_2(\hat{\sigma}_2 - \hat{\sigma}_2'\hat{V}_i^T\mathcal{X}_i)\zeta_i^T\hat{W}_i^T\hat{\sigma}_1')\big) \\ & + tr\big(\tilde{V}_i^T(\gamma_i^{-1}\dot{\tilde{V}}_i + k_2\mathcal{X}_i\zeta_i^T\hat{W}_i^T\hat{\sigma}_1'\hat{Z}_i^T\hat{\sigma}_2')\big)\Big).\end{aligned} \tag{6.65}$$

By substituting (6.43) and (6.55) in (6.65), one can get

$$\begin{aligned}\dot{V} \leq & \mathbf{e}^T(\zeta - k_1\mathbf{e}) + \frac{1}{2}\zeta^T\Pi(r - k_2\zeta) + r^T(-k_2\zeta - (k_3 + k_4)r) \\ & + \sum_{i=1}^{N}\Bigg(\|\zeta_i\|_1\Big(tr(\tilde{W}_i^T\hat{W}_i) + tr(\tilde{Z}_i^T\hat{Z}_i) + tr(\tilde{V}_i^T\hat{V}_i)\Big) \\ & - (W_m^2 + V_m^2 + Z_m^2)\zeta_i^T\text{Sgn}(\zeta_i)\Bigg).\end{aligned} \tag{6.66}$$

Applying Young's inequality for $tr(\tilde{W}_i^T\hat{W}_i)$, one has $tr(\tilde{W}_i^T\hat{W}_i) \leq \frac{W_m^2}{2} - \frac{\|\hat{W}_i\|_F^2}{2}$. Following the same procedure for $tr(\tilde{Z}_i^T\hat{Z}_i)$ and $tr(\tilde{V}_i^T\hat{V}_i)$, one can write

$$\dot{V} \leq \mathbf{e}^T(\zeta - k_1\mathbf{e}) + \frac{1}{2}\zeta^T\Pi(r - k_2\zeta) + r^T(-k_2\zeta - (k_3 + k_4)r) + \sum_{i=1}^{N}\big(\tilde{\kappa}_i^T\dot{\kappa}_i - \tilde{\kappa}_i^T r_i^T\text{Sgn}(\zeta_i)\big). \tag{6.67}$$

From (2.7) and applying Cauchy–Schwarz inequality and Young's inequality, the following result can be obtained

$$-k_2r^T\zeta \leq \frac{k_2}{2}\underline{\sigma}(P(L+B))||\zeta||^2 + k_2\frac{||r||^2}{2\underline{\sigma}(P(L+B))}. \tag{6.68}$$

Substituting (6.68) in (5.27) and from (2.7) one can write

$$\begin{aligned}\dot{V} \leq &-(k_1-\frac{1}{2})||\mathbf{e}||^2-(\frac{k_2}{2}\underline{\sigma}(P(L+B))-\frac{1+\bar{\sigma}(P(L+B))}{2})||\zeta||^2-(k_3+k_4\\&-\frac{\bar{\sigma}(P(L+B))}{2}-\frac{k_2}{2\underline{\sigma}(P(L+B))})||r||^2).\end{aligned} \tag{6.69}$$

From the given conditions for gains k_1, k_2, k_3, k_4 in the Theorem 6.1, one has

$$\dot{V} \leq -\lambda_1||\mathbf{e}||^2-\lambda_2||\zeta||^2-\lambda_3||r||^2, \tag{6.70}$$

where λ_1, λ_2, and λ_3 are positive constants. Consequently, (6.70) can be rewritten as

$$\dot{V} \leq -U(\chi), \tag{6.71}$$

where $U(\chi) \triangleq -\underline{\lambda}||[\mathbf{e}^T, \zeta^T, r^T]^T||^2$, with $\underline{\lambda} = \min(\lambda_1, \lambda_2, \lambda_3)$. Note that in (6.71), $U(\chi)$ is a positive semi-definite function over $\Omega_{\mathcal{X}}$. From (6.56) and (6.71), one has $V \in L_\infty$ over $\Omega_{\mathcal{X}}$; hence, $\mathbf{e}, \zeta, r, \tilde{W}, \tilde{Z}, \tilde{V}$ and $\tilde{\kappa}$ are bounded on set $\Omega_{\mathcal{X}}$. Consequently, from (6.28) $\delta \in L_\infty$. From Assumption 6.1 and (6.27), one can conclude that $\mathbf{x} \in L_\infty$. From (6.30), as $r \in L_\infty$ and $\zeta \in L_\infty$, one can obtain $\dot{\zeta} \in L_\infty$. Using Lemma 2.2, Assumptions 6.1-6.3, and (6.29), it can be deduced that $u \in L_\infty$. Based on Assumption 2.3, (6.37) and (6.40) are also bounded. From the boundedness of $\mathbf{e}, \delta, \zeta, r$ and the closed-loop terms, $U(\chi)$ is uniformly continuous, where Lemma 6.3 can be applied. Let $\Omega_{\mathcal{X}} = \{\chi| \; ||\chi|| \in B(0, R)\}$, and the initial conditions belong to the compact set $\mathcal{S} \subset \Omega_{\mathcal{X}}$ as

$$\mathcal{S} \triangleq \{\chi \in \Omega_{\mathcal{X}} | U_b(\chi) \leq \underline{\eta} R^2\}, \tag{6.72}$$

where the origin is within the set of $\mathcal{S}$. Then, the Lemma 6.3 is used to conclude $||\mathbf{e}||^2 \to 0, ||\zeta||^2 \to 0, ||r||^2 \to 0$, as $t \to \infty$, $\forall \chi(0) \in \mathcal{S}$. From (6.27) and (6.28), one can conclude that as $||\mathbf{e}|| \to 0$, and $||\delta|| \to 0$, (6.7) holds. Consequently, by increasing R, the semi-global asymptotic stability is obtained [88]. This completes the proof. $\square$

6.4 Simulation Results

In order to demonstrate the performance of the proposed method, we consider a multi-agent system with five two-link robot arms. The directed graph that models the system is shown in Figure 6.2. The dynamics of each agent is given by [28]

$$\begin{aligned} \dot{p}_{i1} &= p_{i2}, \\ M_i(p_{i1})\dot{p}_{i2} + V_i(p_{i1}, p_{i2})p_{i2} + G_i(p_{i1}) + w_i &= \tau_i, \end{aligned} \tag{6.73}$$

for $i = 1, ..., 5$, where $p_{i1} = [p_{i11}, p_{i12}]^T \in \mathbb{R}^2$ and $p_{i2} = [p_{i21}, p_{i22}]^T \in \mathbb{R}^2$ are the joint position and velocity states of i-th robot arm, respectively. In (6.73), the control input is $\tau_i \triangleq u_i$. Expressions for the inertia matrix $M_i(p_{i1})$, the Coriolis matrix $V_i(p_{i1}, p_{i2})$, and the gravitational vector $G_i(p_{i1})$ in (6.73) can be found in [28, 96]. In (6.73), w_i represents a bounded disturbance in the dynamics of each two-link robot arm. The parameters of the each robot arm are $g = 9.8m/s^2$, $r_{i1} = 1m$, $r_{i1} = 1m$, $m_{i1} = 0.8kg$, and $m_{i2} = 1.7kg$, $w_i = [-0.12cos(t), 0.1sin(t)]^T$, $i = 1, ..., 5$. The leader dynamics is given by

$$\begin{aligned} \dot{p}_l &= v_l, \\ \dot{v}_l &= \begin{bmatrix} -p_{l_1} + 0.2(1 - p_{l_1}^2)v_{l_1} \\ -p_{l_2} + 0.3(1 - p_{l_2}^2)v_{l_2} \end{bmatrix}, \end{aligned} \tag{6.74}$$

where $p_l = [p_{l_1}, p_{l_2}]^T \in \mathbb{R}^2$ and $v_l = [v_{l_1}, v_{l_2}]^T \in \mathbb{R}^2$ are the position and velocity states of the leader. The initial conditions for the five robots are given as: $p_{11}(0) = [2.1, 0]^T$, $p_{21}(0) = [0, 2.5]^T$, $p_{31}(0) = [-1.1, 2]^T$, $p_{41}(0) = [-1.8, 0.7]^T$, $p_{51}(0) = [-1, -1.7]^T$, $p_{i2}(0) = [0, 0]^T$, for $i = 1, ..., 5$. The desired displacement with respect to the leader for each agent is given as: $d_1 = [0, d]^T$, $d_2 = [-dsin(\frac{2\pi}{5}), dcos(\frac{2\pi}{5})]^T$, $d_3 = [-dsin(\frac{\pi}{5}), -dcos(\frac{\pi}{5})]^T$, $d_4 = [dsin(\frac{\pi}{5}), -dcos(\frac{\pi}{5})]^T$ and $d_5 = [dsin(\frac{2\pi}{5}), dcos(\frac{2\pi}{5})]^T$ with $d = 1$. The leader initial states are $p_l(0) = [1, -1]^T$ and $v_l(0) = [0, 0]^T$, respectively. All weights of edges in Figure 6.2 are equal to *one*, as well as the leader's edge weight ($b_1 = 1$). Therefore, the adjacency matrix and graph Laplacian are given by

$$A = \begin{bmatrix} 0 & 0 & 0 & 0 & 1 \\ 1 & 0 & 0 & 0 & 0 \\ 1 & 1 & 0 & 0 & 0 \\ 0 & 0 & 1 & 0 & 1 \\ 0 & 0 & 1 & 0 & 0 \end{bmatrix}, L = \begin{bmatrix} 1 & 0 & 0 & 0 & -1 \\ -1 & 1 & 0 & 0 & 0 \\ -1 & -1 & 2 & 0 & 0 \\ 0 & 0 & -1 & 2 & -1 \\ 0 & 0 & -1 & 0 & 1 \end{bmatrix}. \tag{6.75}$$

We selected 10 neurons for the input layer, 10 neurons for the first hidden layer, 22 neurons for the second hidden layer, and 2 neurons for the output layer for each agent. The activation function for these layers is a sigmoid function. The activation function for the output layer is linear. The constants α_i, β_i, γ_i, $\forall i$, are chosen as $\alpha_i = \frac{1}{20}$, $\beta_i = \frac{1}{20}$, $\gamma_i = \frac{1}{20}$. The gains were selected as: $k_1 = 4$, $k_2 = 37.5$, $k_3 = 380$, and $k_4 = 2$.

Figures 6.3-6.9 show the simulation results for the multi-agent system (6.73). In Figure 6.3, the performance of the multi-agent system is shown where dash-dotted lines indicate the multi-agent system achieving its desired formation. Figure 6.4 illustrates the trajectories of agents and the leader. The velocities of agents, as well as the leader, are shown in Figure 6.5, where the velocities of agents become identical to the leader velocity. The Frobenius norm of the NN weights matrices of $\hat{V}_i$, $\hat{Z}_i$ and $\hat{W}_i$ are displayed as Figure 6.6. Figure 6.7 demonstrates the time-varying gains κ_i. To avoid that $\kappa_i(t)$ reaching high values, a dead-zone with a size of $b = 0.005$, has been implemented, similar to [87, 97]. The error signals $e_i(t)$, their time derivatives $\delta_i(t)$, and the filtered errors $\zeta_i(t)$ are shown in Figure 6.8. The control input of each agent is shown in Figure 6.9.

These results verify the performance of the proposed method based on RISE feedback and the NN-based controller. To compare our proposed method with other existing works, we considered results on leader-following consensus control of the nonlinear system with unknown nonlinearities [14, 28]. The selected parameters for the controller in [14] are: number of neurons is 9, $\varphi_m = 1$, $\kappa = 0.3$ and $c = 102.45$. Moreover, the selected parameters for the controller in [28] are: number of neurons is 25, $k_i = 250.5$, $\kappa = 0.5$ and $\sigma_i = 0.2$.

. We included the desired displacements and applied these methods similar to [20, p. 127]. We define the average of the control inputs cost function (ACI), $\nu(t)$ and the average of the formation

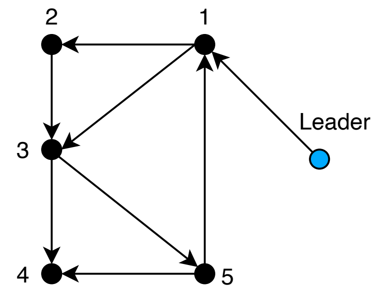

Figure 6.2: The directed graph of five agents with the leader as the root of the spanning tree.

errors cost function (AFE), $\vartheta(t)$, as follows:

$$\begin{aligned} \nu(t) =& \frac{1}{2N}\sum_{i=1}^{N} u_i^T(t)u_i(t), \\ \vartheta(t) =& \frac{1}{2N}\sum_{i=1}^{N} ||e_i(t)||_1. \end{aligned} \tag{6.76}$$

These two functions are used as performance indices to evaluate the effectiveness of the proposed methods in comparison with [14, 28]. Figure 6.10(a) shows the semi-logarithmic graph of the ACI function.

However, the proposed method (solid-line) energy consumption is almost the same as the other two methods. Figure 6.10(b) indicates that our proposed method settled faster and converged to zeros in contrast with two other methods where the error remains bounded.

6.5 Conclusion

In this chapter, we developed the leader-following formation control of the heterogeneous, second-order, uncertain, input-affine, nonlinear multi-agent systems modeled by a directed graph. The unknown nonlinearity in the dynamics of a multi-agent system was approximated by a tunable, three-layer NN consisting of an input layer, two hidden layers, and an output layer. The proposed method can *a priori* set the number of neurons in each layer of the NN. The NN weights tuning laws were derived using the Lyapunov theory. A robust integral of the sign of the error feedback control

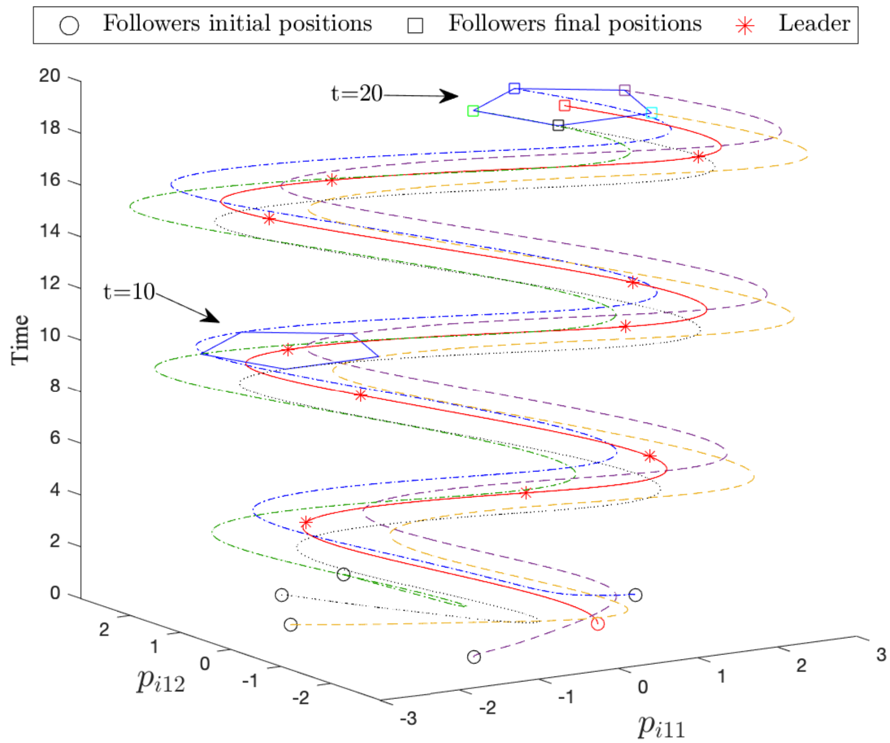

Figure 6.3: Performance of the multi-agent system (6.73).

with an NN was developed that guarantees semi-global asymptotic leader tracking. The boundedness of the closed-loop signals and asymptotic leader tracking formation were proven using the Lyapunov stability theory. The results were compared with two previous results, which showed the effectiveness of the proposed method.

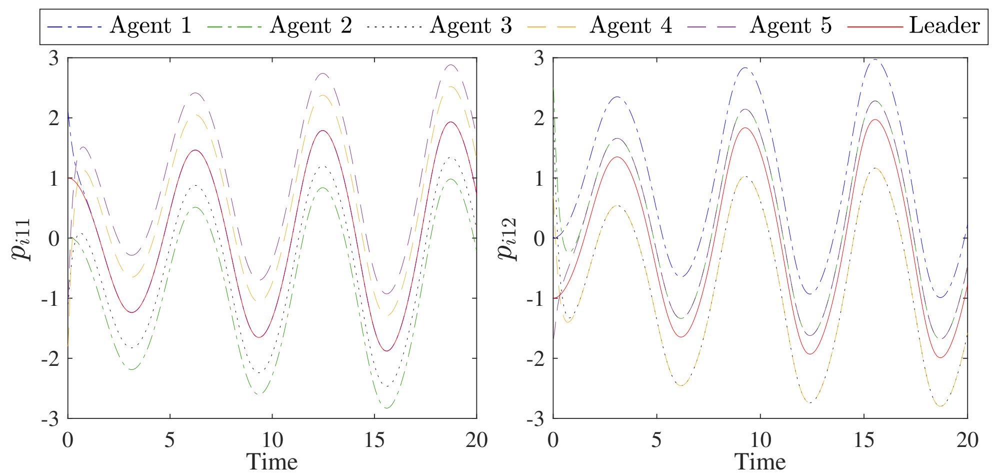

Figure 6.4: Evolution of agents and the leader (solid line) position states.

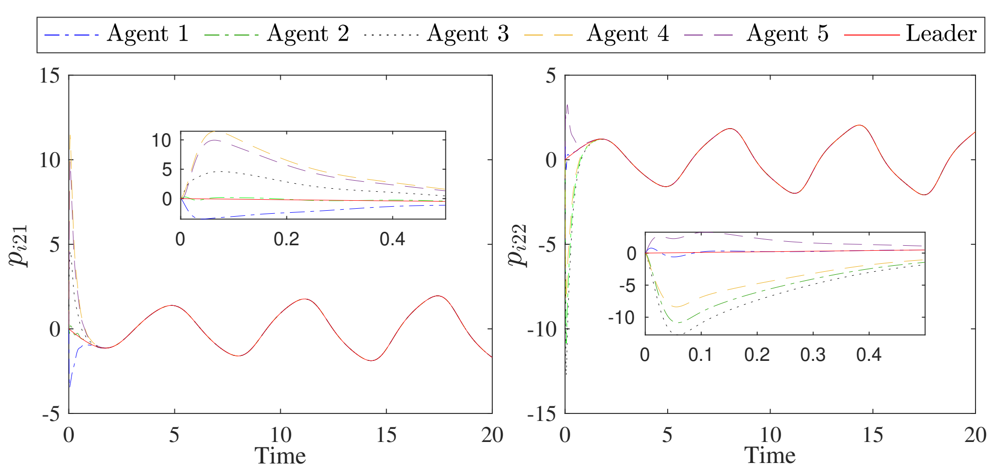

Figure 6.5: Evolution of agents and the leader (solid line) velocity states.

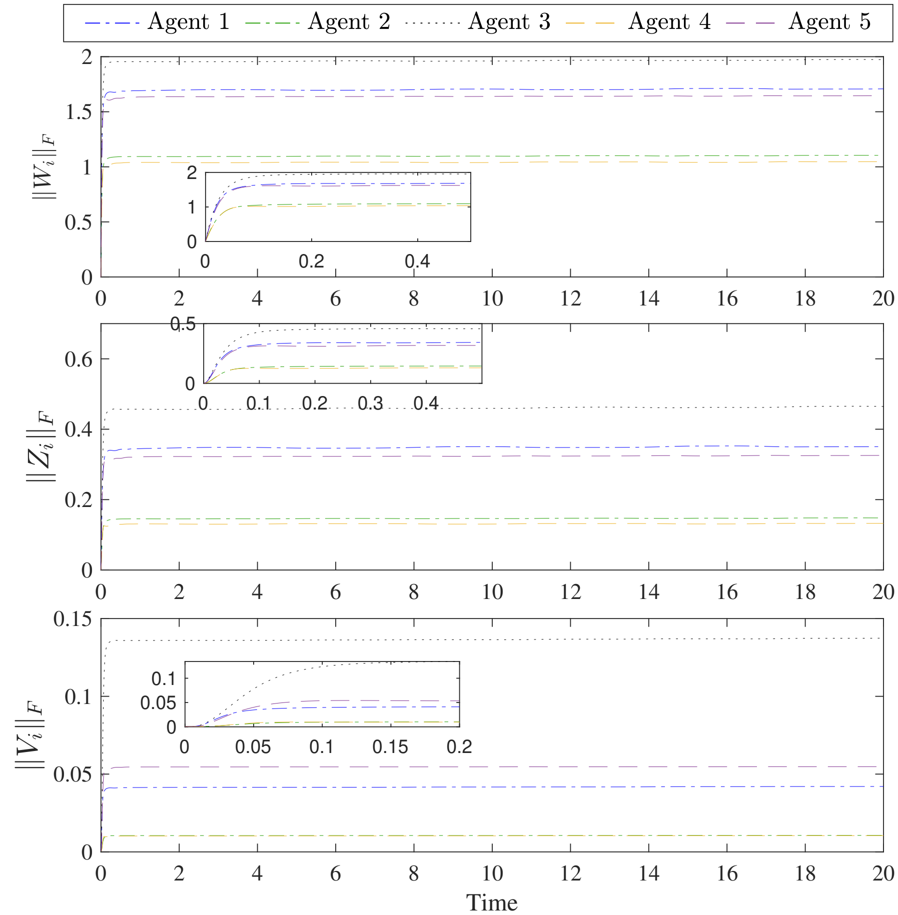

Figure 6.6: Frobenius Norm of NN weights matrices for agents.

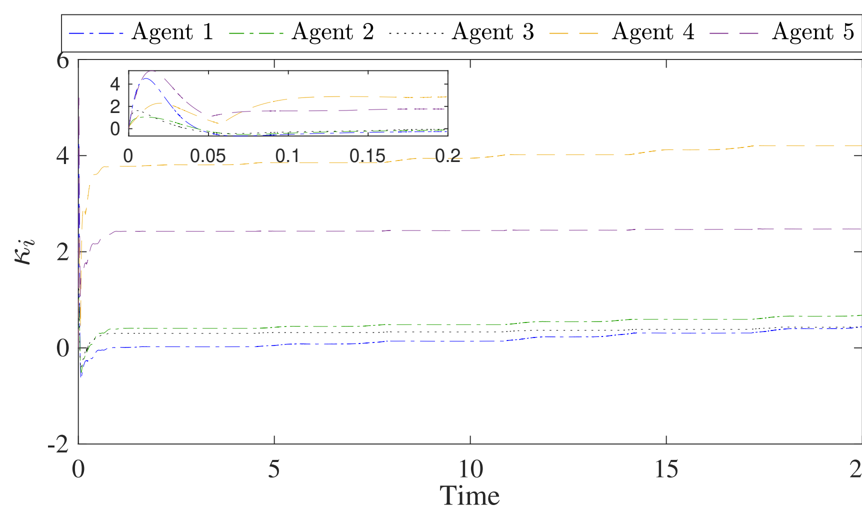

Figure 6.7: Time-variant gain κ_i of each agent.

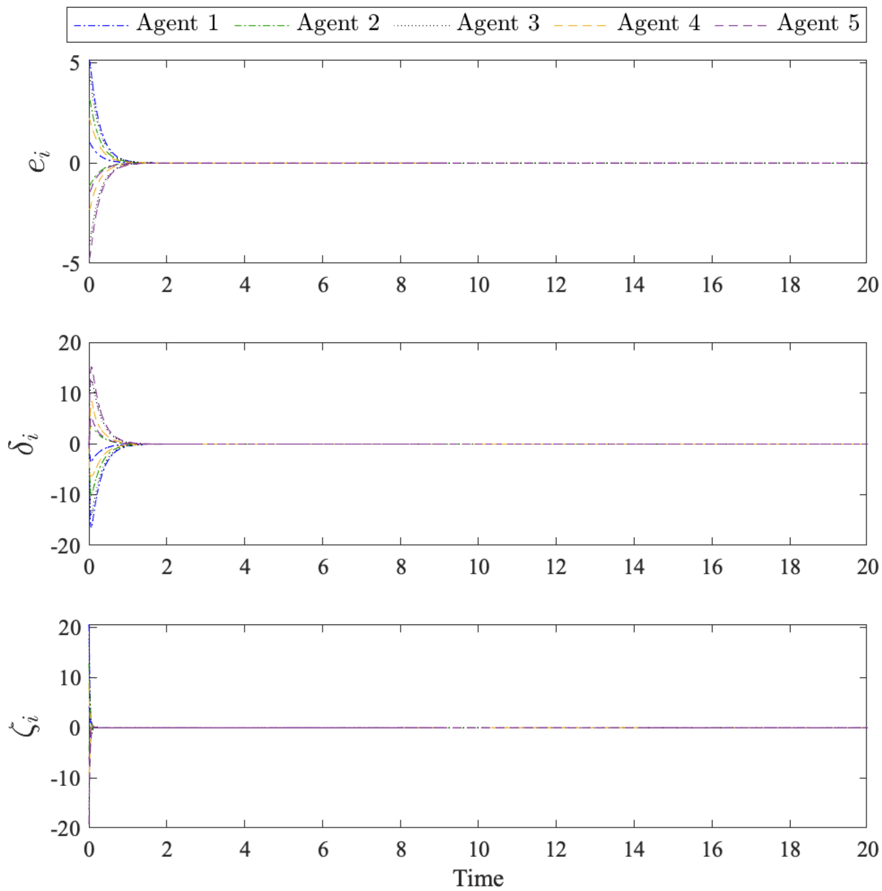

Figure 6.8: Error signals of $\mathbf{e}$, δ, and ζ for each agent.

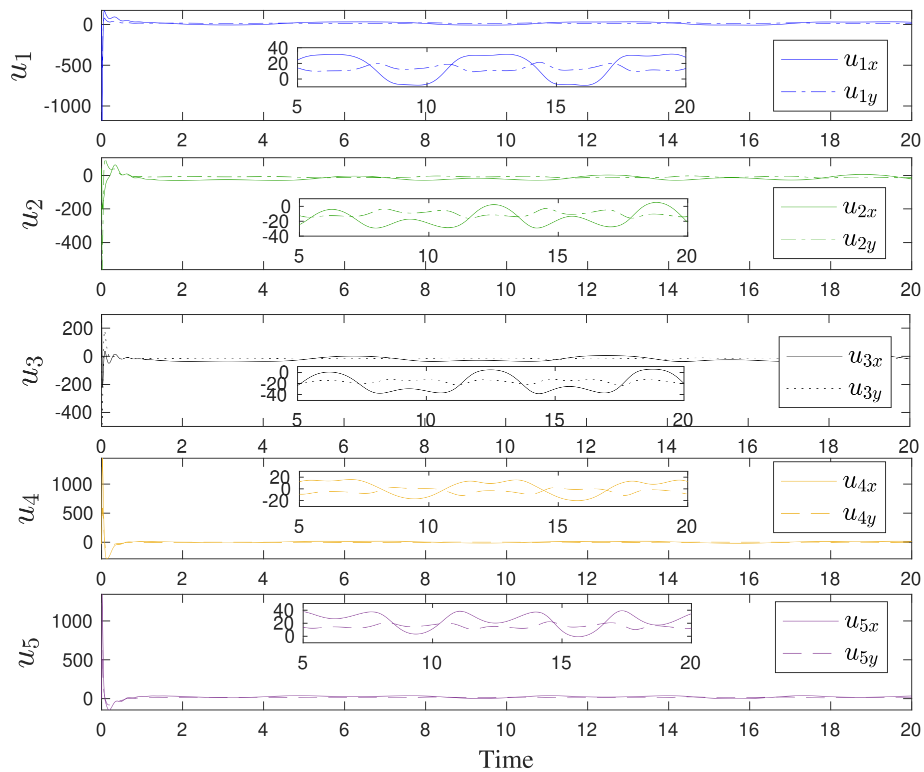

Figure 6.9: Control input of each agent.

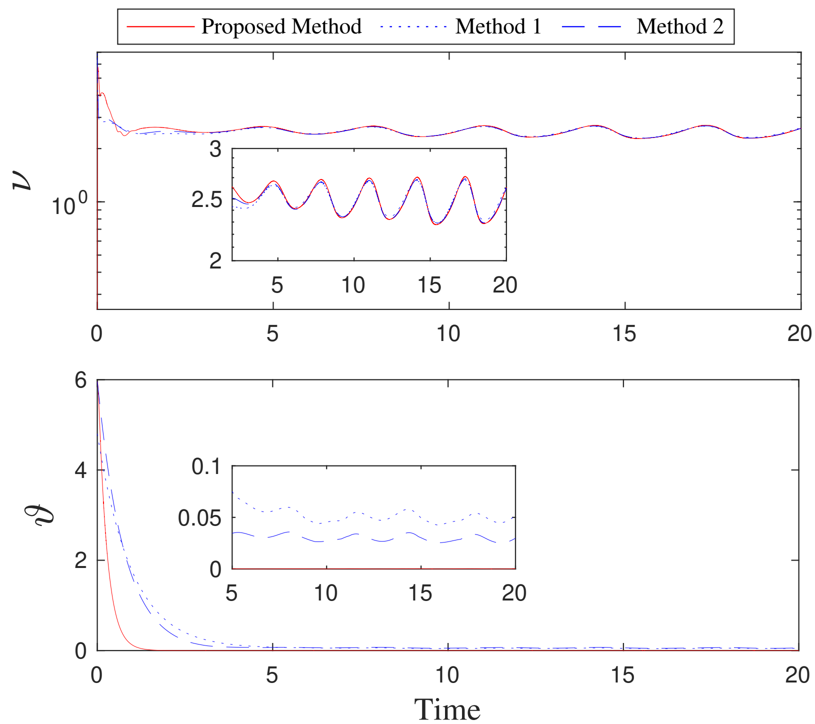

Figure 6.10: (a) ACI function comparison between proposed method, Method 1 [28], and Method 2 [14] (y-axis is in logarithmic scale); (b) AFE function comparison between proposed method, Method 1 [28], and Method 2 [14].

Chapter 7

Neuro-Adaptive Undirected Formation Control of Nonlinear Multi-Agent Systems With Communication Delays

7.1 Introduction

The chapter focuses on formation control with constant communication delays for second-order, uncertain, nonlinear multi-agents with nonsymmetric control gain matrix and unknown control direction. The multi-agent system is modeled by an undirected graph. A three-layer neural network (NN) is used to approximate an unknown nonlinearity. Unlike a conventional one- or two-layer NN, the three-layer NN allows the user apriori to set up the number of neurons in each layer. In this case, only the weights norms of the two consecutive outer layers are tunable, alleviating the computational complexity. The tuning law is derived using the Lyapunov stability theory. The leader-following formation control problem with communication delay is addressed by a delayed integral of error variables, an NN-based control, and a robustifying term. The semi-globally uniformly ultimately bounded (SGUUB) solution of the closed-loop system is rigorously proven using a barrier Lyapunov function. In order to evaluate the efficiency and performance of the proposed method, simulation results are provided.

Formation control problems of nonlinear multi-agent systems have been studied over the last two decades. One of the challenging problems in this domain is to consider the time delay. The time delay can either exist in the dynamics of multi-agent systems, e.g., [60, 63, 93, 94, 102], or as a communication delay among the neighboring agents. The multi-agent systems with communication time-invariant delays and time-varying delays are studied in the literature [103–111]. Most of the proposed techniques use linear matrix inequality (LMI) to establish the stability of the closed-loop system in the presence of a communication delay.

7.1.1 Related Works on Formation Control of Nonlinear Multi-Agent Systems With Communication Delays Using Neural Networks

In a study [112], considering that an undirected graph represents the interaction among agents, authors addressed the time-invariant communication delay when a single-integrator dynamics models each agent. This work was extended in [113], where an average consensus problem has been studied for multi-agent systems modeled by an undirected graph with fixed, switching typologies and time-varying communication delays. The consensus control problem of multi-agent systems with double-integrator dynamics, when a weighted digraph represents the communication topology in the presence of time-varying communication delays, has been studied in [114].

Constant communication delay for formation control problem of nonlinear multi-agent systems was studied in [103–105, 107]. For a class of second-order, Brunovsky form, nonlinear multi-agent systems, a weighted average consensus problem has been addressed in [103], where the system's stability has been proven using the Lyapunov stability theory and frequency-domain input-output analysis. The leader-following and collision avoidance problems for a second-order, Brunovsky form, nonlinear multi-agent with heterogeneous communication delays, when an undirected graph describes the interaction topology, have been studied in [115]. The target tracking problem of first-order, nonlinear multi-agent systems with constant communication delays, when a directed graph describes the interaction topology, has been studied in [107]. An upper bound of the communication delay and sufficient stability conditions were acquired in terms of LMIs.

For high-order, nonlinear multi-agent systems modeled by an undirected graph, an average consensus problem has been addressed in the presence of a constant communication delay in [104].

This work has been extended in [105], where authors considered that a directed graph had described the interaction topology. For a linear, high-order multi-agent system in the presence of the constant communication time delay and undirected graph, authors in [106], investigated a leader-following, fault-tolerant control problem. In [106], the authors used the LMI technique to establish the stability of the closed-loop systems.

Time-varying communication delay for formation control problem of nonlinear multi-agent systems has been studied in [108–111]. In [108], authors addressed sampled-data leader-following consensus for first-order, nonlinear multi-agent systems with a Markovian switching network and communication delay. In this study, the controller gains are obtained upon solving a set of LMIs. For a directed graph, the Leader-following consensus problem for first-order, nonlinear multi-agent systems with a Lipschitz continuous nonlinear function has been studied in [109], where sufficient stability conditions were derived in terms of LMIs using Lyapunov stability theory.

Although some literature assumes that the sign of control direction is known [60, 93, 94], this may not be the case. It is possible to resolve the problem of unknown control directions for nonlinear systems using Nussbaum functions [33–35, 104, 116–122]. Authors in [33–35, 104, 116, 121], used Nussbaum functions to tackle a scalar, unknown control direction in system dynamics. However, authors in [117–121] considered the control gain matrix has an unknown direction. Formation control of nonlinear multi-agent systems with unknown control directions can be found in [123–125]. Authors in [123], using a constructed Nussbaum function, have addressed the adaptive consensus of multi-agent systems for first-order and second-order linearly parameterized dynamics representing agent dynamics when an undirected graph has represented the interactions among agents. For a directed graph, consensus protocols (leaderless and leader-following cases) for second-order nonlinear multi-agent systems have been studied in [125].

Most of the literature on formation control of nonlinear multi-agent uses one-layer radial basis function neural networks (RBFNN) [57, 60, 104] or two-layer NN [54], to compensate for the unknown nonlinearities in system dynamics. In [89], authors use two-layer NN (input, hidden, and output layers), where only the weights between two outer layers can be tuned. The tuning laws in [89] were derived using the Lyapunov stability theory. In this study, a three-layer NN comprised of an input layer, two hidden layers, and an output layer is employed to compensate for a nonlinearity, and the number of neurons in each layer is given.

In this work, we consider a second-order, nonlinear multi-agent system with unknown nonlinearity in the system dynamics in the presence of a bounded disturbance. The undirected graph models the interaction topology. We consider the transmission time delay between the agents and from the leader to the agents. We consider that the control direction is unknown, and we use the Nusbbaum function to resolve this issue. Unknown nonlinearity in the closed-loop systems is compensated using a three-layer NN when only the norm of the weights between the two last consecutive layers is dynamic. We use a hyperbolic function to estimate the upper bound for the NN approximation error and bounded disturbance to avoid right-hand side discontinuity.

The main contributions of this chapter are:

(1) Compared with the literature on the formation control problems of multi-agent systems [106–109, 113], our method does not require the existence or solvability of LMIs. Moreover, we address the unknown control direction in the presence of the time-invariant communication delay. In comparison with [103, 112–114], we addressed leader-following formation control of second-order, nonlinear multi-agent systems with time-invariant communication delay. We also consider a three-layer NN to approximate the nonlinearity in closed-loop systems with a predetermined number of neurons in each layer.

(2) While authors in [104, 105] considered the average consensus problem, here we considered the leader-following formation control problem where we used the barrier Lyapunov function to prove the stability of the closed-loop system. Moreover, we considered a nonsymmetric control gain matrix in each agent's dynamics that distinguishes our work from [104, 105].

(3) The leader-following formation control of second-order, nonlinear multi-agent systems with communication delay is shown to be semi-globally uniformly ultimately bounded (SGUUB).

7.1.2 Related Works on Upper Bound of Time Delay

This section uses previously established results for an upper bound on a time delay when the interaction topology among the agents is modeled with an undirected graph. The following lemma is used later in the proof.

Lemma 7.1 ([112]). *Consider a network of agents with an equal communication time delay τ in all links. For a given Laplace transform of a function $f(t)$ in the form of $\mathcal{F}(s) = sI_N + e^{-\tau s}\mathcal{M}$, where $\mathcal{M}$ is the Laplacian matrix of an undirected, and connected graph, if the nonzero, real constant τ satisfies $\bar{\lambda}(\mathcal{M})\tau < \pi/2$, then all non-trivial zeros of $\mathcal{F}(s)$ are placed in the open left-half-plane.*

These results have been extended in [105] and consider a directed graph topology.

7.2 Problem Formulation

We consider the multi-agent system composed of N agents, each with a dynamics that is given by

$$\begin{aligned} \dot{p}_i(t) &= v_i(t), \\ \dot{v}_i(t) &= f_i(p_i, v_i) + g_i(p_i, v_i)u_i(t) + w_i(t), \end{aligned} \tag{7.1}$$

for $i = 1, ..., N$, where each agent's position and velocity are $p_i \in \mathbb{R}^n$ and $v_i \in \mathbb{R}^n$, respectively. The function $f_i(p_i, v_i) \in \mathbb{R}^n$ is considered to be an unknown, Lipschitz continuous function, and the matrix $g_i(p_i, v_i) \in \mathbb{R}^{n\times n}$ is an unknown function. The control input is $u_i \in \mathbb{R}^n$, and a disturbance on each agent is $w_i \in \mathbb{R}^n$. We define the stacked vector of states as $z_i = [p_i^T, v_i^T]^T$.

Assumption 7.1. *The gain matrix $g_i(p_i, v_i)$ is either a symmetric or regular, non-singular matrix and satisfies the following*

$$\underline{g}||x||^2 \leq x^T g_i x \leq \bar{g}||x||^2, \tag{7.2}$$

where $x \in \mathbb{R}^n$ and $\underline{g}$, and $\bar{g}$ are nonzero constants.

Remark 7.1. *Assumption 7.1 states a condition for the controllability of the system (7.1). Since these bounds are only considered for analytic purposes, knowing their exact values for control design is not necessary. As a result, we did not incorporate $\underline{g}$ or its sign into our control design. Based on these considerations, our work differs from [14, 28, 60, 96], where bounds are used for* *control design. This assumption is a standard assumption in an unknown control direction problem which can be found in [117–120, 122].*

Lemma 7.2 ([118, 122])**.** *Let g_i be a symmetric matrix and x be a nonzero vector with an appropriate vector length. If $\Gamma_i = \frac{x^T g_i x}{x^T x}$, then there exists at least one eigenvalue of g_i in the interval $(-\infty, \Gamma_i]$ and at least one in $[\Gamma_i, +\infty)$.*

The control gain matrix $g_i(.)$ is not necessarily a symmetric matrix. However, if we consider its symmetric part as g_{i_1}, for a nonzero vector x, from Assumption 7.1 one has $\Gamma_i(t) = \frac{x^T g_{i_1} x}{x^T x} \neq 0$. Then, using the fact that the spectral radius of a matrix $\rho(A) \leq \|A\|$ [118], and Lemma 5.1, the following is valid

$$g^- \leq \underline{\lambda}(g_{i_1}(t)) \leq \Gamma_i(t) \leq \bar{\lambda}(g_{i_1}(t)) \leq g^+, \tag{7.3}$$

where g^- and g^+ are some constants. Note that for all x, the following is valid

$$x^T g_{i_1} x = \Gamma_i(t) \|x\|^2. \tag{7.4}$$

Assumption 4.2 is valid for w_i such that $\|w_i\| \leq w_M, \forall i$.

The leader dynamics is defined as follows:

$$\begin{aligned} \dot{p}_l(t) &= v_l(t), \\ \dot{v}_l(t) &= f_l(p_l(t), v_l(t)), \end{aligned} \tag{7.5}$$

where $p_l \in \mathbb{R}^n$ and $v_l \in \mathbb{R}^n$ denote the position and velocity states of the leader. In addition, we consider f_l to be an unknown, continuously differentiable function. The stacked vector of leader states is defined by $z_l = [p_l^T, v_l^T]^T$.

Assumption 7.2. *The leader's trajectory, velocity, and acceleration are assumed to be bounded, i.e., $p_l, v_l, f_l \in \mathcal{L}_\infty$. Moreover, the leader is connected to at least one of the agents and can broadcast its position and velocity to all agents.*

The formation control of multi-agent systems with communication time delay where the leader is connected to all agents was studied in [110, 111]. In a similar approach, authors in [8, 96, 107] considered that the target's information is available for all agents. In [126], authors considered that all agents were able to receive the leader's information directly or indirectly. However, we assume that the leader is not directly connected to all agents, i.e., no star topology exists. We consider that the undirected graph $G = (V, E)$ is connected, and the leader is connected to at least one of the agents. The leader's information is transferred to that agent and propagated to other agents with a delay.

Between any two neighboring agents, we consider that there exists a communication time delay. For an arbitrary pair of agents $(v_j, v_i) \in E$, we denote the communication time delay by $\tau_{ij}(t)$, $\tau_{ij}(t) > 0$. We also denote the time delay corresponding to the received information of the leader by the i-th agent with $\tau_{il}(t) > 0$.

Assumption 7.3. *There exists a communication time delay τ such that the delayed stacked vectors $z_k(t-\tau)$ are available for i-th agent $k \in N_i$, $i = 1, ..., N$. We also consider that the leader's delayed stacked vector of states $z_l(t-\tau)$ is available for agents.*

Remark 7.2. *Note that there exists positive constant τ in Assumption 7.3 such that $\tau \geq \max_{k \in \mathcal{S}} \big(\tau_{ik}(t)\big)$. Each agent receives the leader's information after an admissible propagation delay. This consideration justifies Assumption 7.3, which can be seen in [104–106, 127].*

Definition 7.1 ([102])**.** *A vector $\mathcal{V}(t) \in \mathbb{R}^n$ is said to be SGUUB, if for any compact $\Omega \in \mathbb{R}^n$, and all initial conditions $\mathcal{V}(t_0) \in \Omega$, there exists an $\varepsilon > 0$, and a time $T_f\big((\varepsilon, \mathcal{V}(t_0)\big)$ such that $\|\mathcal{V}(t)\| < \varepsilon$ for all $t > t_0 + T_f$.*

From (7.1) and (7.5), let us define the variable e_{x_i} and e_{v_i} as follows:

$$\begin{aligned} e_{x_i}(t) &= p_i(t) - p_l(t) - d_i, \\ e_{v_i}(t) &= v_i(t) - v_l(t), \end{aligned} \tag{7.6}$$

where d_i is a bounded, relative time-independent displacement between the agent i-th and the leader, i.e., $\|d_i\| \leq d_M$.

The control objective is to develop a distributed controller using the local time-delayed information of the neighboring agents such that all closed-loop signals remain SGUUB and to ensure that all agents achieve the desired relative position and maintain relative velocity to the leader

$$
\begin{aligned}
&\lim_{t\to\infty} \|p_i(t) - p_l(t) - d_i\| \le \varepsilon_x \\
&\lim_{t\to\infty} \|v_i(t) - v_l(t)\| \le \varepsilon_v,
\end{aligned}
\tag{7.7}
$$

where ε_x and ε_v are positive constants.

7.3 Controller Design

Let us define the following error signals

$$
\begin{aligned}
\chi_i &= \sum_{j\in N_i} a_{ij}\big(e_{x_i}(t) - e_{x_j}(t)\big) + e_{x_i}(t), \\
\nu_i &= \sum_{j\in N_i} a_{ij}\big(e_{v_i}(t) - e_{v_j}(t)\big) + e_{v_i}(t).
\end{aligned}
\tag{7.8}
$$

Using (7.8), Assumptions 7.2 and 7.3, let us define r_{xi}, r_{vi} as

$$
\begin{aligned}
r_{xi}(t) &= p_i(t) - p_l(t-\tau) - d_i + k_1 u_s(t-\tau)\int_0^{t-\tau} \chi_i(\iota)d\iota, \\
r_{vi}(t) &= v_i(t) - v_l(t-\tau) + k_1 u_s(t-\tau)\int_0^{t-\tau} \nu_i(\iota)d\iota,
\end{aligned}
\tag{7.9}
$$

where $u_s(t-\tau)$ denotes a delayed unit step function and the constant k_1 is positive, $k_1 > 0$. The control signal $u_i(t)$ is a function of r_{x_i} and r_{v_i} in which only the delayed information of neighboring agents is required. As each agent receives the information of the leader with a time delay, we define $B = diag(\mathbf{1}_N)$.

Remark 7.3. *Note that r_{x_i} and r_{v_i} are time-varying functions, which include local, time-delayed information of the neighbors, the leader, as well as the information of the agent i at time instance t.*

Theorem 7.1. *Let the multi-agent system (7.1) be modeled by a connected, undirected graph. For a positive constant k_1, let the communication time delay be bounded by $\tau < \pi/(2k_1\bar{\lambda}(L+B))$. If for all agents, terms r_{xi} and r_{vi} are bounded such that $\lim_{t\to\infty}\|r_{xi}(t)\| \le \delta$, $\lim_{t\to\infty}\|r_{vi}(t)\| \le \delta$,* *then the following inequalities hold*

$$\lim_{t\to\infty}\|\xi_x(t)\|\le\bar{\xi}_x\delta,\quad \lim_{t\to\infty}\|\xi_v(t)\|\le\bar{\xi}_v\delta, \tag{7.10}$$

where constants $\bar{\xi}_x$, $\bar{\xi}_v$ are given later in the proof.

Proof. From (7.6), for the agent i, one can define the auxiliary variables ξ_{xi}, and ξ_{vi}

$$\begin{aligned}\xi_{xi}(t)&=\int_0^t e_{x_i}(\iota)d\iota,\ \ t\ge 0,\\ \xi_{vi}(t)&=\int_0^t e_{v_i}(\iota)d\iota,\ \ t\ge 0.\end{aligned} \tag{7.11}$$

Let us define the stacked vectors $d=[d_1^T,...,d_N^T]^T, e_x=[e_{x_1}^T,...,e_{x_N}^T]^T$, $e_v=[e_{v_1}^T,...,e_{v_N}^T]^T$, $\xi_x=[\xi_{x1}^T,...,\xi_{xN}^T]^T$, $\xi_v=[\xi_{v1}^T,...,\xi_{vN}^T]^T$, $r_x=[r_{x_1}^T,...,r_{x_N}^T]^T$, $r_v=[r_{v_1}^T,...,r_{v_N}^T]^T\in\mathbb{R}^{nN}$. Note that $\xi_{xi}(t)=0$, $\xi_{vi}(t)=0$ for $t\in[-\tau,0)$. From (7.8) and (7.9), and by taking the time derivative of (7.11) for $t>0$, one has

$$\begin{aligned}\dot{\xi}_x(t)=&-k_1\big((L+B)\otimes I_n\big)\xi_x(t-\tau)+r_x(t)+\mathbf{1}_N\otimes(p_l(t-\tau)-p_l(t)),\\ \dot{\xi}_v(t)=&-k_1\big((L+B)\otimes I_n\big)\xi_v(t-\tau)+r_v(t)+\mathbf{1}_N\otimes(v_l(t-\tau)-v_l(t)).\end{aligned} \tag{7.12}$$

Considering (7.11), and by taking the Laplace transform of (7.12), one has

$$\begin{aligned}\xi_x(s)=&\Big(sI_{nN}+k_1\big((L+B)\otimes I_n\big)e^{-\tau s}\Big)^{-1}\Big(R_x(s)+(e^{-\tau s}-1)\mathbf{1}_N\otimes P_l(s)\Big),\\ \xi_v(s)=&\Big(sI_{nN}+k_1\big((L+B)\otimes I_n\big)e^{-\tau s}\Big)^{-1}\Big(R_v(s)+(e^{-\tau s}-1)\mathbf{1}_N\otimes V_l(s)\Big).\end{aligned} \tag{7.13}$$

One can conclude that the matrix $L+B$ is a full rank. Therefore, one can write the Jordan decomposition of the matrix as $L+B=MJQ^T$, where $MQ^T=I_N$ and $J\in\mathbb{R}^{N\times N}$. One has $M=[m_1,....,m_N]$ and $Q=[q_1,...,q_N]\in\mathbb{R}^{N\times N}$, where m_i, q_i are column vectors. Thus, one can write

$$\Big(sI_{nN}+k_1\big((L+B)\otimes I_n\big)e^{-\tau s}\Big)^{-1}=\sum_{i=1}^{N}\frac{1}{s+k_1\lambda_i e^{-s\tau}}(m_iq_i^T)\otimes I_n, \tag{7.14}$$

where $\lambda_i > 0$ is the i-th eigenvalue of the matrix $L + B$. Similar to [104], one can define

$$o_i(t) \triangleq \mathcal{L}^{-1}\left[\frac{1}{s+k_1\lambda_i e^{-s\tau}}\right]. \tag{7.15}$$

From (7.14), (7.15), and by taking the inverse Laplace transform of (7.13), one has

$$\begin{aligned} \xi_x(t) &= \sum_{i=1}^{N}\left(\int_0^t o_i(t-s)(m_i q_i^T)\otimes I_n\Big(r_x(s)+\mathbf{1}_N\otimes(p_l(s-\tau)-p_l(s))\Big)ds\right), \\ \xi_v(t) &= \sum_{i=1}^{N}\left(\int_0^t o_i(t-s)(m_i q_i^T)\otimes I_n\Big(r_v(s)+\mathbf{1}_N\otimes(v_l(s-\tau)-v_l(s))\Big)ds\right). \end{aligned} \tag{7.16}$$

For some positive constants α_i, β_i, if all poles of $\mathcal{O}_i(s)$ are placed in the open left-half-plane, from [104, 128], one has

$$\|o_i(t)\| \leq \alpha_i e^{-\beta_i t}. \tag{7.17}$$

In Lemma 7.1, let $\mathcal{M} \triangleq k_1(L+B)$, $k_1\tau < \pi/(2\bar{\lambda}(L+B))$, then all poles of $\mathcal{O}_i(s)$ are placed in the open left-half-plane. Recall that for two arbitrary matrices A, B, $\|A\otimes B\| = \|A\|\|B\|$. Then, for (7.16) one has

$$\begin{aligned} \|\xi_x(t)\| &\leq \sum_{i=1}^{N}\left(\int_0^t \alpha_i e^{-\beta_i(t-s)}\Big(\|r_x(s)\|+\sqrt{N}\|p_l(s-\tau)-p_l(s))\|\Big)ds\right), \\ \|\xi_v(t)\| &\leq \sum_{i=1}^{N}\left(\int_0^t \alpha_i e^{-\beta_i(t-s)}\Big(\|r_v(s)\|+\sqrt{N}\|v_l(s-\tau)-v_l(s))\|\Big)ds\right). \end{aligned} \tag{7.18}$$

Consider (7.5), and recall the fact that continuous differentiability is a sufficient condition for being locally Lipschitz [98, Corollary 4.1.1], then there exist positive scalars p_M and v_M such that

$$\begin{aligned} \|p_l(t)-p_l(t-\tau)\| &\leq p_M\tau, \\ \|v_l(t)-v_l(t-\tau)\| &\leq v_M\tau. \end{aligned} \tag{7.19}$$

Then, one has

$$\begin{aligned}\lim_{t\to\infty}\|\xi_x(t)\| \leq & \bar{\xi}_x\delta,\\ \lim_{t\to\infty}\|\xi_v(t)\| \leq & \bar{\xi}_v\delta,\end{aligned} \tag{7.20}$$

with $\bar{\xi}_x = \sqrt{N}(1+p_M\tau/\delta)\sum_{i=1}^{N}\alpha_i/\beta_i$ and $\bar{\xi}_v = \sqrt{N}(1+v_M\tau/\delta)\sum_{i=1}^{N}\alpha_i/\beta_i$. This completes the proof. □

From (7.11), and (7.12), one can write

$$\begin{aligned}\|e_x(t)\| =& \|r_x(t) - k_1\big((L+B)\otimes I_n\big)\xi_x(t-\tau) + \mathbf{1}_N\otimes(p_l(t-\tau)-p_l(t))\|,\\ \|e_v(t)\| =& \|r_v(t) - k_1\big((L+B)\otimes I_n\big)\xi_v(t-\tau) + \mathbf{1}_N\otimes(v_l(t-\tau)-v_l(t))\|.\end{aligned} \tag{7.21}$$

From (7.20), Assumption 7.2, we conclude that

$$\begin{aligned}\lim_{t\to\infty}\|e_x(t)\| \leq & (k_1\bar{\sigma}(L+B)\bar{\xi}_x + \sqrt{N}(p_M\tau/\delta+1))\delta \triangleq \varepsilon_x,\\ \lim_{t\to\infty}\|e_v(t)\| \leq & (k_1\bar{\sigma}(L+B)\bar{\xi}_v + \sqrt{N}(v_M\tau/\delta+1))\delta \triangleq \varepsilon_v.\end{aligned} \tag{7.22}$$

Let us define $r_i(t) = r_{vi}(t) + r_{xi}(t)$. Considering (7.1) and (7.9), the dynamics of $r_i(t)$ can be given by

$$\begin{aligned}\dot{r}_i(t) =& (v_i(t) - v_l(t-\tau) + k_1u_s(t-\tau)\chi_i(t-\tau)) + f_i(p_i,v_i) + g_i(p_i,v_i)u_i(t) + w_i(t)\\ & - f_l(p_l(t-\tau), v_l(t-\tau)) + k_1u_s(t-\tau)\nu_i(t-\tau).\end{aligned} \tag{7.23}$$

From (7.23), define an auxiliary variable as

$$h_i = v_i(t) - v_l(t-\tau) + k_1u_s(t-\tau)\big(\chi_i(t-\tau)+\nu_i(t-\tau)\big). \tag{7.24}$$

Remark 7.4. *For each agent, we consider the neural network with three layers (2.17), and set the first and second hidden layers' neurons to $m_1 = 4n$ and $m_2 = 2(4n)+2$, respectively. A three-layer neural network with $4n$ input neurons (see (7.35)), $4n$ neurons in the first hidden layer, $2(4n)+2$ neurons in the second hidden layer, and sigmoid activation functions is able to approximate $y(\mathcal{X})$*

with arbitrary accuracy [100].

For agent i, from (2.17), define the $\varpi_i \triangleq \|W_i\|_F^2$. The estimation of ϖ_i is denoted by $\hat{\varpi}_i$. The estimated error is $\tilde{\varpi}_i \triangleq \varpi_i - \hat{\varpi}_i$. We propose the NN-based, adaptive control law as

$$u_i(t) = \mathcal{N}(\zeta_i)\vartheta_i r_i, \tag{7.25}$$

where

$$\begin{aligned}
\dot{\zeta}_i &= \theta_i \vartheta_i, \\
\vartheta_i &= \bar{\vartheta}_{f_i} + \bar{\vartheta}_{u_i}, \\
\bar{\vartheta}_{f_i} &= (\hat{\varpi}_i \|\sigma_{1_i}(Z_i^T \sigma_{2_i}(V_i^T \mathcal{X}_i))\|^2 + \|h_i\|^2), \\
\bar{\vartheta}_{u_i} &= (k_{c_i} + \hat{b}_{m_i} \tanh \frac{\theta_i}{\varsigma}), \\
\theta_i &= \frac{1}{(k_{b_i}^2 - r_i^T r_i)^2} \|r_i\|^2,
\end{aligned} \tag{7.26}$$

where $\hat{b}_{m_i}$ is an adaptive, robustifying term that is used to estimate the unknown b_{m_i}, and the estimation error is $\tilde{b}_{m_i} \triangleq b_{m_i} - \hat{b}_{m_i}$. The term b_{m_i} is defined by $b_{m_i} \triangleq \|\epsilon_i + w_i\|^2$. From Assumptions 2.2, and 4.2, it is clear that b_{m_i} is bounded by $b_{m_i} \leq \epsilon_M + w_M \triangleq b_{M_i}$.

Let the tuning laws for $\hat{\varpi}_i$ and $\hat{b}_{m_i}$ be given by

$$\begin{aligned}
\dot{\hat{\varpi}}_i &= \Pi_i(\theta_i \|\sigma_{1_i}(Z_i^T \sigma_{2_i}(V_i^T \mathcal{X}_i)\|^2 - \kappa_i \hat{\varpi}_i), \\
\dot{\hat{b}}_{m_i} &= \gamma_i(\theta_i \tanh \frac{\theta_i}{\varsigma} - \mu_i \hat{b}_{m_i}),
\end{aligned} \tag{7.27}$$

where $\Pi_i, \kappa_i, \gamma_i$, and μ_i are positive constants. The block diagram of proposed control law is illustrated in Figure 7.1.

7.3.1 Stability Analysis

In this section, we prove that the proposed control law (7.25) guarantees the stability of the leader-following formation control problem for nonlinear multi-agent systems (7.1). The following Lemmas are stated, which are used later in the proof of the main theorem.

Lemma 7.3 ([129]). *For any positive scalar k_b, and any $z \in \mathbb{R}$ satisfying $|z| < k_b$, the following*

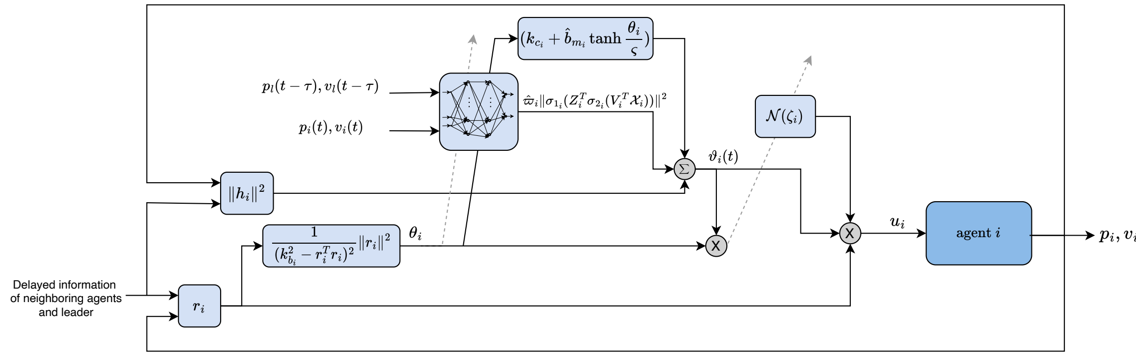

Figure 7.1: The block diagram of proposed control law.

inequality holds

$$\log \frac{k_b^2}{k_b^2 - z^2} < \frac{z^2}{k_b^2 - z^2}, \tag{7.28}$$

where log *denotes the natural logarithm.*

Lemma 7.4 ([130])**.** *For any $\varepsilon > 0$ and for any $\chi \in \mathbb{R}$, we have $0 \leq |\chi| - \chi \tanh\left(\frac{\chi}{\varepsilon}\right) \leq \Delta\varepsilon$, where Δ is a constant that satisfies $\Delta = e^{-(\Delta+1)}$, ($\Delta \simeq 0.2785$).*

Let us define the barrier Lyapunov function (BLF) as

$$V_{i_1} = \frac{1}{2} \log \frac{k_{b_i}^2}{k_{b_i}^2 - r_i^T r_i}. \tag{7.29}$$

Remark 7.5. *The symmetric BLF in (7.29) was proposed in [131], and asymmetric BLFs have been proposed [132]. It is clear that the function (7.29) is positive over the set $\Omega_{b_i} = \{r_i \mid \|r_i\| < k_{b_i}\}$, and $V_{i_1} \to \infty$, for $\|r_i\| = k_{b_i}$.*

The time derivative of (7.29) is given by

$$\begin{aligned}\dot{V}_{i_1} =& \frac{r_i^T}{k_{b_i}^2 - r_i^T r_i}\Big(\big(v_i(t) + k_1 u_s(t-\tau)\chi_i(t-\tau)\big) + f_i(p_i, v_i) + g_i(p_i, v_i)u_i(t) + w_i(t) \\ &+ k_1 u_s(t-\tau)\nu_i(t-\tau)\Big).\end{aligned} \tag{7.30}$$

Remark 7.6. *Note that one can define the stack vector of $r = [r_1^T, ..., r_N^T]^T \in \mathbb{R}^{Nn}$ and write the BLF as $\frac{1}{2}\log\frac{k_b^2}{k_b^2 - r^T r}$ similar to [133]. In this case, the stacked control input ($u = [u_1^T, ..., u_N^T]^T \in$*

$\mathbb{R}^{Nn}$) *signal may consists of* $\frac{1}{k_b^2 - r^T r}$. *Consequently, each agent's controller requires the stacked vector* r *to generate its control input. To avoid this, we consider the BLF as (7.29).*

Theorem 7.2. *Let a connected, undirected graph model the multi-agent system (7.1). Under Assumptions 2.2, 2.3, 4.2, and 7.1-7.3, select the control input as (7.25), the NN tuning law, and robustifying term dynamics as (7.27). Then all closed-loop signals remain semi-globally uniformly ultimately bounded. Moreover, the convergence of tracking errors to an arbitrarily small neighborhood of zero is ensured by appropriately selecting design parameters.*

Proof. Let us define the Lyapunov function candidate

$$V_i = V_{i_1} + \frac{1}{2}\Pi_i^{-1}\tilde{\varpi}_i^2 + \frac{1}{2}\gamma_i^{-1}\tilde{b}_{m_i}^2, \tag{7.31}$$

where Π_i and γ_i are positive scalars. The time derivative of (7.31) is given by

$$\dot{V}_i = \frac{r_i^T}{k_{b_i}^2 - r_i^T r_i}\big(h_i + f_i + w_i(t)\big) + r_i^T g_1 \mathcal{N}(\zeta_i)\vartheta_i r_i + \dot{\zeta}_i - \dot{\zeta}_i + \Pi_i^{-1}\tilde{\varpi}_i\dot{\tilde{\varpi}}_i + \gamma_i^{-1}\tilde{b}_{m_i}\dot{\tilde{b}}_{m_i}. \tag{7.32}$$

From Assumption 7.1, one can write symmetric part of control gain matrix as $g_{i_1} = (g_i + g_i^T)/2$, and its skew-symmetric part as $g_{i_2} = (g_i - g_i^T)/2$. Note that Assumption 7.1 guarantees that $g_{i_1} \neq \mathbf{0}_{N\times N}$. Thus, using the fact that $r_i^T g_2 r_i = 0$, one has

$$\dot{V}_i = \frac{r_i^T}{k_{b_i}^2 - r_i^T r_i}\big(h_i + f_i + w_i(t)\big) + r_i^T g_1 \mathcal{N}(\zeta_i)\vartheta_i r_i + \dot{\zeta}_i - \dot{\zeta}_i + \Pi_i^{-1}\tilde{\varpi}_i\dot{\tilde{\varpi}}_i + \gamma_i^{-1}\tilde{b}_{m_i}\dot{\tilde{b}}_{m_i}. \tag{7.33}$$

Using Lemma 7.2, (7.4), and (7.26), one has

$$\dot{V}_i = \frac{r_i^T}{k_{b_i}^2 - r_i^T r_i}\big(h_i + f_i + w_i(t)\big) + (\Gamma_i(t)\mathcal{N}(\zeta_i) + 1)\dot{\zeta}_i - \dot{\zeta}_i + \Pi_i^{-1}\tilde{\varpi}_i\dot{\tilde{\varpi}}_i + \gamma_i^{-1}\tilde{b}_{m_i}\dot{\tilde{b}}_{m_i}. \tag{7.34}$$

Let us consider $y_i(\bar{\mathcal{X}}_i) \triangleq f_i(t) - f_l\big(p_l(t-\tau), v_l(t-\tau)\big)$ as (2.17), where $\bar{\mathcal{X}}_i = [p_i^T(t), v_i^T(t), p_l(t-$

$\tau), v_l(t-\tau)]^T \in \mathbb{R}^{4n}$. Then, the following result over set $\Omega_{\mathcal{X}_i} \subset \Omega_{b_i}$ can be obtained

$$
\begin{aligned}
\dot{V}_i =& \frac{r_i^T}{k_{b_i}^2 - r_i^T r_i}\big(W_i^T \sigma_{1_i}(Z_i^T \sigma_{2_i}(V_i^T \mathcal{X}_i))\big) + \frac{r_i^T}{k_{b_i}^2 - r_i^T r_i}(\epsilon_i + w_i(t)) + (\Gamma_i(t)\mathcal{N}(\zeta_i) + 1)\dot{\zeta}_i \\
& - \|r_i\|^2 \vartheta_i + \Pi_i^{-1} \tilde{\varpi}_i \dot{\hat{\varpi}}_i + \gamma_i^{-1} \tilde{b}_{m_i} \dot{\hat{b}}_{m_i},
\end{aligned}
\tag{7.35}
$$

where $\mathcal{X}_i = [1, \bar{\mathcal{X}}_i^T]^T$. Let us define $T(\mathcal{X}_i) \triangleq W_i^T \sigma_{1_i}(Z_i^T \sigma_{2_i}(V_i^T \mathcal{X}_i))$.

An a priori knowledge (the number of position/velocity states n) is required to determine the number of neurons in each layer.

Using the fact that $\|.\|_2 \leq \|.\|_F$ and by applying Cauchy–Schwarz and Young's inequalities, one has

$$
\begin{aligned}
\frac{r_i^T}{k_{b_i}^2 - r_i^T r_i} T_i(\mathcal{X}_i) \leq& \theta_i \varpi_i \|\sigma_{1_i}(Z_i^T \sigma_{2_i}(V_i^T \mathcal{X}_i))\|^2 + \frac{1}{4a_1^2}, \\
\frac{r_i^T}{k_{b_i}^2 - r_i^T r_i}(w_i + \epsilon_i) \leq& \theta_i b_{m_i} + \frac{1}{4a_2^2},
\end{aligned}
\tag{7.36}
$$

where a_1 and a_2 are positive constants. From Assumptions 2.2 and 4.2, it is clear that the unknown term b_{m_i} is bounded. From (7.26), and by substituting (7.36) in (7.35), one has

$$
\begin{aligned}
\dot{V}_i \leq& \theta_i \varpi_i \|\sigma_{1_i}(Z_i^T \sigma_{2_i}(V_i^T \mathcal{X}_i)\|^2 + \frac{1}{4a_1^2} - \frac{k_c}{k_{b_i}^2 - r_i^T r_i} r_i^T r_i + \frac{1}{(k_{b_i}^2 - r_i^T r_i)^2}\|r_i\|^2 b_{m_i} \\
& + (\Gamma_i(t)\mathcal{N}(\zeta_i) + 1)\dot{\zeta}_i - \frac{1}{(k_{b_i}^2 - r_i^T r_i)^2}\|r_i\|^2 \hat{b}_{m_i} \tanh\frac{\theta_i}{\varsigma} \\
& + \frac{1}{4a_2^2} - \hat{\varpi}_i \|\sigma_{1_i}(Z_i^T \sigma_{2_i}(V_i^T \mathcal{X}_i)\|^2 \theta_i - \Pi_i^{-1} \tilde{\varpi}_i \dot{\hat{\varpi}}_i - \gamma_i^{-1} \tilde{b}_{m_i} \dot{\hat{b}}_{m_i}.
\end{aligned}
\tag{7.37}
$$

From Lemma 6.4, and substituting (7.27) in (7.37), one has

$$
\begin{aligned}
\dot{V}_i \leq& -\frac{k_c}{k_{b_i}^2 - r_i^T r_i} r_i^T r_i + (\Gamma_i(t)\mathcal{N}(\zeta_i) + 1)\dot{\zeta}_i + \frac{1}{4a_1^2} + \frac{1}{4a_2^2} + 0.2785 b_{M_i} \varsigma \\
& + \kappa_i \tilde{\varpi}_i \hat{\varpi}_i + \mu_i \tilde{b}_{m_i} \hat{b}_{m_i}.
\end{aligned}
\tag{7.38}
$$

Using Lemma 7.3, and applying Young's inequality, yields

$$\begin{aligned}\dot{V}_i \leq & -k_c \log \frac{k_{b_i}^2}{k_{b_i}^2 - r_i^T r_i} + (\Gamma_i(t)\mathcal{N}(\zeta_i)+1)\dot{\zeta}_i + \frac{1}{4a_1^2} + \frac{1}{4a_2^2} + 0.2785 b_{M_i}\varsigma - \frac{1}{2}\kappa_i \tilde{\varpi}_i^2 \\ & - \frac{1}{2}\mu_i \tilde{b}_{m_i}^2 + \frac{1}{2}\kappa_i \varpi_i^2 + \frac{1}{2}\mu_i b_{m_i}^2.\end{aligned} \tag{7.39}$$

Let us define constants $c_{1_i} \triangleq \min(k_c, \kappa_i \Pi_i^{-1}, \mu_i \gamma_i^{-1})$, and $c_{\epsilon_i} \triangleq \frac{1}{4a_1^2} + \frac{1}{4a_2^2} + 0.2785 b_{M_i}\varsigma + \frac{1}{2}\kappa_i W_{M_i}^2 + \frac{1}{2}\mu_i b_{M_i}^2$. Then, (7.39) can be written as

$$\dot{V}_i \leq -c_{1_i} V_i + (\Gamma_i(t)\mathcal{N}(\zeta_i)+1)\dot{\zeta}_i + c_{\epsilon_i}. \tag{7.40}$$

Taking the integral over the interval $t \in [0, t_f)$, one can obtain

$$V_i(t) \leq (V_i(0) - \frac{c_{\epsilon_i}}{c_{1_i}})e^{-c_{1_i}t} + \frac{c_{\epsilon_i}}{c_{1_i}} + \int_0^t (\Gamma_i(\tau)\mathcal{N}(\zeta_i)+1)e^{-c_{1_i}(t-\tau)}\dot{\zeta}_i d\tau. \tag{7.41}$$

One can see that for $V = \sum_{i=1}^N V_i$, the boundedness of all closed-loop signals is guaranteed. Consider the augmented closed-loop system with respect to (7.1), (7.23), (7.25), (7.26), and (7.27), then the system dynamics for each agent can be written as [104]:

$$\dot{\mathbf{x}}_i(t) = \begin{cases} F_{i_1}(\mathbf{x}_i(t)), & \text{if } t \in [0, \tau), \\ F_{i_2}(\mathbf{x}_i(t), \mathbf{x}_i(t-\tau)), & \text{if } t \in [\tau, \infty). \end{cases} \tag{7.42}$$

In (7.1), we considered $f_i(p_i, v_i)$ to be locally Lipschitz continuous and a solution of $\varphi_i(t)$ exists for $\dot{\mathbf{x}}_i(t) = F_{i_1}(\mathbf{x}_i(t))$ when $t \in [0, \tau)$. From the control input (7.25) and (7.41), one can see that $r_i(t)$, $\hat{\varpi}_i(t)$, and $\hat{b}_{m_i}(t)$ remain bounded for $t \in [0, \tau)$. Using Assumption 7.2, Theorem 7.1, (7.21), and upon proper selection of k_1, variables $\xi_{xi}(t)$, $\xi_{vi}(t)$, $p_i(t)$, and $v_i(t)$ are bounded for $t \in [0, \tau)$. Therefore, the solution of $\varphi_i(t)$ is bounded for $t \in [0, \tau]$, and the continuation of this solution can be obtained along $\dot{\mathbf{x}}_i(t) = F_{i_2}(\mathbf{x}_i(t), \mathbf{x}_i(t-\tau))$ with initial condition of $\varphi_i(t)$ [104]. Similarly, since $F_{i_2}(\mathbf{x}_i(t), \mathbf{x}_i(t-\tau))$ is locally Lipschitz, a solutions exists for $t \in [0, t_f)$. Define $c_{0_i} \triangleq V_i(0) + \frac{c_{\epsilon_i}}{c_{1_i}}$ and recall Lemma 2.5. From (7.41), one can note that $V_i(t), \zeta_i(t)$, and $\int_0^t (\Gamma_i(\tau)\mathcal{N}(\zeta_i)+1)\dot{\zeta}_i d\tau$ are bounded over $[0, t_f)$. As the closed-loop system is bounded, we can extend the solution to $t_f = +\infty$ [35]. From Lemma 2.5 and similar to [35, 129], let us consider the bound $|(\Gamma_i(t)\mathcal{N}(\zeta_i)+1)\dot{\zeta}_1| < N_{b_i}$, and define $\bar{\delta}_i \triangleq (\frac{c_{\epsilon_i}}{c_{1_i}} + V_i(0)e^{-c_{1_i}t} + N_{b_i})$. From (7.29), and (7.41), one can write

$$\begin{aligned} \|r_i(t)\| \leq & k_{b_i}\sqrt{1-e^{-2\bar{\delta}_i}}, \\ |\tilde{\varpi}_i(t)| \leq & \gamma_i^{-1}\bar{\delta}_i. \end{aligned} \tag{7.43}$$

Since $V(t)$ is bounded, we have $r_i \in \mathcal{L}_\infty$, it is clear that $r_{vi}(t) \in \mathcal{L}_\infty$, and $r_{xi}(t) \in \mathcal{L}_\infty$. From Assumption 7.2, and (7.21), one can conclude that $p_i(t)$ and $v_i(t)$ are bounded, namely $\|p_i(t)\| \leq P_M$ and $\|v_i(t)\| \leq V_M$. From Assumption 7.2, we know that there exist scalars $\bar{p}_l$ and $\bar{v}_l$ such that $\|p_l(t)\| \leq \bar{p}_l$ and $\|v_l(t)\| \leq \bar{v}_l$. Then, the NN compact set can be defined as follows:

$$\Omega_{\mathcal{X}_i} \triangleq \{\|p_i\| \leq P_M, \|v_i\| \leq V_M, \|r_i\| \leq k_b\sqrt{1-e^{-2\bar{\delta}_i}}, \|p_l(t)\| \leq \bar{p}_l, \|v_l(t)\| \leq \bar{v}_l\}. \tag{7.44}$$

This completes the proof. □

Remark 7.7. *In this chapter, we utilized the NN to approximate the nonlinearity $y_i(\bar{\mathcal{X}}_i)$, which has an intrinsic approximation error, see (2.17). In the robustifying terms in (7.27), if we use signum function instead of $\tanh(.)$, we would obtain another controller that achieves the asymptotic stability of the closed-loop signal, similar to [104, 116, 120, 134, 135]. In these works, authors showed that as $r_i \in \mathcal{L}_2 \cap \mathcal{L}_\infty$ and $\dot{r}_i \in \mathcal{L}_\infty$, then from Barbalat's lemma $\lim_{t\to\infty} r_i(t) \to 0$. However, if we use $\hat{b}_{m_i}$ to compensate for disturbance in system dynamics (7.1), as well as the NN intrinsic approximation error, and design it in the form of $\dot{\hat{b}}_{m_i} = \gamma_i\theta_i sgn(r_i)$, we impose the right-hand side discontinuity on the closed-loop system dynamics. Consequently, by employing differential inclusion [72, 73], the existence of an absolutely continuous Filipov's solution should be studied. To avoid these issues, we used $\tanh(.)$ in our control design and proved the stability of the continuous closed-loop system.*

Remark 7.8. *Note that from the results of Theorem 7.2, the proposed control law $r_i(t)$ and the closed-loop signals are SGUUB. From the results of Theorem 7.1, we have shown that if $r_i(t)$ is bounded, then the desired control objective is achieved. To reduce the tracking error bounds in*

(7.7), δ in (7.10) should be kept small, which can be achieved by selecting appropriate design parameters. From (7.43), one can select larger values of k_c and μ_i, and smaller values of k_1 and k_{b_i}.

7.4 Simulation Results

In order to demonstrate the performance of the proposed method, we simulated a multi-agent system with five agents and the leader. The undirected graph that models the system is shown in Figure 7.2. Consider a multi-agent system (7.1) where the dynamics of each agent is given by [118],

$$\begin{cases} \dot{x}_{11_i} = x_{12_i}, \\ \dot{x}_{12_i} = x_{21_i} + a_{1_i}\sin(x_{11_i}x_{12_i}) + x_{12_i}^2 + (a_{2_i} + \cos(x_{11_i}))u_{1_i} + (1 + x_{21_i}^2 + x_{22_i}^2)u_{2_i} \\ \qquad + 0.6\sin(\frac{\pi}{4}t), \\ \dot{x}_{21_i} = x_{22_i}, \\ \dot{x}_{22_i} = x_{11_i} + x_{12_i}^2 + x_{22_i}^2 - (\cos(x_{12_i}) + \cos(x_{22_i}))\, u_{1_i} + \left(1 + x_{12_i} + x_{21_i}^2\right) u_{2_i} \\ \qquad + 0.8\cos(\frac{\pi}{4}t), \end{cases} \tag{7.45}$$

where constants of a_{1_i}, and a_{2_i} for each agent are given in Table 7.1. Let $p_i = [x_{11_i}, x_{21_i}]^T, v_i = [x_{12_i}, x_{22_i}]^T$, and $u_i = [u_{1_i}, u_{2_i}]^T$. Using the following definitions, (7.45) can be written in the form (7.1).

$$\begin{aligned} f_i(p_i, v_i) &= \begin{bmatrix} x_{21_i} + a_{1_i}\sin(x_{11_i}, x_{12_i}) + x_{12_i}^2 \\ x_{11_i} + x_{12_i}^2 + x_{22_i}^2 \end{bmatrix}, \\ g_i(p_i, v_i) &= \begin{bmatrix} a_{2_i} + \cos(x_{11_i}) & 1 + x_{21_i}^2 + x_{22_i}^2 \\ -(\cos(x_{12_i}) + \cos(x_{22_i})) & 1 + x_{12_i} + x_{21_i}^2 \end{bmatrix}, \\ w_i &= \begin{bmatrix} 0.6\sin(\frac{\pi}{4}t) \\ 0.8\cos(\frac{\pi}{3}t) \end{bmatrix}, \end{aligned} \tag{7.46}$$

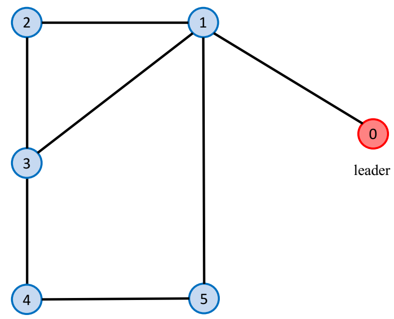

Figure 7.2: The communication topology of an undirected graph with five agents and the leader.

Table 7.1: Values of a_{1_i}, and a_{2_i} in the i-th agent.

i	1	2	3	4	5
a_{1_i}	-0.2	-0.4	-0.6	0.7	0.5
a_{2_i}	4	3.5	4	3	2

The leader dynamics is given by

$$\begin{aligned} \dot{p}_l &= v_l, \\ \dot{v}_l &= \begin{bmatrix} -0.03p_{l_1} + 0.2(1 - p_{l_1}^2)v_{l_1}, \\ -0.06p_{l_2} + 0.3(1 - p_{l_2}^2)v_{l_2}. \end{bmatrix}, \end{aligned} \tag{7.47}$$

where $p_l = [p_{l_1}, p_{l_2}]^T \in \mathbb{R}^2$ and $v_l = [v_{l_1}, v_{l_2}]^T \in \mathbb{R}^2$ are the position and velocity states of the leader. The initial conditions for agents are given as: $p_{11}(0) = [1.2, 0]^T$, $p_{21}(0) = [-1, 2]^T$, $p_{31}(0) = [1.1, -2]^T$, $p_{41}(0) = [-1, -0.8]^T$, $p_{51}(0) = [-1.3, 0.5]^T$, $p_{i2}(0) = [0, 0]^T$, for $i = 1, ..., 5$. The desired displacement with respect to the leader for each agent is given as: $d_1 = [0, d]^T$, $d_2 = [-dsin(\frac{2\pi}{5}), dcos(\frac{2\pi}{5})]^T$, $d_3 = [-dsin(\frac{\pi}{5}), -dcos(\frac{\pi}{5})]^T$, $d_4 = [dsin(\frac{\pi}{5}), -dcos(\frac{\pi}{5})]^T$, and $d_5 = [dsin(\frac{2\pi}{5}), dcos(\frac{2\pi}{5})]^T$ with $d = 1$. The leader initial states are $p_l(0) = [1, -1]^T$ and $v_l(0) = [0, 0]^T$, respectively. All weights of edges in Figure 7.2 are equal to *one*. Without a loss of generality, we consider that the leader is connected the first agent. Moreover, as the graph is connected, all agents can obtain the leader's information.

We selected 8 neurons for the input layer, 8 neurons for the first hidden layer, 18 neurons for the second hidden layer, and 2 neurons for the output layer for each agent. The NN's initial weights

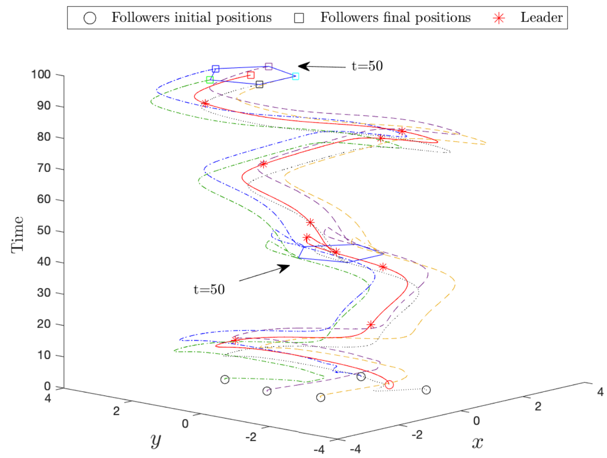

Figure 7.3: Trajectories of agents and the leader in xy-plane.

are chosen randomly in the interval of $[-0.01, 0.01]$. The activation function for these layers is a sigmoid function. The activation function for the output layer is linear. The parameters were selected as $\gamma_i = 1, \varsigma = 0.1, \mu_i = 0.1, \kappa_i = 0.1, \Pi_i = 10$, $k_{b_i} = 0.5$. Also we selected the gains as $k_{c_i} = 50$. Let the time delay be $\tau = 0.25$, then from Theorem 7.1, one can get $k_1\tau < 0.2796$, and we selected $k_1 = 1$.

Figures 7.3-7.9 demonstrate the simulation results where a time delay τ is considered. The performance of the multi-agent system (7.45) is illustrated in Figure 7.3 where the evolution of position states in $xy-$plane are shown. Trajectories and velocities of each agent are shown in Figures 7.4-7.5, respectively. It can be seen that the agents have maintained the leader velocity (see Figure 7.5). The tracking errors e_{x_i} and e_{v_i} (7.6) are provided in Figure 7.6. Evolution of Frobenius norm of the NN weights $\varpi_i(t)$, gain b_{m_i}, and Nussbaum parameter $\zeta_i(t)$ for each agent. From Theorems 7.1, 7.2, Figure 7.7, one can note that as $r_i(t)$ is bounded, the errors of e_{x_i}, and e_{v_i} remain bounded. Thus, the SGUUB of e_{x_i}, and e_{v_i} can be seen in Figure 7.6. The control inputs of each agent are given in Figure 7.9.

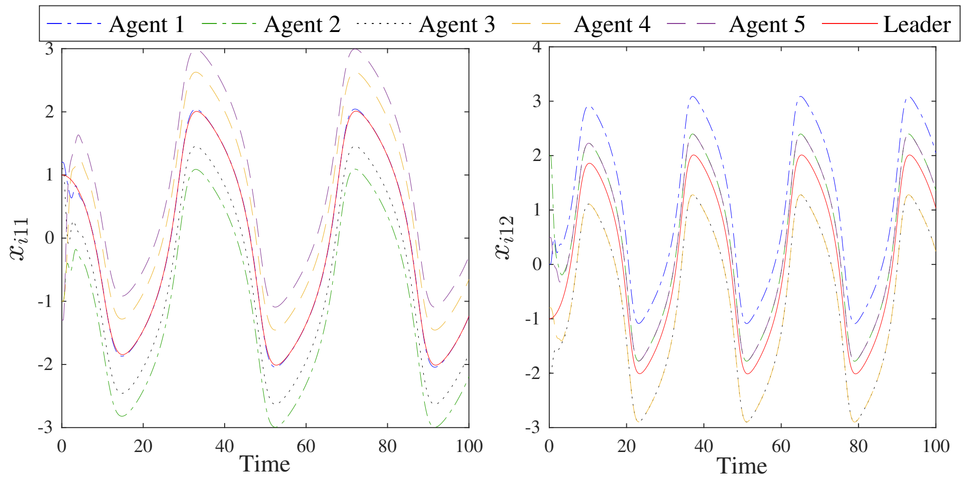

Figure 7.4: Trajectories of agents and the leader.

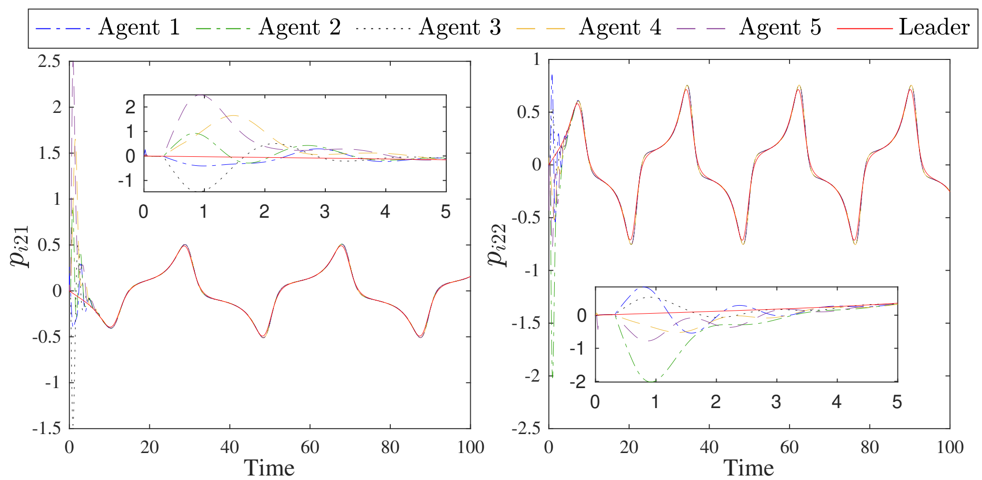

Figure 7.5: Velocities of agents and the leader.

7.5 Conclusion

This chapter addressed a leader-following formation control problem for second-order, uncertain, nonlinear multi-agent systems in the presence of communication delays. An undirected graph modeled a multi-agent system's communication topology where a leader can broadcast information to agents. The number of states is an a priori knowledge that specifies the number of neurons in the three-layer NN. To alleviate the computational burden, only the weights norms of two consecutive outer layers were tunable. The leader-following formation control problem with communication

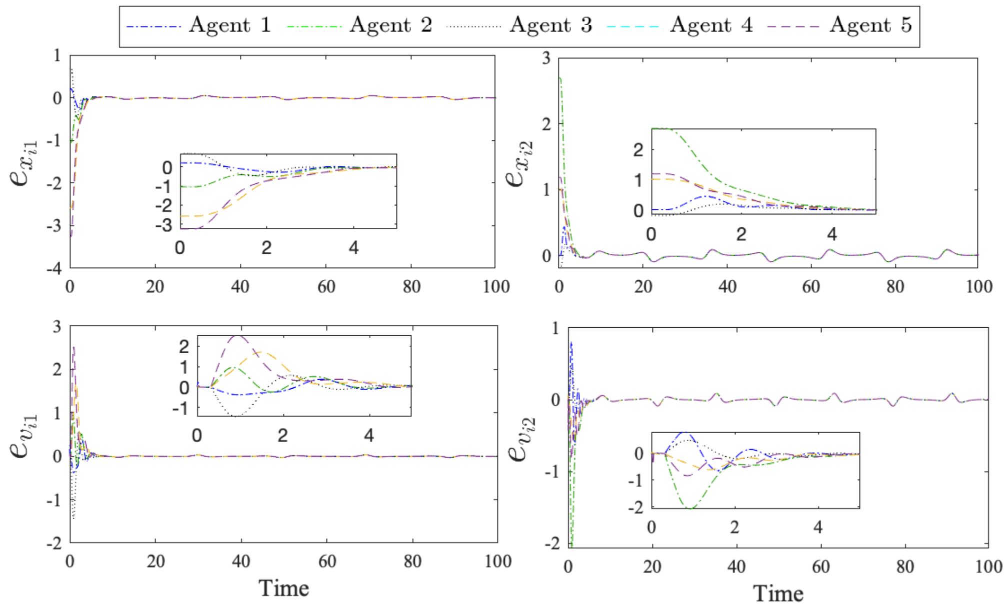

Figure 7.6: Error signals of e_{x_i}, e_{v_i} for each agent.

delay was addressed by a delayed integral of error variables, an NN-based control, and a robustifying term. Using a barrier Lyapunov function, the SGUUB of a closed-loop system was rigorously proven.

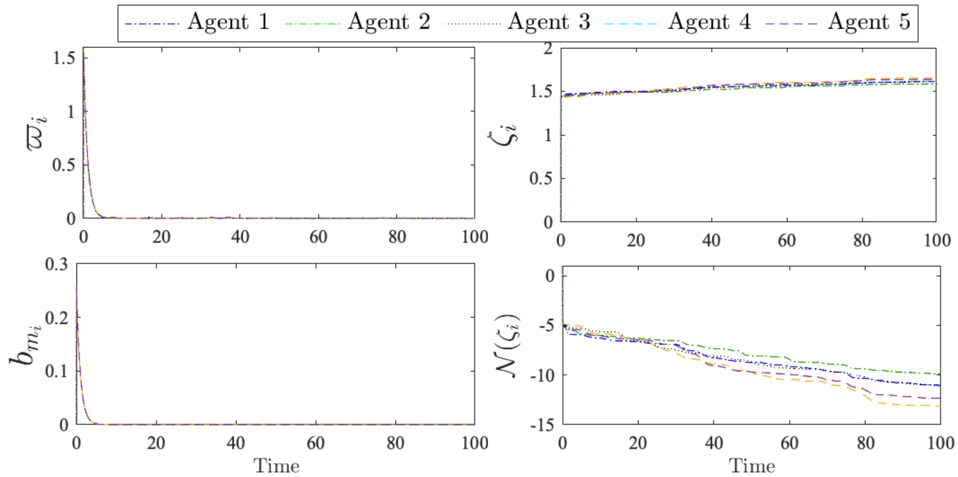

Figure 7.7: Evolution of $\varpi_i(t)$, time-variant gain b_{m_i}, and parameters $\zeta_i(t)$ for each agent.

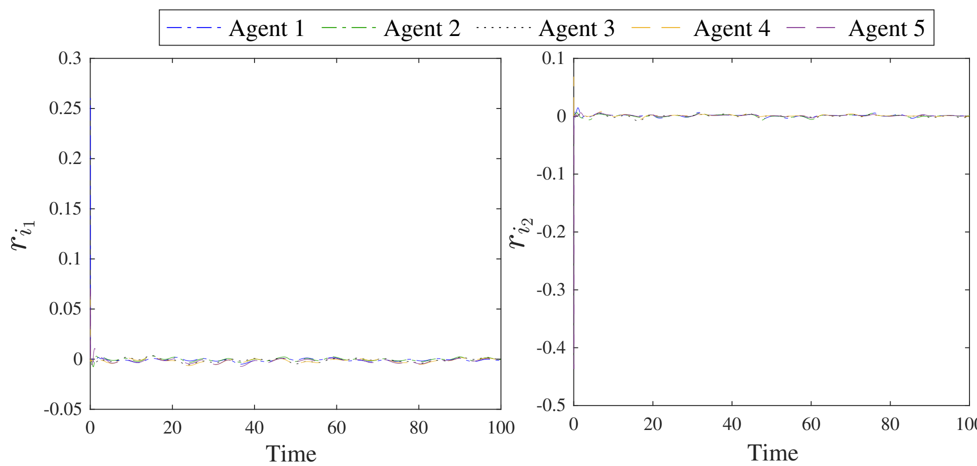

Figure 7.8: Evolution of signal of $r_i(t)$ for each agent.

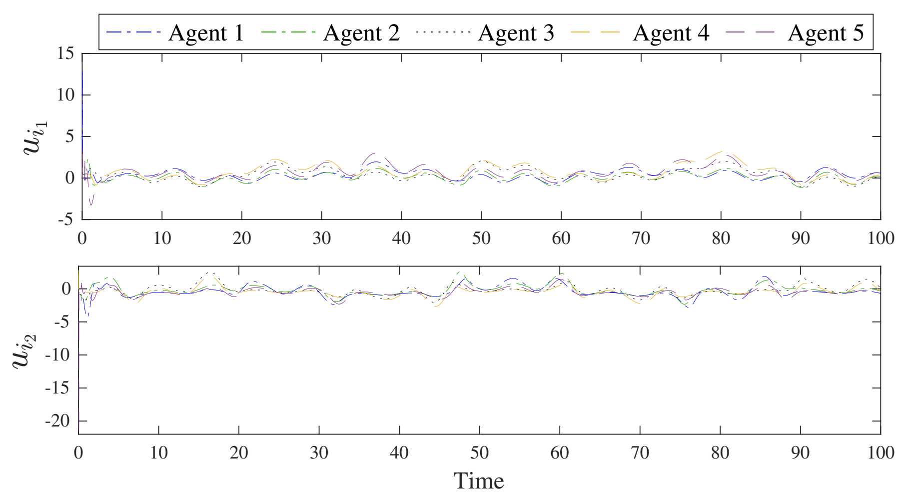

Figure 7.9: Control inputs of each agent.

Chapter 8

Conclusion and Future Works

8.1 Summary

In this dissertation, we explored the spectral properties of the normalized rigidity matrix in 2D and 3D spaces. The necessary and sufficient conditions for reaching the maximum smallest singular value of the matrix in a rigid framework with three vertices in 2D space were presented and validated through numerical simulations and a robot experimentation platform.

We then proposed a distance-based formation control and target tracking method for nonlinear multi-agent systems with unknown dynamics and disturbances. The method used an RBFNN to compensate for unknown agent dynamics and a stable NN tuning law paired with a target-tracking backstepping controller to ensure the formation's stability. The proposed method was shown to have improved performance compared to two other displacement-based methods through simulation results and the introduced performance index.

In addition, a distance-based formation control and target tracking scheme using a neuro-adaptive backstepping and rigid graph theory was developed for second-order nonlinear multi-agent systems with bounded disturbances and unknown state time delays. The scheme used RBFNN to compensate for disturbances and unknown nonlinearities, and its stability was proven through the Lyapunov stability theory. Simulation results verified the proposed method's effectiveness and improvements compared to recent literature results.

A leader-following formation control scheme for heterogeneous, second-order, uncertain, input-affine, nonlinear multi-agent systems using a directed graph was also developed. A three-layer NN was used to approximate the nonlinearity of multi-agent dynamics, and NN error feedback control with RISE feedback ensured semi-global asymptotic leader-following formation control. The stability of the closed-loop signals and asymptotic leader tracking formation was proven through a Lyapunov stability theory, and the proposed method was shown to be effective through comparisons with previous studies.

Finally, we investigated the leader-following formation control problem of second-order, uncertain, nonlinear multi-agent systems in the presence of communication delays. A three-layer NN with tunable weight norms was used, along with a delayed integral of error variables, an NN-based control, and a robustifying term, to solve the formation control problem. The solution was proven to be SGUUB through a barrier Lyapunov function, and the performance of the proposed method was demonstrated through simulation results.

8.2 Limitations

In Chapter 3, we only investigated the maximum smallest singular value of the normalized rigidity matrix for a rigid graph with three vertices in 2D space. It would be interesting to extend this analysis to MIR graphs with four or more vertices or in 3D space.

In Chapter 4, we assumed that the first agent could track the trajectory and broadcast information to the other agents. It would be worth considering scenarios where there is no broadcasting, and each agent has access to only local information. Additionally, we used RBFNN, which requires a trial and error process to determine the number of neurons, centers of the activation function, and widths of the Gaussian function. We partially addressed hyperparameters' tuning issue with a three-layer NN for a leader-following formation control problem in Chapter 6. Investigating other methods for compensating for unknown agent dynamics would be a valuable future direction.

In Chapter 5, in addition to the considerations in Chapter 4, we considered the time delay in the dynamics of the multi-agent system to be bounded. Still, we did not investigate the bound for the time delay. Future work could explore how to determine the time delay bound and how to design controllers that are robust to time delays.

In Chapter 6, we removed the broadcasting information of the trajectory from one agent to others and alleviated the assumption regarding the control gain matrix. Thus, the control design did not require the lower bound of the control gain matrix. However, the sign of the matrix was known. To resolve the limitation in Chapters 4 and 5, we used a three-layer NN, where the number of neurons in each layer was given. We established the tuning law for NN weights matrices in the proposed scheme. The system's stability has been improved compared to Chapters 4 and 5.

In Chapter 7, we removed the assumption regarding the knowledge of the control gain matrix in the system dynamics of a multi-agent system. This consideration distinguishes this work from Chapters 4, 5, and 6. Moreover, we considered that the leader is connected to at least one of the agents, and that agent can propagate the leader's information to other agents. We also considered that there exists a bounded, constant propagation delay among the agents. Unlike Chapter 4 and Chapter 5, we considered an undirected graph to model the interactions among the agents.

8.3 Future Works

- Study and investigate the properties of the normalized rigidity matrix in 3D. In addition, the maximum smallest singular value of the normalized rigidity matrix for a MIR graph of four vertices or more can be established. A possible relation between the number of vertices and this value can be derived.

- An experimental setup using a set of UGVs or UAVs can be run for the proposed controllers of this dissertation.

- The dynamics of the multi-agent system in this work is deterministic. Further investigation is required to address the distance-based and leader-following formation control of stochastic nonlinear multi-agent systems. In that case, the Itô calculus is required to derive the stability of the multi-agent systems. An interested reader may start from the following references [136–138].

- The other direction may include the formation control of nonlinear multi-agent systems with actuator hysteresis or a dead zone. An interested reader may start from the following references [139, 140].

- Cyberattack detection on multi-agent systems' formation control problems has recently gained attention. However, attack detection and mitigation of the distance-based formation control of nonlinear multi-agent with unknown nonlinearity in the system dynamics is an open question that requires further studies. An interested reader may start from the following reference [141].

References

[1] X. Li, D. Zhu, and Y. Qian, “A survey on formation control algorithms for multi-auv system,” *Unmanned Systems*, vol. 2, no. 04, pp. 351–359, 2014.

[2] K.-K. Oh, M.-C. Park, and H.-S. Ahn, “A survey of multi-agent formation control,” *Automatica*, vol. 53, pp. 424–440, 2015.

[3] P. B. S. Lissaman and C. A. Shollenberger, “Formation flight of birds,” *Science*, vol. 168, no. 3934, pp. 1003–1005, 1970.

[4] “fello’fly: Airbus’ wake energy retrieval concept shows promise for operational fuel savings,” Accessed on 28 March 2023, chapter 6, Climate Change Mitigation: Operations, ICAO Environmental Report 2022. [Online]. Available: https://www.icao.int/environmental-protection/Documents/EnvironmentalReports/2022/ENVReport2022_Art39.pdf

[5] S. J. Portugal, T. Y. Hubel, J. Fritz, S. Heese, D. Trobe, B. Voelkl, S. Hailes, A. M. Wilson, and J. R. Usherwood, “Upwash exploitation and downwash avoidance by flap phasing in ibis formation flight,” *Nature*, vol. 505, no. 7483, pp. 399–402, 2014.

[6] I. Newton, *The Migration Ecology of Birds*. Elsevier, 2010.

[7] S. Ramazani, R. R. Selmic, and M. De Queiroz, “Rigidity-based multiagent layered formation control,” *IEEE Transactions on Cybernetics*, vol. 47, no. 8, pp. 1902–1913, 2017.

[8] M. De Queiroz, X. Cai, and M. Feemster, *Formation Control of Multi-agent Systems: A Graph Rigidity Approach*. John Wiley & Sons, 2019.

[9] Y. Q. Chen and Z. Wang, “Formation control: a review and a new consideration,” in *2005 IEEE/RSJ International conference on intelligent robots and systems*. IEEE, 2005, pp. 3181–3186.

[10] C. Sabol, R. Burns, and C. A. McLaughlin, “Satellite formation flying design and evolution,” *Journal of spacecraft and rockets*, vol. 38, no. 2, pp. 270–278, 2001.

[11] S. Ramazani, A. Gardner, and R. R. Selmic, “Neural network-based formation control of unmanned vehicles in 3d space,” in *Control and Automation (MED), 2016 24th Mediterranean Conference on*. IEEE, 2016, pp. 1065–1070.

[12] W. C. Wah, *Synchronization in Complex Networks of Nonlinear Dynamical Systems*. World scientific, 2007.

[13] Z. Qu, *Cooperative Control of Dynamical Systems: Applications to Autonomous Vehicles*. Springer Science & Business Media, 2009.

[14] A. Das and F. L. Lewis, “Cooperative adaptive control for synchronization of second-order systems with unknown nonlinearities,” *International Journal of Robust and Nonlinear Control*, vol. 21, no. 13, pp. 1509–1524, 2011.

[15] ——, “Distributed adaptive control for synchronization of unknown nonlinear networked systems,” *Automatica*, vol. 46, no. 12, pp. 2014–2021, 2010.

[16] H. Zhang and F. L. Lewis, “Adaptive cooperative tracking control of higher-order nonlinear systems with unknown dynamics,” *Automatica*, vol. 48, no. 7, pp. 1432–1439, 2012.

[17] X. Cai and M. De Queiroz, “Multi-agent formation maneuvering and target interception with double-integrator model,” in *2014 American Control Conference*. IEEE, 2014, pp. 287–292.

[18] A. R. Berg and T. Jordán, “A proof of connelly’s conjecture on 3-connected circuits of the rigidity matroid,” *Journal of Combinatorial Theory, Series B*, vol. 88, no. 1, pp. 77–97, 2003.

[19] L. Asimow and B. Roth, “The rigidity of graphs, ii,” *Journal of Mathematical Analysis and Applications*, vol. 68, no. 1, pp. 171–190, 1979.

[20] M. Mesbahi and M. Egerstedt, *Graph Theoretic Methods in Multiagent Networks*. Princeton University Press, 2010.

[21] X. Cai and M. De Queiroz, "Adaptive rigidity-based formation control for multirobotic vehicles with dynamics," *IEEE Transactions on Control Systems Technology*, vol. 23, no. 1, pp. 389–396, 2014.

[22] G. Laman, "On graphs and rigidity of plane skeletal structures," *Journal of Engineering Mathematics*, vol. 4, no. 4, pp. 331–340, 1970.

[23] L. Asimow and B. Roth, "The rigidity of graphs, ii," *Journal of Mathematical Analysis and Applications*, vol. 68, no. 1, pp. 171–190, 1979.

[24] C. Borcea and I. Streinu, "The number of embeddings of minimally rigid graphs," *Discrete & Computational Geometry*, vol. 31, no. 2, pp. 287–303, 2004.

[25] H. Maehara, "Geometry of frameworks," *Yokohama Mathematical Journal*, vol. 47, pp. 41–65, 1999.

[26] R. Babazadeh and R. R. Selmic, "Distance-based multi-agent formation control with energy constraints using sdre," *IEEE Transactions on Aerospace and Electronic Systems*, 2019.

[27] F. Lewis, S. Jagannathan, and A. Yesildirak, *Neural Network Control of Robot Manipulators and Non-linear Systems*. CRC Press, 1998.

[28] G.-X. Wen, C. P. Chen, Y.-J. Liu, and Z. Liu, "Neural-network-based adaptive leader-following consensus control for second-order non-linear multi-agent systems," *IET Control Theory & Applications*, vol. 9, no. 13, pp. 1927–1934, 2015.

[29] M. H. Stone, "The generalized weierstrass approximation theorem," *Mathematics Magazine*, vol. 21, no. 5, pp. 237–254, 1948.

[30] K. Hornik, M. Stinchcombe, and H. White, "Multilayer feedforward networks are universal approximators," *Neural Networks*, vol. 2, no. 5, pp. 359–366, 1989.

[31] J. Shin, S. Kim, and A. Tsourdos, “Neural-networks-based adaptive control for an uncertain nonlinear system with asymptotic stability,” *International Journal of Control, Automation and Systems*, vol. 16, no. 4, pp. 1989–2001, 2018.

[32] P. M. Patre, W. MacKunis, K. Kaiser, and W. E. Dixon, “Asymptotic tracking for uncertain dynamic systems via a multilayer neural network feedforward and rise feedback control structure,” *IEEE Transactions on Automatic Control*, vol. 53, no. 9, pp. 2180–2185, 2008.

[33] R. D. Nussbaum, “Some remarks on a conjecture in parameter adaptive control,” *Systems & control letters*, vol. 3, no. 5, pp. 243–246, 1983.

[34] Z. Chen, “Nussbaum functions in adaptive control with time-varying unknown control coefficients,” *Automatica*, vol. 102, pp. 72–79, 2019.

[35] S. S. Ge, F. Hong, and T. H. Lee, “Adaptive neural control of nonlinear time-delay systems with unknown virtual control coefficients,” *IEEE Transactions on Systems, Man, and Cybernetics, Part B (Cybernetics)*, vol. 34, no. 1, pp. 499–516, 2004.

[36] D. Zelazo, A. Franchi, H. H. Bülthoff, and P. Robuffo Giordano, “Decentralized rigidity maintenance control with range measurements for multi-robot systems,” *The International Journal of Robotics Research*, vol. 34, no. 1, pp. 105–128, 2015.

[37] S. M. Cioabă and X. Gu, “Spectral conditions for graph rigidity in the euclidean plane,” *arXiv preprint arXiv:2001.06934*, 2020.

[38] D. Zelazo, A. Franchi, F. Allgöwer, H. H. Bülthoff, and P. R. Giordano, “Rigidity maintenance control for multi-robot systems,” in *Robotics: science and systems*, 2012, pp. 473–480.

[39] K. Aryankia and R. R. Selmic, “Formation control and target tracking for a class of nonlinear multi-agent systems using neural networks,” in *2020 European Control Conference (ECC)*, 2020, pp. 160–165.

[40] E. Rohmer, S. P. Singh, and M. Freese, “V-rep: A versatile and scalable robot simulation framework,” in *2013 IEEE/RSJ International Conference on Intelligent Robots and Systems*. IEEE, 2013, pp. 1321–1326.

[41] C. Jiang, Z. Chen, and Y. Guo, “Multi-robot formation control: a comparison between model-based and learning-based methods,” *Journal of Control and Decision*, vol. 7, no. 1, pp. 90–108, 2020.

[42] K.-K. Oh and H.-S. Ahn, “Formation control of mobile agents based on inter-agent distance dynamics,” *Automatica*, vol. 47, no. 10, pp. 2306–2312, 2011.

[43] M. Aranda, G. López-Nicolás, C. Sagüés, and M. M. Zavlanos, “Coordinate-free formation stabilization based on relative position measurements,” *Automatica*, vol. 57, pp. 11–20, 2015.

[44] M.-C. Park, K. Jeong, and H.-S. Ahn, “Formation stabilization and resizing based on the control of inter-agent distances,” *International Journal of Robust and Nonlinear Control*, vol. 25, no. 14, pp. 2532–2546, 2015.

[45] L. Krick, M. E. Broucke, and B. A. Francis, “Stabilisation of infinitesimally rigid formations of multi-robot networks,” *International Journal of Control*, vol. 82, no. 3, pp. 423–439, 2009.

[46] K.-K. Oh and H.-S. Ahn, “Distance-based undirected formations of single-integrator and double-integrator modeled agents in n-dimensional space,” *International Journal of Robust and Nonlinear Control*, vol. 24, no. 12, pp. 1809–1820, 2014.

[47] T. H. Summers, C. Yu, S. Dasgupta, and B. D. Anderson, “Control of minimally persistent leader-remote-follower and coleader formations in the plane,” *IEEE Transactions on Automatic Control*, vol. 56, no. 12, pp. 2778–2792, 2011.

[48] K.-K. Oh and H.-S. Ahn, “Leader-follower type distance-based formation control of a group of autonomous agents,” *International Journal of Control, Automation and Systems*, vol. 15, no. 4, pp. 1738–1745, 2017.

[49] B. Tian, H. Lu, Z. Zuo, and W. Yang, “Fixed-time leader–follower output feedback consensus for second-order multiagent systems,” *IEEE Transactions on Cybernetics*, vol. 49, no. 4, pp. 1545–1550, 2018.

[50] B. Jiang, M. Deghat, and B. D. Anderson, “Simultaneous velocity and position estimation via distance-only measurements with application to multi-agent system control,” *IEEE Transactions on Automatic Control*, vol. 62, no. 2, pp. 869–875, 2016.

[51] Q. Wang, Q. Hua, Y. Yi, and T. Zhang, “Multi-agent formation control in switching networks using backstepping design,” *International Journal of Control, Automation and Systems*, vol. 15, no. 4, pp. 1569–1576, 2017.

[52] E. D. Ferreira-Vazquez, E. Hernandez-Martinez, J.-J. Flores-Godoy, G. Fernandez-Anaya, and P. Paniagua-Contro, “Distance-based formation control using angular information between robots,” *Journal of Intelligent & Robotic Systems*, vol. 83, no. 3-4, pp. 543–560, 2016.

[53] C. P. Chen, G.-X. Wen, Y.-J. Liu, and F.-Y. Wang, “Adaptive consensus control for a class of nonlinear multiagent time-delay systems using neural networks,” *IEEE Transactions on Neural Networks and Learning Systems*, vol. 25, no. 6, pp. 1217–1226, 2014.

[54] G. Chen and Y.-D. Song, “Cooperative tracking control of nonlinear multiagent systems using self-structuring neural networks,” *IEEE Transactions on Neural Networks and Learning Systems*, vol. 25, no. 8, pp. 1496–1507, 2013.

[55] J. Yu, X. Dong, Q. Li, and Z. Ren, “Practical time-varying formation tracking for second-order nonlinear multiagent systems with multiple leaders using adaptive neural networks,” *IEEE Transactions on Neural Networks and Learning Systems*, vol. 29, no. 12, pp. 6015–6025, 2018.

[56] J. Mei, W. Ren, B. Li, and G. Ma, “Distributed containment control for multiple unknown second-order nonlinear systems with application to networked lagrangian systems,” *IEEE Transactions on Neural Networks and Learning Systems*, vol. 26, no. 9, pp. 1885–1899, 2014.

[57] L. Tan, C. Li, and J. Huang, “Neural network–based event-triggered adaptive control algorithms for uncertain nonlinear systems with actuator failures,” *Cognitive Computation*, pp. 1–11, 2020.

[58] S.-M. Kang, M.-C. Park, B.-H. Lee, and H.-S. Ahn, "Distance-based formation control with a single moving leader," in *2014 American Control Conference*. IEEE, 2014, pp. 305–310.

[59] R. Olfati-Saber and R. M. Murray, "Consensus problems in networks of agents with switching topology and time-delays," *IEEE Transactions on Automatic Control*, vol. 49, no. 9, pp. 1520–1533, 2004.

[60] G. Wen, C. P. Chen, Y.-J. Liu, and Z. Liu, "Neural network-based adaptive leader-following consensus control for a class of nonlinear multiagent state-delay systems," *IEEE Transactions on Cybernetics*, vol. 47, no. 8, pp. 2151–2160, 2016.

[61] T. Zhang, S. S. Ge, and C. C. Hang, "Adaptive neural network control for strict-feedback nonlinear systems using backstepping design," *Automatica*, vol. 36, no. 12, pp. 1835–1846, 2000.

[62] X. Cai and M. De Queiroz, "Rigidity-based stabilization of multi-agent formations," *Journal of Dynamic Systems, Measurement, and Control*, vol. 136, no. 1, 2014.

[63] K. Aryankia and R. R. Selmic, "Neuro-adaptive formation control and target tracking for nonlinear multi-agent systems with time-delay," *IEEE Control Systems Letters*, vol. 5, no. 3, pp. 791–796, 2021.

[64] X. Tang, X. Zhang, J. Shi, S. Wei, and B. Tian, "Ground moving target 2-d velocity estimation and refocusing for multichannel maneuvering sar with fixed acceleration," *Sensors*, vol. 19, no. 17, p. 3695, 2019.

[65] I. S. Reed, R. M. Gagliardi, and L. B. Stotts, "A recursive moving-target-indication algorithm for optical image sequences," *IEEE Transactions on Aerospace and Electronic Systems*, vol. 26, no. 3, pp. 434–440, 1990.

[66] B. D. Anderson, C. Yu, B. Fidan, and J. M. Hendrickx, "Rigid graph control architectures for autonomous formations," *IEEE Control Systems Magazine*, vol. 28, no. 6, pp. 48–63, 2008.

[67] C. Yu, B. D. Anderson, S. Dasgupta, and B. Fidan, "Control of minimally persistent formations in the plane," *SIAM Journal on Control and Optimization*, vol. 48, no. 1, pp. 206–233, 2009.

[68] M. Ye, B. D. Anderson, and C. Yu, "Bearing-only measurement self-localization, velocity consensus and formation control," *IEEE Transactions on Aerospace and Electronic Systems*, vol. 53, no. 2, pp. 575–586, 2017.

[69] B. Jiang, B. D. Anderson, and H. Hmam, "3-d relative localization of mobile systems using distance-only measurements via semidefinite optimization," *IEEE Transactions on Aerospace and Electronic Systems*, vol. 56, no. 3, pp. 1903–1916, 2019.

[70] T. Eren, "Using angle of arrival (bearing) information for localization in robot networks," *Turkish Journal of Electrical Engineering & Computer Sciences*, vol. 15, no. 2, pp. 169–186, 2007.

[71] H. K. Khalil, "Nonlinear systems," *Upper Saddle River*, 2002.

[72] A. F. Filippov, *Differential Equations with Discontinuous Righthand Sides: Control Systems*. Springer Science & Business Media, 2013, vol. 18.

[73] J.-P. Aubin and A. Cellina, *Differential Inclusions: Set-valued Maps and Viability Theory*. Springer Science & Business Media, 2012, vol. 264.

[74] Y. Wang, G. Pin, A. Serrani, and T. Parisini, "Switching-based sinusoidal disturbance rejection for uncertain stable linear systems," in *2018 Annual American Control Conference (ACC)*. IEEE, 2018, pp. 4502–4507.

[75] H. Ma, Z. Wang, D. Wang, D. Liu, P. Yan, and Q. Wei, "Neural-network-based distributed adaptive robust control for a class of nonlinear multiagent systems with time delays and external noises," *IEEE Transactions on Systems, Man, and Cybernetics: Systems*, vol. 46, no. 6, pp. 750–758, 2015.

[76] K. Chen, J. Wang, Y. Zhang, and Z. Liu, "Leader-following consensus for a class of nonlinear strick-feedback multiagent systems with state time-delays," *IEEE Transactions on Systems, Man, and Cybernetics: Systems*, 2018.

[77] S. S. Ge and C. Wang, "Adaptive neural control of uncertain mimo nonlinear systems," *IEEE Transactions on Neural Networks*, vol. 15, no. 3, pp. 674–692, 2004.

[78] H. Zhang, D. Yue, X. Yin, S. Hu, and C. Xia Dou, "Finite-time distributed event-triggered consensus control for multi-agent systems," *Information Sciences*, vol. 339, pp. 132–142, 2016.

[79] W. Ren, "Multi-vehicle consensus with a time-varying reference state," *Systems & Control Letters*, vol. 56, no. 7-8, pp. 474–483, 2007.

[80] Q. Shi, T. Li, J. Li, C. P. Chen, Y. Xiao, and Q. Shan, "Adaptive leader-following formation control with collision avoidance for a class of second-order nonlinear multi-agent systems," *Neurocomputing*, vol. 350, pp. 282–290, 2019.

[81] J. L. Castro, "Fuzzy logic controllers are universal approximators," *IEEE Transactions on Systems, Man, and Cybernetics*, vol. 25, no. 4, pp. 629–635, 1995.

[82] J.-H. Park, S.-H. Huh, S.-H. Kim, S.-J. Seo, and G.-T. Park, "Direct adaptive controller for nonaffine nonlinear systems using self-structuring neural networks," *IEEE Transactions on Neural Networks*, vol. 16, no. 2, pp. 414–422, 2005.

[83] X. Wang, H. Wang, T. Huang, and J. Kurths, "Neural-network-based adaptive tracking control for nonlinear multiagent systems: The observer case," *IEEE Transactions on Cybernetics*, vol. 53, no. 1, pp. 138–150, 2023.

[84] K. Lu, Z. Liu, G. Lai, C. L. P. Chen, and Y. Zhang, "Adaptive consensus tracking control of uncertain nonlinear multiagent systems with predefined accuracy," *IEEE Transactions on Cybernetics*, vol. 51, no. 1, pp. 405–415, 2021.

[85] C. Wang and D. J. Hill, "Learning from neural control," *IEEE Transactions on Neural Networks*, vol. 17, no. 1, pp. 130–146, 2006.

[86] J. Moody and C. Darken, *Learning with Localized Receptive Fields*. Yale Univ., Department of Computer Science, 1988.

[87] Q. Yang, S. Jagannathan, and Y. Sun, "Robust integral of neural network and error sign control of mimo nonlinear systems," *IEEE Transactions on Neural Networks and Learning Systems*, vol. 26, no. 12, pp. 3278–3286, 2015.

[88] B. Xian, D. M. Dawson, M. S. de Queiroz, and J. Chen, "A continuous asymptotic tracking control strategy for uncertain nonlinear systems," *IEEE Transactions on Automatic Control*, vol. 49, no. 7, pp. 1206–1211, 2004.

[89] T. Dierks and S. Jagannathan, "Neural network control of mobile robot formations using rise feedback," *IEEE Transactions on Systems, Man, and Cybernetics, Part B (Cybernetics)*, vol. 39, no. 2, pp. 332–347, 2008.

[90] N. Fischer, Z. Kan, R. Kamalapurkar, and W. E. Dixon, "Saturated rise feedback control for a class of second-order nonlinear systems," *IEEE Transactions on Automatic Control*, vol. 59, no. 4, pp. 1094–1099, 2013.

[91] Z. Yao, J. Yao, and W. Sun, "Adaptive rise control of hydraulic systems with multilayer neural-networks," *IEEE Transactions on Industrial Electronics*, vol. 66, no. 11, pp. 8638–8647, 2018.

[92] B. Yao and M. Tomizuka, "Adaptive robust control of siso nonlinear systems in a semi-strict feedback form," *Automatica*, vol. 33, no. 5, pp. 893–900, 1997.

[93] S. S. Ge, F. Hong, and T. H. Lee, "Adaptive neural network control of nonlinear systems with unknown time delays," *IEEE Transactions on Automatic Control*, vol. 48, no. 11, pp. 2004–2010, 2003.

[94] M. Wang, B. Chen, and P. Shi, "Adaptive neural control for a class of perturbed strict-feedback nonlinear time-delay systems," *IEEE Transactions on Systems, Man, and Cybernetics, Part B (Cybernetics)*, vol. 38, no. 3, pp. 721–730, 2008.

[95] G. Wen, C. P. Chen, Y.-J. Liu, and Z. Liu, "Neural network-based adaptive leader-following consensus control for a class of nonlinear multiagent state-delay systems," *IEEE Transactions on Cybernetics*, vol. 47, no. 8, pp. 2151–2160, 2017.

[96] K. Aryankia and R. R. Selmic, "Neural network-based formation control with target tracking for second-order nonlinear multi-agent systems," *IEEE Transactions on Aerospace and Electronic Systems*, pp. 1–1, 2021.

[97] B. Fan, Q. Yang, S. Jagannathan, and Y. Sun, "Asymptotic tracking controller design for nonlinear systems with guaranteed performance," *IEEE Transactions on Cybernetics*, vol. 48, no. 7, pp. 2001–2011, 2017.

[98] S. Scholtes, *Introduction To Piecewise Differentiable Equations*. Springer Science & Business Media, 2012.

[99] J. Cortes, "Discontinuous dynamical systems," *IEEE Control systems magazine*, vol. 28, no. 3, pp. 36–73, 2008.

[100] V. E. Ismailov, "On the approximation by neural networks with bounded number of neurons in hidden layers," *Journal of Mathematical Analysis and Applications*, vol. 417, no. 2, pp. 963–969, 2014.

[101] D. Shevitz and B. Paden, "Lyapunov stability theory of nonsmooth systems," *IEEE Transactions on automatic control*, vol. 39, no. 9, pp. 1910–1914, 1994.

[102] Q. Zhou, P. Shi, S. Xu, and H. Li, "Adaptive output feedback control for nonlinear time-delay systems by fuzzy approximation approach," *IEEE Transactions on Fuzzy Systems*, vol. 21, no. 2, pp. 301–313, 2012.

[103] L. Ma, H. Min, S. Wang, and Y. Liu, "Consensus of nonlinear multi-agent systems with self and communication time delays: A unified framework," *Journal of the Franklin Institute*, vol. 352, no. 3, pp. 745–760, 2015.

[104] H. E. Psillakis, "Adaptive nn cooperative control of unknown nonlinear multiagent systems with communication delays," *IEEE Transactions on Systems, Man, and Cybernetics: Systems*, vol. 51, no. 9, pp. 5311–5321, 2021.

[105] A. K. Gkesoulis, H. E. Psillakis, and Q. Wang, "Pdi regulation for consensus: Application to unknown pure-feedback agents with state and communication delays," *IEEE Transactions on Control of Network Systems*, vol. 8, no. 4, pp. 1964–1974, 2021.

[106] Y. Zhong, G. Lyu, X. He, Y. Zhang, and S. S. Ge, "Distributed active fault-tolerant cooperative control for multiagent systems with communication delays and external disturbances," *IEEE Transactions on Cybernetics*, 2021.

[107] Y. Kang, D. Luo, B. Xin, J. Cheng, T. Yang, and S. Zhou, "Robust leaderless time-varying formation control for nonlinear unmanned aerial vehicle swarm system with communication delays," *IEEE Transactions on Cybernetics*, 2022.

[108] L. Ding and G. Guo, "Sampled-data leader-following consensus for nonlinear multi-agent systems with markovian switching topologies and communication delay," *Journal of the Franklin Institute*, vol. 352, no. 1, pp. 369–383, 2015.

[109] K. Subramanian, P. Muthukumar, and Y. H. Joo, "Leader-following consensus of nonlinear multi-agent systems via reliable control with time-varying communication delay," *International Journal of Control, Automation and Systems*, vol. 17, no. 2, pp. 298–306, 2019.

[110] M. Sharifi and M. J. Yazdanpanah, "Finite time consensus of nonlinear multi-agent systems in the presence of communication time delays," *European Journal of Control*, vol. 53, pp. 10–19, 2020.

[111] A. Izadipour, J. Ghaisari, and J. Askari, "Distributed robust adaptive flocking for uncertain nonlinear multi-agent systems with time-varying communication delay," *International Journal of Systems Science*, vol. 51, no. 1, pp. 72–86, 2020.

[112] R. Olfati-Saber and R. M. Murray, “Consensus problems in networks of agents with switching topology and time-delays,” *IEEE Transactions on automatic control*, vol. 49, no. 9, pp. 1520–1533, 2004.

[113] Y. G. Sun, L. Wang, and G. Xie, “Average consensus in networks of dynamic agents with switching topologies and multiple time-varying delays,” *Systems & Control Letters*, vol. 57, no. 2, pp. 175–183, 2008.

[114] K. Liu, G. Xie, and L. Wang, “Consensus for multi-agent systems under double integrator dynamics with time-varying communication delays,” *International Journal of Robust and Nonlinear Control*, vol. 22, no. 17, pp. 1881–1898, 2012.

[115] Y. Guo, J. Zhou, G. Li, and J. Zhang, “Robust formation tracking and collision avoidance for uncertain nonlinear multi-agent systems subjected to heterogeneous communication delays,” *Neurocomputing*, vol. 395, pp. 107–116, 2020.

[116] Y. Xudong and J. Jingping, “Adaptive nonlinear design without a priori knowledge of control directions,” *IEEE Transactions on Automatic Control*, vol. 43, no. 11, pp. 1617–1621, 1998.

[117] H. Xu and P. A. Ioannou, “Robust adaptive control for a class of mimo nonlinear systems with guaranteed error bounds,” *IEEE Transactions on Automatic Control*, vol. 48, no. 5, pp. 728–742, 2003.

[118] W. Shi, “Adaptive fuzzy control for mimo nonlinear systems with nonsymmetric control gain matrix and unknown control direction,” *IEEE Transactions on Fuzzy Systems*, vol. 22, no. 5, pp. 1288–1300, 2013.

[119] Y. Song, X. Huang, and C. Wen, “Robust adaptive fault-tolerant pid control of mimo nonlinear systems with unknown control direction,” *IEEE Transactions on Industrial Electronics*, vol. 64, no. 6, pp. 4876–4884, 2017.

[120] K. Sachan and R. Padhi, “Output-constrained robust adaptive control for uncertain nonlinear mimo systems with unknown control directions,” *IEEE Control Systems Letters*, vol. 3, no. 4, pp. 823–828, 2019.

[121] J. Yu, P. Shi, C. Lin, and H. Yu, “Adaptive neural command filtering control for nonlinear mimo systems with saturation input and unknown control direction,” *IEEE Transactions on Cybernetics*, vol. 50, no. 6, pp. 2536–2545, 2019.

[122] Z. Ruan, Q. Yang, S. S. Ge, and Y. Sun, “Adaptive fuzzy fault tolerant control of uncertain mimo nonlinear systems with output constraints and unknown control directions,” *IEEE Transactions on Fuzzy Systems*, 2021.

[123] W. Chen, X. Li, W. Ren, and C. Wen, “Adaptive consensus of multi-agent systems with unknown identical control directions based on a novel nussbaum-type function,” *IEEE Transactions on Automatic Control*, vol. 59, no. 7, pp. 1887–1892, 2013.

[124] M. Guo, D. Xu, and L. Liu, “Cooperative output regulation of heterogeneous nonlinear multi-agent systems with unknown control directions,” *IEEE Transactions on Automatic Control*, vol. 62, no. 6, pp. 3039–3045, 2016.

[125] G. Wang, C. Wang, L. Li, and Z. Zhang, “Designing distributed consensus protocols for second-order nonlinear multi-agents with unknown control directions under directed graphs,” *Journal of the Franklin Institute*, vol. 354, no. 1, pp. 571–592, 2017.

[126] D. G. Lui, A. Petrillo, and S. Santini, “Exponential bipartite tracking consensus in cooperative-antagonistic nonlinear multi-agent systems with multiple communication time-varying delays,” *IFAC Journal of Systems and Control*, p. 100209, 2022.

[127] C. Yuan and X. Mao, “Robust stability and controllability of stochastic differential delay equations with markovian switching,” *Automatica*, vol. 40, no. 3, pp. 343–354, 2004.

[128] J. K. Hale and S. M. V. Lunel, *Introduction to Functional Differential Equations*. Springer Science & Business Media, 2013, vol. 99.

[129] B. Ren, S. S. Ge, K. P. Tee, and T. H. Lee, “Adaptive neural control for output feedback nonlinear systems using a barrier lyapunov function,” *IEEE Transactions on Neural Networks*, vol. 21, no. 8, pp. 1339–1345, 2010.

[130] M. M. Polycarpou and P. A. Ioannou, "A robust adaptive nonlinear control design," in *1993 American control conference*. IEEE, 1993, pp. 1365–1369.

[131] K. B. Ngo, R. Mahony, and Z.-P. Jiang, "Integrator backstepping using barrier functions for systems with multiple state constraints," in *Proceedings of the 44th IEEE Conference on Decision and Control*. IEEE, 2005, pp. 8306–8312.

[132] K. P. Tee, S. S. Ge, and E. H. Tay, "Barrier lyapunov functions for the control of output-constrained nonlinear systems," *Automatica*, vol. 45, no. 4, pp. 918–927, 2009.

[133] Y. Zhang, H. Liang, H. Ma, Q. Zhou, and Z. Yu, "Distributed adaptive consensus tracking control for nonlinear multi-agent systems with state constraints," *Applied Mathematics and Computation*, vol. 326, pp. 16–32, 2018.

[134] A. Boulkroune, M. Tadjine, M. M'Saad, and M. Farza, "Fuzzy adaptive controller for mimo nonlinear systems with known and unknown control direction," *Fuzzy sets and systems*, vol. 161, no. 6, pp. 797–820, 2010.

[135] S. Labiod, M. S. Boucherit, and T. M. Guerra, "Adaptive fuzzy control of a class of mimo nonlinear systems," *Fuzzy sets and systems*, vol. 151, no. 1, pp. 59–77, 2005.

[136] Y. Zhao, C. Liu, X. Liu, H. Wang, and Y. Zhou, "Adaptive tracking control for stochastic nonlinear systems with unknown virtual control coefficients," *International Journal of Robust and Nonlinear Control*, vol. 32, no. 3, pp. 1331–1354, 2022.

[137] W. Sun, S.-F. Su, Y. Wu, and J. Xia, "Novel adaptive fuzzy control for output constrained stochastic nonstrict feedback nonlinear systems," *IEEE Transactions on Fuzzy Systems*, vol. 29, no. 5, pp. 1188–1197, 2020.

[138] P. Jagtap and D. V. Dimarogonas, "Distributed consensus of stochastic multi-agent systems with prescribed performance constraints," in *2021 60th IEEE Conference on Decision and Control (CDC)*. IEEE, 2021, pp. 1911–1916.

[139] J. Wang, K. Chen, Q. Liu, and Q. Ma, “Observer-based adaptive consensus tracking control for nonlinear multi-agent systems with actuator hysteresis,” *Nonlinear Dynamics*, vol. 95, no. 3, pp. 2181–2195, 2019.

[140] D. Liu, Z. Liu, C. Chen, and Y. Zhang, “Distributed adaptive fuzzy control approach for prescribed-time containment of uncertain nonlinear multi-agent systems with unknown hysteresis,” *Nonlinear Dynamics*, vol. 105, no. 1, pp. 257–275, 2021.

[141] A. Mousavi, K. Aryankia, and R. R. Selmic, “A distributed fdi cyber-attack detection in discrete-time nonlinear multi-agent systems using neural networks,” *European Journal of Control*, vol. 66, p. 100646, 2022.